ESTIMATION OF TENSION IN THE GEOMEMBRANE OF GCL

A Thesis Submitted

in Partial Fulfilment of the Requirements

for the Degree of

MASTER OF TECHNOLOGY

by

K. V. S. Krishna Prasad

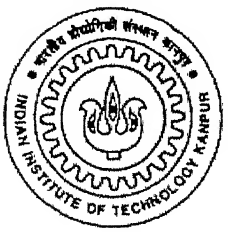

to the

DEPARTMENT OF CIVIL ENGINEERING

INDIAN INSTITUTE OF TECHNOLOGY, KANPUR

May, 2000

Dedicated to

My Parents and
Teachers

CERTIFICATE

It is certified that the work contained in this thesis entitled "***Estimation of Tension in the Geomembrane of GCL***" by **K. V. S. Krishna Prasad** has been carried out under my supervision and that this work has not been submitted elsewhere for a degree.

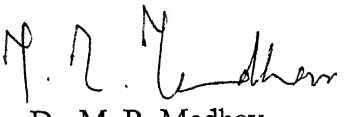

Dr. M. R. Madhav
Professor
Department of Civil Engineering

May, 2000
I. I. T, Kanpur

Acknowledgements

I take this opportunity to express my profound sense of gratitude and indebtedness to Prof. Madhira R. Madhav for his valuable guidance and encouragement at any time, any day at any place, throughout the course of my work. I sincerely appreciate the lively interest and constructive criticisms, which inspired me in carrying out this work.

It is my privilege to be extremely grateful to my teachers, Prof. Sarvesh Chandra, Prof. P.K. Basudhar, Prof. N. S. V. Kameswara Rao and Prof. Umesh Dayal for giving me a thorough professional knowledge of geotechnical engineering. I acknowledge the help rendered by them in my academics. I express my sincere gratitude to Dr. N. S. V. Kameshwara Rao for his guidence and supervision during this work.

I thank the Geotechnical Engineering Laboratory staff members Shri. R. P. Trivedi, Shri. A. K. Srivastava, Shri. Gulab Chand and Shri. Kishan for their timely help.

I will be always indebted to my friends and colleagues Lakshmi, Raghava, Aruna, Mallikarjun, Vivek, Saha, Dipanjan, Nem, Surendra, Srinu, Anil, Kushal, Subhojeet, Venkat, Debu, Aveek, Rajan, Balaji, Kaliprasad, Mohit, Rao ji, Anna, Amit, Chandana, Rohini, Supriya, Kapil, and Krishna for their sincere encouragement for this thesis work and making my stay at IIT Kanpur memorable. My special thanks to all my juniors for a nice pen as a farewell gift, which helped me a lot during write up of this work. My special thanks to Shri. K. Ramu for his immense help and co-operation.

K. V. S. Krishna Prasad

ABSTRACT

The present day solution for proper management of waste is disposal in an engineered landfill. The main component of an engineered landfill is the liner system, which acts as a barrier to the percolating leachate. Generally, a single liner system, with a clay layer and a geomembrane over it or a double liner system with two clay layers and geomembranes, are generally used in most of the present day landfills. As construction of a landfill involves placement of waste and soil as per design specifications over the liner system, tension is induced in the geomembrane because of substantial down-slope shear stresses induced due to the overburden. As most of the geomembranes have limited tensile strength, the tension induced in the geomembrane needs to be estimated as it is a design parameter. An attempt has been made to estimate the tension induced in the liner system. Many factors effect the tension induced. Some of these, like the stress-strain behavior of the geomembrane material, the shear stress-displacement characteristics of the geomembrane-clay interface, settlement of the subgrade, etc. have been included in the analyses. The problem was modeled into a three parameter mathematical model by modeling the clay layer underneath the geomembrane with Winkler springs and Pasternak shear layer.

Results obtained indicate that all the aspects considered have an effect on the tension induced in the geomembrane. In all cases, the maximum tension was mobilised near the anchorage. The normalised tension in all the cases was of the order of 10^{-4} to 10^{-2} and significant variations in normalised tensions was noticed with the geometric parameters of the landfill and the stress-strain parameters of the liner system. The effect of strain softening was phenomenal and so it is essential to consider the actual shear stress-displacement response of the lower interface for a proper estimate of tension. The effect of an initial non-linear stress-strain response of the geomembrane doesn't have a drastic effect on tension. From the analysis of the model of the problem, the observed settlements in the clay liner were high and its contribution to the tension induced needs to be considered.

CONTENTS

List of Figures

List of Tables

CHAPTER 1
INTRODUCTION

In the last two decades, there has been a significant growth in the general awareness towards the environmental aspects in the living habitat. This is primarily because of sharp increase in the production of waste. The harmful hazards of waste could be quite devastating. Therefore proper management of enormous quantities of wastes safely is absolutely essential.

Wastes can be classified into three groups depending on their physical state of existence as solid, liquid or gaseous waste. Liquid wastes are the most difficult to handle as they get mixed with ground water and disappear from sight. Gaseous wastes disperse into the atmosphere while solid wastes are transported and stored in and through the living spaces of a society and have great potential for adversely effecting the quality of the environment. Solid wastes are of three types: (1) Municipal, (2) Industrial and (3) Agricultural. Industrial waste contains many types of chemicals, which are specific to the industry. They may not pose a threat to the environment if they are treated in situ and disposed off safely. Most of the agricultural wastes are non-toxic, harmless and can be reused as manure. The most problematic are the municipal wastes. They generally have a very wide variety of materials, most of which are difficult to treat. At the same time, municipal waste gets collected in such high volumes that treating them would be costly.

One of the major drawbacks with municipal solid wastes is that apart from their potential to damage the environment, they remain highly visible. The remedy for the menace of municipal solid wastes is either reduction at the source and/or containment with proper treatment.

Despite all efforts, the requirement for disposal/storage of the solid waste that cannot be recycled and the residual waste after all types of processing have been undertaken, would remain. Thus, planning for proper disposal of these types of waste becomes essential. The normally adopted practice is disposal on land. But, when waste is stored on land, it becomes a part of the hydrological cycle. During infiltration of water

through waste as well as during runoff of water from the surface of waste, numerous contaminants are removed from the waste and transferred to the adjacent areas as well as to the strata below the waste by the action of percolating water. This action of water has a significant impact on the environment. To minimise the impact of waste on the environment, final disposal is done in an 'Engineered Landfill' which offers an environmentally sustainable methodology for disposal of waste on land.

The term **'engineered landfill'** is used to denote a landfill designed and operated to minimise environmental impact due to the waste. The components of a modern engineering landfill are (Fig. 1):

(a) A liner system at the base and sides of the landfill which prevents migration of leachate or gas to the surrounding soil. Liner material usually comprises of compacted clays and/or geomembranes.

(b) A leachate collection system which collects and extracts leachate from within and from the base of the landfill and then treats the leachate.

(c) A gas control facility which collects and extracts gas from within and from the top of the landfill and then treats it or uses it for energy recovery.

(d) A final cover system which enhances surface drainage, intercepts infiltrating water and supports surface vegetation. The final cover system comprises of multiple layers of soils and/or geomembrane materials.

(e) A surface water drainage system which collects and removes all surface runoff from the landfill site.

(f) An environmental monitoring system which periodically collects and analyses air, surface water, soil-gas and ground water samples around the landfill site.

(g) A closure and post closure plan which lists the steps that must be taken to close and secure a landfill site once the filling operation has been completed and the activities for long-term monitoring and maintenance are completed for the landfill (typically 30 to 50 years).

Landfill Liner System

Landfill liner systems comprise of a combination of leachate drainage and collection layer(s) and barrier layer(s) (Fig.1). A competent liner system should have low

permeability, be robust, durable and resistant to chemical attack, puncture and rupture. A liner system may comprise of a combination of barrier materials such as natural clays, amended soils, flexible geomembranes or combinations, e.g. geosynthetic clay liners. Three types of liner systems are usually adopted. They are:

(1) Single Liner System: Comprises of a single primary barrier overlain by a leachate collection system. A system of this type is used for low vulnerability landfills.

(2) Single Composite Liner System: Comprises of two barriers, made of different materials, placed in intimate contact with each other to provide a beneficial combined effect of both the barriers. Usually a flexible geomembrane is placed over a clay or amended soil barrier. A leachate collection system is placed over the composite barrier.

(3) Double Liner System: Comprises of two single liner systems placed over each other. The top barrier is overlain by a leachate collection system. Beneath the primary barrier, another leachate collection system (often called as leak detection system) is placed followed by the secondary barrier. This type of system offers double safety and is generally preferred for industrial waste fills.

Even though engineered landfills offer a good solution to the nuisance caused by waste, construction of these engineered landfills pose a lot of problem to the present day engineer and to a geotechnical engineer in particular. Considerable effort is required to control the quality of the work. Most of the problems arise from the same component, the liner system. The selection of an appropriate geosynthetic or set of geosynthetics for the liner system and clay for the underlying clay liner as per the prevalent site conditions and to check the quality of work during installation are some of these problems. The design and the construction of a landfill should be comprehensive enough to tackle all varieties of problems that can be expected during the design life of the landfill.

In most landfills that are constructed or being constructed in recent times, geosynthetic liners are normally placed on slopes and anchored at the crest level. Subsequent construction involves placement of soil cover and waste layers up to a certain height based on the design. The load that comes on the geosynthetic results in the application of substantial down-slope shear stresses on the liners. These down-

slope shear stresses induce tension in the geomembrane. Considering the fact that most of the geosynthetics have a limited tensile strength, it becomes highly imperative to predict the tension induced in the geosynthetic liner.

Analyses have been proposed in this thesis to estimate the tension induced in the geosynthetic liner system under various conditions. The procedure adopted and the results achieved are presented herein.

A literature review has been carried out to study the work carried out till date. The review has been presented in Chapter 2. Most of the experimental studies on the geomembrane–clay interface response reveal that in most of the cases, the shear stress–displacement are interrelated through hyperbolic response. This assumption has been considered in the model used to solve the problem. The statement of the problem and the analysis are presented in Chapter 3 and the results obtained are presented and discussed in Chapter 4. Results from experiments also reveal that in a few cases, the geomembrane-clay interface response has strain-softening phenomenon. This assumption has also been covered in Chapter 3 and results obtained presented in Chapter 4. Most of the geosynthetics have an initial nonlinear stress-strain response. This aspect has been covered by considering the geosynthetic stress-strain response to be bilinear. The procedure adopted is presented in Chapter 3 and results obtained presentedd and discussed in Chapter 4. In order to estimate the amount of settlements in the clay liner and the tension induced in the geomembrane because of the settlements, the problem has been modeled by a three – parameter model originally proposed by Madhav and Pooroshasb. The description of the model and the procedure adopted is presented in Chapter 3. Results obtained by modeling the problem are presented in Chapter 4.

Some salient conclusions on the methodology adopted and the results obtained are presented in Chapter 5. The details of derivations involved in the analyses are presented in Appendix A.

CHAPTER 2
REVIEW OF LITERATURE

2.1 Introduction

In the last two decades, pollution of the environment has become an issue of concern for engineers all around the world. Considerable efforts are being made to minimise the quantity of waste generated and to save the environment from the harmful effects of waste. Pollution of land, air and water has become serious and there is a need for proper management of waste. Many solutions have been adopted for a proper management of various types waste. One such solution for handling solid waste is disposal with or without treatment. However, for safe disposal of solid waste, the present day technique is to dispose the wastes in engineered landfills.

The term landfill refers to all the natural or man-made depressions that are used for the purpose of waste disposal. Though natural or man-made depressions have been used for waste disposal for a long time, it would not be proper to say that the wastes have been disposed off safely. In most of the cases, rainwater gets leached with the wastes. The resulting leachate percolates into the strata and finally mixes with the ground water thereby rendering it harmful for usage. In order to check that wastes don't get into the hydrological cycle in the form of leachate, the present day solution is engineered landfills.

Most of the present day engineered landfills have a liner system with geosynthetic clay liners, which act as a barrier to the percolating leachate. Landfill liner systems comprise of a combination of leachate drainage and collection layer(s) and barrier layer(s) (Figure 2.1). A competent liner system should have low permeability, be robust, durable and resistant to chemical attack, puncture and rupture. A liner system may comprise of a combination of barrier materials such as natural clays, amended soils, flexible geomembranes or combinations, e.g. geosynthetic clay liners. Three types of liner systems are usually adopted. They are:

(1) Single Liner System;

(2) Single Composite Liner System;

(3) Double Liner System.

Even though landfills offer one of the best possible solution for management of waste, construction of a landfill has always been a challenging job for all the engineers in general and to a geotechnical engineer in particular. The variety of wastes that are to be handled, selection of a proper site, proper designing of the landfill taking various constraints like the design period, the stability of slopes of the landfill and the variation in various properties of the materials used and in situ conditions often pose as challenges before the designer. As the liner system of a landfill is by far the most important component of a landfill, its assessment is required during the design of the liner system. For a good design of the liner system, one must consider various properties of the materials used in its construction. These include virtually all the properties of clay that are to be used, the hydraulic conductivity of geosynthetics that are to be used, shear stress charecteristics of clay and the geosynthetic – clay interface under various conditions, prevailing field conditions, etc. In a landfill, after the construction of the liner system, subsequent construction involves placement of wastes and soil over the liner system as per the design specifications upto the design height. Because of this overburden material, substantial down slope shear stresses are induced on the top surface of the geomembrane. These shear stresses induce tension in the geomembrane. Though the main purpose of a geomembrane in the liner system is to act as a barrier to the percolating leachate, as most of the geomembranes have a limited tensile capacity, tension induced in the geomembrane has to be considered as an important design parameter.

A review of literature was carried out to study various factors influencing the performance of a liner system in general and to study the methods adopted till date to estimate tension induced in the geomembrane. The review was carried out and presented under the following topics:

(1) Selection of suitable site and construction material;
(2) Hydraulic conductivity and drainage considerations for a liner system;
(3) Shear stress characteristics of clay and the geosynthetic – clay interface;
(4) Tension induced in the geomembrane;
(5) Some aspects that effect the amount of tension induced.

2.2 Selection of Suitable Site and Construction Material

2.2.1 Selection of a Suitable Site

A properly sited and designed secure landfill minimises the adverse impacts on environment. The efficiency of any landfill for solid waste disposal depends upon selection of proper site and there are several issues that have an impact for site selection (Rao, 1997). Broadly, they can be into three categories i.e., environmental, economic and socio-economic. The geological, geotechnical and hydrological considerations fall with in the environmental category.

Rao (1997) proposed a methodology for selection of a suitable site. The process of site selection for waste treatment and disposal involves comparison of different options based on social evaluation of each of them for detailed environmental, social and community impacts. The methodology comprises the following steps:

(1) Selecting criteria for evaluation of sites;
(2) Apportioning a total score of 1000 among the assessment criteria based on their importance;
(3) Developing site sensitivity index (SSIS);
(4) Estimating score for each parameter for various site alternatives using SSIS;
(5) Adding the score for individual site alternatives to rank the alternatives based on total score;
(6) Classification of site, based on total score.

Classification of sites was proposed based on the total score. Details of classification based on total score are as given in Table 2.1. A summary of site ranking and classification based on the proposed methodology for some of the sites in Delhi are as given in Table 2.2.

However it can be concluded that no standardised procedure for selection of a proper site is available and one has to select the best possible alternative by one's own judgment and assessment of the alternatives available.

2.2.2 Selection of Suitable Construction Material

For construction of liner system for an engineered landfill, the materials required are clay with very low permeability and geosynthetics. There are a few other materials required, but a liner system is more or less constructed of these two materials.

2.2.2.1 Selection of Clay

Low permeability compacted clays are used as seepage barriers in liner systems of engineered landfills. In most of the cases, locally available clays are used as liner material for the ease of transportation. But these clays may or may not possess the property of low permeability. In order to make them competent enough to be used as liner material, additives in the form of natural clays or commercially available clays (e.g. Bentonite) may be mixed with local clays to form amended soils, which are a good option for liners. Grain size distribution, plasticity, overburden stress, degree of saturation, compaction and soil structure, clay clods (peds), shrinkage cracking (desiccation), and permeant characteristics, all influence hydraulic conductivity of low permeability soils to varying degree (Datta and Juneja, 1997).

2.2.2.2 Selection of Geosynthetics

Geosynthetics are factory manufactured materials which are typically produced in sheet form and seamed together in field. The main advantage with geosynthetics over other materials is their thinness, light weight, good quality control, ease of installation and general cost effectiveness in comparison to natural soil materials. They also have the characteristics of being very unforgiving in their installation procedures thereby requiring constant vigilance via construction quality control and assurance (Wilson Fahmy and Koerner, 1993).

Almost all types of geosynthetics could be of use in landfills. Figure 2.2 presents a typical view of a sanitary landfill with geosynthetics and Table 2.3 summarises the primary functions that the geosynthetics perform. The main funtions of the geosynthetics installed in a landfill liner system are:

(1) Absorption: The process of fluid being assimilated or incorporated into a geotextile or a bioproduct.

(2) Barrier (to fluid): The ability of a geosynthetic to prevent migration of fluids (both liquids and gasses).

(3) Cushion: The ability of a gesynthetic to control and eventually damp dynamic mechanical actions.

(4) Drainage: The ability to collect and carry off fluids (water, leachate, gases, etc.) within a geosynthetic liner eventually within a biodegradable natural composite drain.

(5) Surficial Erosion Control: the complex function carried out by a geosynthetic or by a bioproduct to prevent ground surface soil particles from detachment and transport.

(6) Filtration: The ability of a geosynthetic to retain soil particles while being crossed by flowing water or leachate.

(7) Interlayer: The ability of a geosynthetic to improve shear resistance between two layers of geosynthetic products and or earth materials. This property is applicable in geocomposite liner systems.

(8) Protection: The ability of a geosynthetic to prevent local damage to a geomembrane due to concentrated mechanical stresses. This property is applicable in geocomposite liner systems.

(9) Reinforcement: The result of stress transfer from soil to geosynthetic.

(10) Seperation: The ability of a geosynthetic or a bioproduct to prevent intermixing of adjacent soil and or fill material.

The most important function in a liner system is that of barrier to the percolating fluids which is performed by a geomembrane (Rao,1997). Thus selection of a suitable geomembrane is the most important aspect.

2.3 Hydraulic Conductivity and Drainage Considerations for a Liner System

The main purpose of construction of a landfill is to prevent toxic leachates from percolating into the strata below and there by contaminating the ground water. The general technique adopted is to isolate the wastes with the help of a impervious barrier there by preventing the percolation of leachates. The function of a barrier is performed by the liner system. Thus, it is very essential for the liner system to be impervious. It is therefore necessary to check for the hydraulic conductivity of the

liner system. If a perfect barrier is provided but with out any drainage facility to the percolating leachates, it would result in pooling of leachates and result in unhygienic condition around the landfill. Thus, for a good design of the landfill, a good design of the drainage system also becomes essential. Leachate is formed when rainwater percolates through wastes and carries some toxic compounds along with it. As waste contains mostly of organic compounds, leachate in most of the cases is an organic compound.

Many tests for hydraulic conductivity of the clay used as a liner material have been reported. Daniel *et al.* (1985) conducted a series of tests on compacted clays using fixed wall permeameter and flexible wall permeameter and compared the results achieved. Bowders and Daniel (1987) have studied the hydraulic conductivity of compacted clays to dilute organic chemicals. These organic chemicals are very similar to the organic chemicals that are generally found in most landfills. Daniel (1989) reported some in-situ tests for hydraulic conductivity of compacted clays. Benson and Daniel (1990) have studied the influence of clods on hydraulic conductivity of compacted clays. Datta and Juneja (1997) have listed some important parameters that effect the hydraulic conductivity of clays. Laboratory tests by permeating organic solvents, acids, alkalis, exchangeable cations and concentrated salt solutions through clays as well as the mechanism of interaction become necessary for the design of the liner system.

According to various investigators, soils with the following specifications would be suitable for construction of a liner system:

Percentage fines $\geq 20 - 30$ %;

Plasticity index $\geq 7 - 10$ %;

Percentage gravel ≤ 30 % and

Maximum particle size: 25 – 50 mm. (Boynton and Daniel, 1985)

It has been noticed that most of the liner systems that have been constructed with compacted clay only perform inadequately because of various reasons. Effects on hydraulic conductivity due to formation of clods, tension cracks, cracks formed because of cyclic drying and wetting result in improper functioning of the liner

system. Moreover, liners formed with compacted clay only have lesser provision for drainage. Thus, most of the present day landfills have liner systems that are a combination of geosynthetics and clayey materials. Some of the other advantages with the use of geosynthetics is that the drainage system could be easily incorporated in a landfill and construction of a landfill needs far lesser manpower.

Considerable work has been reported over the hydraulic conductivity aspects of various geosynthetics and geosynthetic clay liners. Many field tests and laboratory tests for the hydraulic conductivity of geosynthetics and geosynthetic clay liners, under various conditions have been reported. Broadman (1996) reported a few tests to find the hydraulic conductivity of desiccated geosynthetic clay liners. The effect of cyclic drying and wetting on hydraulic conductivity of several geosynthetic clay liners (GCL) was studied and it was found out that drying caused severe cracking in the clay (Bentonite) component of the (GCL). As the GCL was permeated again it has been noticed that the hydraulic conductivity slowly decreased from an initial high value. Figure 2.3 shows the variation in hydraulic conductivity with time for one of the GCLs. The long-term, steady state value of hydraulic conductivity after the wetting and drying cycle was found to be essentially the same as the value for the undessicated GCL. It has been concluded that GCLs possess the ability to self-heal after a cycle of wetting and drying, which is important for applications in which there may be alternative wetting and drying of a hydraulic barrier like the liner system of a landfill.

Field tests have been reported by Eith and Koerner (1997) over the performance of a HDPE (High density polyethylene) geomembrane in a municipal waste landfill liner system after eight years of service. It has been noticed that the performance levels of the geomembrane remained more or less the same and no substantial degradation was noticed. Other field tests reported also show that GCLs perform as a better barrier material. Thus in most of the present day landfills they are preferred as barriers over the conventional clay liners.

2.4 Shear Stress Characteristics of Clay and the Geosynthetic – Clay Interface

GCLs consist of a thin layer of bentonite sandwiched between two geotextiles or mixed with an adhesive and attached to a geomembrane. While most of the GCLs enjoy favorable hydraulic characteristics, they suffer from limitations as a result of low shear strength of hydrated bentonite. A shear failure involving a GCL can occur at three possible locations:

(1) The external interface between the top of the GCL and the overlying material (soil or geosynthetic);

(2) Internally within the GCL and

(3) The external interface between the bottom of the GCL and the underlying material (soil or geosynthetic).

Current engineering practice is to establish appropriate internal and interface shear strength parameters for design using direct shear tests on a 300-mm^2 test specimens and employing traditional limit equilibrium techniques for analyzing slope stability. However, the low shear strength of bentonite, the limited number of laboratory direct shear test results available, the uncertainty over the use of peak versus residual shear strength, the newness of GCLs, the lack of field experience with GCLs all lead to questions about the long-term stability of GCLs on relatively steep slopes.

Daniel *et al.* (1998) report results from fourteen full-scale field test plots containing five different types of GCLs. The types of GCLs used are shown in Figure 2.4. The test plots were constructed on 2H:1V and 3H:1V slopes for the purpose of assessing slope stability. Slides occurred in two of the 2H:1V test plots along the interfaces between textured geomembranes and the woven geotextile component when the GCL unexpectedly became hydrated. All other test plots were stable. It was observed that the results of laboratory direct shear tests compared favorably with field observations, providing support for the current design procedures that engineers are using for assessing the stability of slopes containing GCLs.

Fox *et al.* (1998) investigated the internal shear strength of three GCLs. The GCLs were adhesive-bonded, stitch-bonded or needle-punched. Tests were performed using a large direct shear apparatus capable of measuring peak and residual shear

strengths. For each product, failure occurred at woven geotextile – bentonite interface. It was noticed that the peak shear strength of the needle-punched GCL increased significantly with increasing normal stress because of the frictional connection of the reinforcing fibers. Figure 2.5 shows the shear stress – displacement curves of the GCLs. It was also noticed that the residual shear-strength failure envelope was dependent on the product type. Figure 2.6 shows the failure envelopes corresponding to the peak and residual shear stresses. Each peak shear strength envelope shows modest nonlinearity and is described as a p-order hyperbola with non-orthogonal asymptotes. The general equation proposed is

$$\tau_p = a_\infty + \sigma_n \tan \delta_\infty - \frac{a_\infty - a_o}{\left(1 + \frac{\sigma_n}{\sigma_o}\right)^p} \qquad (2.1)$$

where a_∞, δ_∞, a_0, σ_0 and p are constants. Equation 2.1 characterizes nonlinear variation of shear strength with respect to normal stress.

Mitchell *et al.* (1990) reported on slope failure of Kettleman Hills landfill. The liner properties were responsible for the failure. The slope failure occurred in a 15 acre hazardous waste landfill in which lateral displacements up to 35 feet and vertical displacements up to 14 feet were measured. Failure developed by sliding along interfaces within the composite, multilayered geosynthetic-compacted clay liner system beneath the waste fill. Testing and analyses were done to determine the liner system interface shear-strength characteristics. This included direct shear and pullout testing program on interfaces between various geosynthetics, and between these materials and compacted clay in the liner system. These interfaces were characterized by low friction resistance, with values of friction angle as low as 8 degrees for some combinations. The most critical interface were determined to be those HDPE geomembrane and geotextile, HDPE geomembrane and geonet, and HDPE geomembrane and compacted clay. The variation measured in the strength parameters for different interfaces in the liner system indicate the necessity of conducting similar test programs to establish design parameters. Seed *et al.* (1990) have analysed the stability of the same landfill by the conventional two-dimensional method of a representative cross-section and three-dimensional analyses of the overall wastefill. It

was concluded that the factor of safety at the time of failure was around 0.85 – 1.25. However, this estimate of factor of safety includes the uncertainties in the strength parameters and analyses methods. Table 2.4 lists the measured values of angle of friction, ϕ_r, and shear strength for some of the interfaces. It was also noted that the frictional resistance was effected by various properties, including the degree of polishing, whether the interfaces were wet or dry, and in some cases the relative orientation of the layers to the direction of shear stress application. Variation in properties between one batch to another batch of HDPE liner and geonet materials was also seen. The values of interface friction angle were not significantly influenced by the magnitude of normal stress. In all cases, it was noticed that the minimum ultimate or residual frictional resistance was fully mobilised at very small deformation levels.

Gilbert (1996) conducted direct shear tests to study the shear strength characteristics of reinforced geosynthetic clay liners. It was noticed that the reinforcement increases the peak internal shear strength when compared to that of unreinforced GCLs. However, the reinforced GCL exhibited a post peak reduction in strength with displacement due to failure of reinforcement. Large-displacement shear strengths for the GCLs were about 50% of the peak shear strength. The shear stress – displacement variation for various GCLs is as shown in Figure 2.7. Direct shear tests were conducted to evaluate the interface shear strength between the reinforced GCL and other geosynthetic materials. It was noticed that the peak interface shear strengths between the GCL and a smooth geomembrane or a drainage geocomposite are less than the internal shear strength. However, the peak interface strength between the GCL and a textured geomembrane is limited by a peak internal strength after normal stresses more than 13.8 kPa. Postpeak reduction in strength with displacement occurs for this interface at higher normal stresses due to reinforcement failure. These results are also shown in Figure 2.7. Extrusion of Bentonite at interfaces with GCLs was observed in all of the interface tests. This might have lowered the shear resistance.

Stark *et al.* (1996) reported on shear strength of high density polyethylene (HDPE) geomembrane/geotextile interfaces. Torsional ring shear tests were performed on interfaces comprised of HDPE geomembranes/nonwoven geotextiles

and a drainage composite. Four textured geomembranes with different manufacturing techniques were utilized to investigate the effect of geomembrane texturing on interface shear resistance. In addition, the effects of geotextile fibre type, fabric style, polymer composition, calendering and mass per unit area on textured HDPE geomembrane interface strengths were investigated. The textured HDPE geomembrane/nonwoven geotextile and drainage geocomposite interfaces exhibit a large postpeak strength loss. This strength loss is attributed to pulling out or tearing of filaments from the nonwoven geotextile and orienting them parallel to shear and polishing of the texturing on the geomembrane. At high normal stresses, damage to or removal of the texturing on the geomembrane can cause the strength loss.

Stark and Poeppel (1994) conducted torsional-ring tests to study the interface shear strength of the geosynthetic - clay interface. The results of these show that for a geomembrane – clay interface:

(1) The interface shear strength depends on plasticity and compaction water content of the clay, and the normal stress;

(2) In general, the interface shear strengths measured with the torsional-ring-shear apparatus were in excellent agreement with back-calculated field strengths;

(3) Peak and residual interface failure envelopes, in most of the cases were non-linear, and this non-linearity should be modeled in stability analysis instead of the conventional method wherein the failure envelope is modeled as a combination of cohesion and friction angle.

(4) It was noticed that in virtually all cases, the interface has undergone strain softening after peak shear stress. The residual shear stress was around 60% of the peak shear stress.

One can conclude that for proper shear stress considerations, all the geosynthetic materials and clay that are to be used have to be tested for shear stress - displacement characteristics. The most important aspect is to study the shear strength of various possible interfaces and in particular the clay and the geosynthetic-clay interface. The most critical section of a clay-geosynthetic interface is the portion of the interface that can be seen in the anchor trenches of a liner system.

Anchor trenches are used at the top of side-slope liners to hold installed geosynthetics in place against the applied loads and to prevent potential tears caused by wind intrusion beneath the geosynthetics. As shown in Figure 2.8, anchor trenches can generally be classified as flat, rectangular or V-shaped. Selection of the appropriate anchor trench depends on the required holding capacity, access considerations, dimensional constraints and available construction equipment.

The holding capacity of anchor trenches is developed by the applied normal load of the soil placed above the geosynthetics, which creates frictional resistance between the geosynthetics and the underlying soil. There is minimal frictional resistance developed between the upper soil and the geosynthetic since the soil above the geosynthetic is likely to move with the geosynthetic. The soil depth, type of soil or other material underlying the geosynthetic and the geosynthetic anchorage length are therefore the key factors in developing the required anchor trench holding capacity (Sharma and Lewis, 1994).

Though there is no ideal solution available for rectangular and V-shaped trenches, however it is quite easy to analyze a flat anchor. The free body diagram and the development of equation 2.2 is shown in Figure 2.9.

$$L = \frac{T\cos\beta - T\sin\beta\tan\delta_l}{\gamma\, d\tan\delta_l} \qquad (2.2)$$

where

T is the tensile force in the geomembrane;

β is the slope angle;

δ_l is the interface friction angle;

d is the depth of cover soil;

γ is the unit weight of cover soil and

L is the run out length of geomembrane in the anchor trench (Koerner, 1990).

An anchor trench should be designed to resist pull out loads caused by applied loading in the form of overburden soil and waste and self weight of geosynthetics. In cases wherein the geomembrane may be exposed to severe temperatures and wind loads, stresses caused by these forces should also be considered. Ideally an anchor should be designed to pull out slightly rather than causing tearing of geosynthetics. Thus, the

maximum holding capacity of an anchor trench should be slightly less than the ultimate tensile strength of geosynthetic to be anchored, irrespective of the applied loads. If the applied loads are higher than the tensile strength of the geosynthetic, measures must be taken to reduce the applied loads or the replace geosynthetic with a geosynthetic of higher tensile strength. Figures 2.10. and 2.11 show typical values required anchorage force required for slope with 9° and 12° interface friction angles respectively (Sharma and Lewis, 1994). It can be noted from these figures that the required anchorage force increases linearly with the slope height.

2.5 Tension Induced in the Geomembrane

Construction of a present day engineered landfill involves placement of geomembrane liners on slopes. These geomembrane liners are generally anchored at the crest level for support. Subsequent construction process involves placement of waste and soil in layers as per design specifications up to the design height. This overburden material results in substantial down-slope shear stresses on the liner system leading to development of significant liner tension. Most of the geomembranes have limited tensile strength. Though the main function of a liner system is containment of waste, cases of wide width tension failures of the underlying geomembrane were reported (Sharma and Lewis, 1994). A tension failure in the geomembrane would be in the form of rupture in the geomembrane. This results in percolation of leachate through the rupture thereby nullifying the very purpose behind the construction of a liner system in particular and a landfill in general. It follows that for proper functioning of a liner system, one must consider tension induced in the geomembrane of a liner system as a design parameter and it becomes imperative to estimate the tension induced.

Work carried out to date on this problem involves predominantly the employment of three approaches; namely, the limit equilibrium method as in slope stability analysis (Koerner and Hwu, 1991); the load-displacement analysis such as the finite element method (Wilson-Fahmy and Koerner, 1993) and a simplified analysis which takes into account the essential stress-strain/displacement compatibility of the slope materials (Kodikara, 1996).

Koerner and Hwu (1991) analysed the problem of tension induced in a geomembrane considering the stability of cover soil and waste placed above the liner system. The shear stresses from the cover soil above the liner act downward on the underlying geomembrane and in doing so mobilise upward shear stresses beneath the geomembrane from the underlying soil. The situation is as shown in Figure 2.12. In order to study the effect of the response of geomembrane to tension, three different scenarios have been envisioned. They are:

(1) If $\tau_U = \tau_L$, no tension is induced in the geomembrane.

(2) If $\tau_U < \tau_L$, no tension is induced in the geomembrane.

(3) If $\tau_U > \tau_L$, the geomembrane goes into a state of pure shear equal to τ_L and the balance of $\tau_U - \tau_L$ must be carried by the geomembrane in tension.

where τ_U and τ_L are the shear stresses acting on the upper and lower interfaces of the geomembrane respectively.

The latter case was considered for the design process. The situation generally occurs when a material with high interface friction (like sand or gravel) is placed above the geomembrane and a material with low interface friction (like clay with high moisture content) is placed beneath the geomembrane. The essential equation for design is given by

$$T/W = [(c_{aU} - c_{aL}) + \gamma H \cos\omega (\tan\delta_U - \tan\delta_L)]L \qquad (2.3)$$

where c_{aU} and c_{aL} are the adhesion between the geomembrane and clay at the upper and lower interfaces of the geomembrane respectively;

γ is the unit weight of the overburden material;

H is the height of the overburden material;

δ_U and δ_L are the interface friction angles at the upper and lower interfaces of the geomembrane;

L is the length of the landfill and

T/W is the tension induced per unit width of the geomembrane.

For the purpose of design, the resulting value of T/W was compared to the allowable strength of the geomembrane which is shown schematically for different geomembranes in Figure 2.13.

In this approach, the slope system is assumed to be at the verge of failure and tension was computed considering the equilibrium of mobilised forces. However, this method ignores the stress-strain laws and the stress-strain behavior of the geomembrane and the clay – geomembrane interface. This system is not suitable for estimating tension induced in case of stable slopes and is not suited for analysis of stable slopes under normal working conditions.

Load – displacement analysis was also adopted for analysis of the problem. Wilson-Fahmy and Koerner (1993) proposed a finite element analysis for the stability of cover soil on liner systems with geomembranes. This method is more general and rigorous over the previous method analysis. However, it would require detailed parametric representation of the slope and materials. Because of the relative newness of geosynthetics and as very few field and laboratory test results are available, application of this method becomes difficult. Moreover, the method is time consuming as it requires a detailed parametric representation.

Kodikara (1996) presented a simple analysis for estimating tension induced in the geomembrane of a liner system. The method considers the stress-strain considerations and the force equilibrium of a small element of the geomembrane as shown in Figure 2.14. For evaluating shear stress on the top surface of the geomembrane, the principle of Mohr's circle was adopted. For evaluation of shear stress on the lower surface, the shear – displacement response of the geomembrane clay interface was assumed to be elastic – ideally plastic as shown in Figure 2.15. As shown in Figure 2.15, the interface characteristics are defined by shear stiffness, k_s, of the clay liner and a limiting shear stress based on Mohr-Coulomb strength parameters (c_l and ϕ_l). The resulting equations were then solved for various ranges of non-dimensional parameters and design charts shown in Figure 2.16 were developed.

The solutions however ignore a few aspects that can be noticed through various laboratory and field tests. The shear stress – displacement response curve for a geomembrane – clay interface is close to a hyperbola in most of the cases. Some of the interfaces show strain softening also (Figure 2.13). Thus the assumption of elastic

– ideally plastic interface response needs to be modified. However, the method is simple and is applicable to both stable and unstable slopes.

2.6 Some Aspects that effect the Amount of Tension Induced

Even though an ideal geosynthetic liner system is the best barrier material for landfills, it is hard to have one in practice. Almost all landfill liner systems suffer with one or more problems. Problems may arise because of many factors like poor workmanship, improper design and construction material, malfunctioning of construction material, etc. These problems lead to some undesirable results, which effect the general functioning of a landfill. Formation of cavity, extrusion of clay into the geomembrane – clay interface thereby resulting in reduction of shear resistance of the interface, small holes in geomembrane due to tearing due to concentrated forces when it is laid upon uneven ground are a few factors that may lead to some undesirable results.

Not much work has been done till date in order to study the effects of all these factors on the tension induced in a geosynthetic clay liner. LaGatta *et al.* (1997) have reported on the effect of differential settlement on the hydraulic conductivity of geosynthetic clay liners. It has been noted that differential settlement induced tensile cracks in almost all clay liners. This resulted in seepage of leachate through the cracks thereby detoriating the liner system. As reported by Broadman (1996), extrusion of bentonite into the interface between two geosynthetics resulted in reduction of the interface shear resistance. This can have an effect on tension induced in the liner system as lesser amount of shear will be mobilised either at the top or the bottom interface. Thus, to estimate the tension accurately, it becomes imperative to take care of some of these aspects and to take these aspects into consideration while designing a liner system for a landfill.

Most of the laboratory and field tests reveal that some geosynthetic – clay interfaces undergo strain softening when subjected to shear stresses (Fig. 2.9). Under these conditions, the tension induced in the geomembrane would be quite different. Thus, it becomes essential to consider this aspect while estimating tension induced in the geomembrane.

For an accurate estimate of tension induced in the geomembrane, it is essential to consider the stress – strain behavior of the geomembrane. Koerner *et al.* (1990) conducted three-dimensional, axi-symmentric tension tests on various geomembranes. The method adopted involves geomembrane being placed and supported in a large pressure vessel and hydrostatically stressed until failure occurs. The center point deflection is monitored during test, thus providing the deflection readings to go along with the pressure readings. The stress – strain data was generated from the pressure – deflection data. The test results show that in most of the cases, the stress – strain behavior is non-linear. The results are shown in Figure 2.17. Thus, it is essential to consider this behavior for proper estimation of tension. These test results also show a marked contrast from one-dimensional tensile tests on geomembranes. Tests on geotextiles also reveal a non-linear stress strain relationship with the modulus of deformation increasing gradually up to a certain peak value. Once the peak value is attained, the modulus of deformation stays fairly constant. The reason for the same could be that in case of a geotextile, at low strain levels the fibers in the geotextile align themselves in the direction of strain. This results in lesser values of modulus of deformation. Once the fibers are aligned in the direction of strain, the geotextile takes more stress even for small increments in strain. Thus, it shows higher values of modulus of deformation after a certain strain level (Sharma and Lewis, 1994).

Wilson-Fahmy *et al.* (1993) conducted confined and unconfined wide width tension tests on geosynthetics. It was concluded that the applied normal stress remains insignificant in most of the cases and has no or very less effect on the stress-strain behavior of geosynthetics. However, in the case of non-woven geotextiles and needle punched non-woven geotextiles, the normal stress had some effect on the stress-strain behavior. Thus it becomes imperative to include the effect of normal stress on tension induced in a geosynthetic clay liner (GCL), particularly if the GCL has a non-woven geotextile and or a needle punched geotextile as its component(s).

Giroud (1994) proposed a mathematical model to describe the stress-strain curves of geomembranes that exhibit a yield peak in a uniaxial tensile test. The model consists of an n-order parabola, with the exponent, n, constant or variable as a function of the strain and it has been calibrated with the results of uniaxial tensile tests. For more precision, an n-order parabola with a variable exponent was suggested.

The proposed equation is given by

$$\sigma = \sigma_Y \left[1 - \left(1 - \frac{\varepsilon}{\varepsilon_Y} \right)^n \right] \tag{2.4}$$

where n is a dimensionless exponent greater than unity,

σ is the stress in the geomembrane corresponding to a given strain level, ε and

σ_Y and ε_Y are respectively the yield stress and strain for the geomembrane.

If the stress, σ_Y, and strain, ε_Y, at yield and the initial modulus, E_o, are known the exponent n can be obtained by

$$n = \varepsilon_Y E_o / \sigma_Y \tag{2.5}$$

Another factor that may effect the amount of tension induced in the geomembrane is the temparature at the time of construction of a liner system. If the geomembrane is exposed to high temparatures, it expands and wrinkles thereby loosing contact with the clay lying underneath. At the same time, if the geomembrane is exposed to low temparatures, then, it shrinks. When the cover soil is placed over a shrunk geomembrane, it restrains the geomembrane from expanding when the geomembrane is exposed to high temparatures. This results in induction of internal stresses. These stresses may count when a geomembrane fails in tension. In order to avoid any undesired effects of such kind, the normal practice is to construct a liner system early in the morning when there is enough light and the temparatures are within tolerable limits (Sharma and Lewis, 1994).

As all these aspects effect the tension induced in the geomembrane in one or other way, it becomes necessary to consider them and their effects for an accurate estimate of the amount of tension induced in the geomembrane. The present work takes a few of these factors into consideration and notes their effect on the liner system.

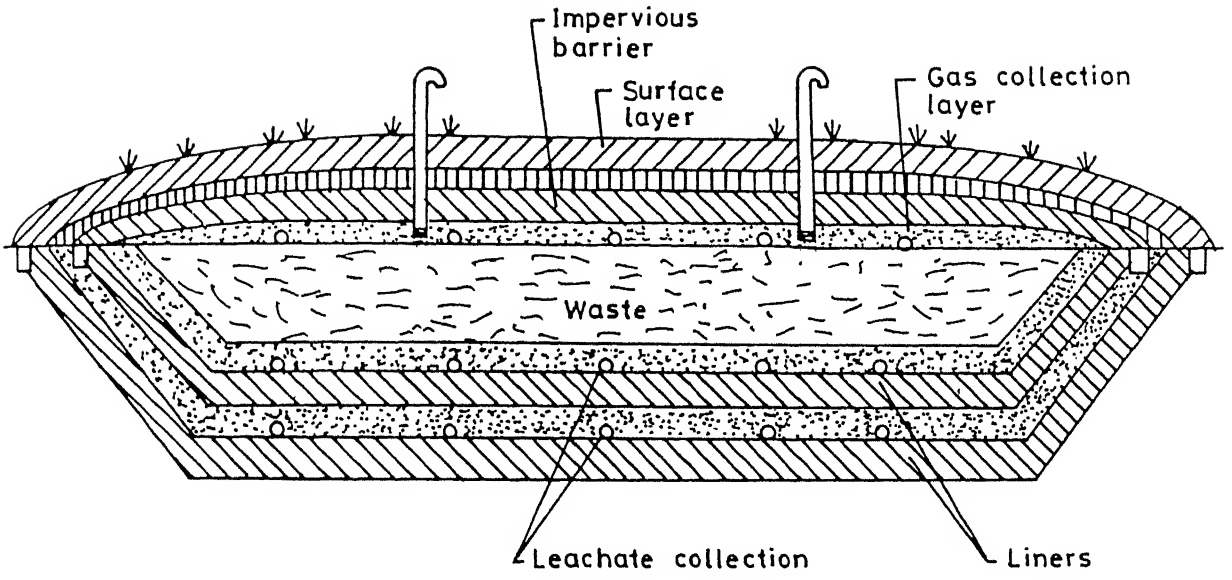

Figure 2.1: Typical Cross-section of an Engineered Landfill

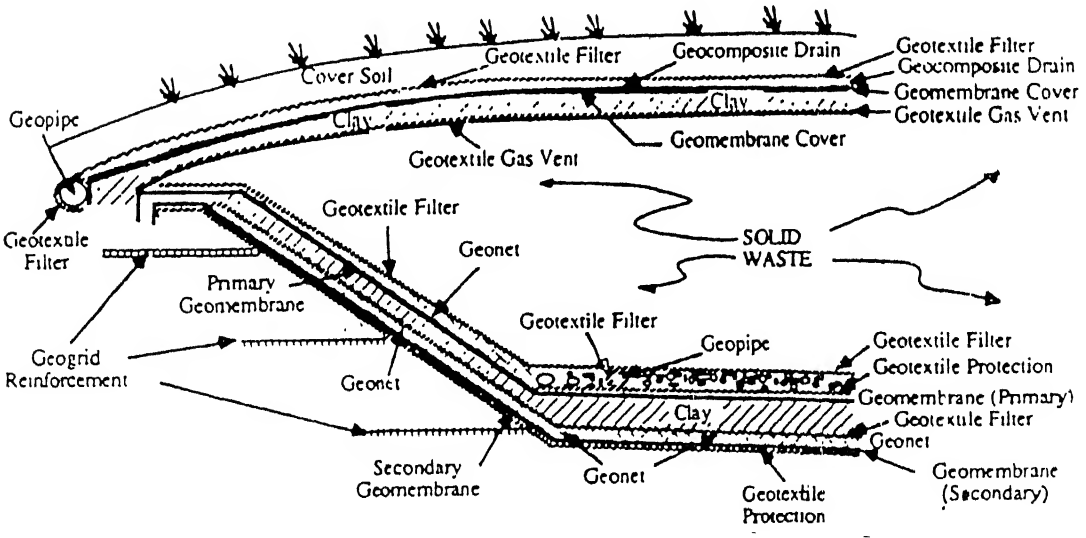

Figure 2.2: Application of Geosynthetics in Landfills

CLASS	OVERALL SCORE	GENERALIZED LEVEL OF SITE
I	800-1000	V.Poor
II	600-800	Poor
III	400-600	Fair
IV	200-400	Good
V	0-200	V.Good

Table 2.1: Details of Site Classification based on Total Score (after Rao)

SITE	RANKING SCORE OBTAINED	CLASS	MEANING OF CLASS
A. MUNICIPAL PRESENT			
1. Ghazipur	426	III	Fair
2. Hastal	548	III	Fair
3. Mandawali	425	III	Fair
4. Bhalwa dairy	403	III	Fair
5. Crossing of GT Karnal and Outer Ring Road	398	IV	Good
6. Rohini PH-III	534	III	Fair
7. Okhla PH-I	533	III	Fair
B. MUNICIPAL PAST			
1. Ring road	472	III	Fair
2. Timarpur	525	III	Fair
3. Tilak Nagar	516	III	Fair
4. Chhatarpur	421	III	Fair
5. Bharaon Road	572	III	Fair
6. SGT Nagar	525	III	Fair
7. I.P. Depot	473	III	Fair
8. Gopalpur	564	III	Fair
9. Sunder Nagri	525	III	Fair
10.Tughlakabad Ext	491	III	Fair
11.Haiderpur	477	III	Fair
C. MUNICIPAL FUTURE			
1. Jaitpur/ Tajpur	543	III	Fair
2. Bhatti Mines	470	III	Fair
3. Mandi Village	470	III	Fair
D. HAZARDOUS FUTURE			
1. Badarpur	497	III	Fair
2. Surajkund Border	429	III	Fair
3. Tughlakabad	472	III	Fair
4. Shakarpur	508	III	Fair

Table 2.2: Proposed Methodology for some Sites in Delhi (after Rao)

Type of GS	Primary Function				
	Separate	Reinforce	Filter	Drain	Barrier
GM					✓
GT	✓	✓	✓	✓	
GN				✓	
GP				✓	
GC				✓	
GG		✓			

Table2.3: Functions of Geosynthetics in Landfills (after Rao)

Interface (1)	Shear Strength τ_r or Residual Angle of Friction, ϕ_r	
	Dry condition (2)	Wet condition (3)
HDPE liner/geotextile	$\phi_r \approx 9° \pm 1°$	$\phi_r \approx 8° \pm 1°$
HDPE liner/geonet	$\phi_r \approx 8.5° \pm 1°$	$\phi_r \approx 8.5° \pm 1°$
HDPE liner/clay	—[a]	$\tau_r \approx 900$ psf ± 250 psf
Geotextile/geonet	$\phi_r > 20°$	$\phi_r > 12°$
Geotextile/clay	—[a]	$\phi_r \approx 24°$

[a]Not available.

Table 2.4: Angle of Friction and Shear Strength between Geosynthetics (after Seed *et al.*)

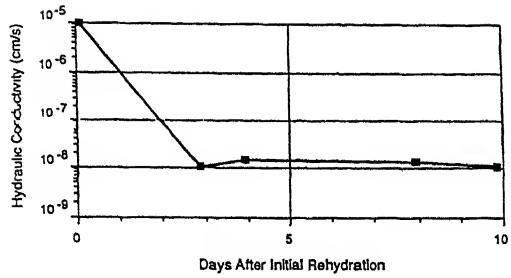

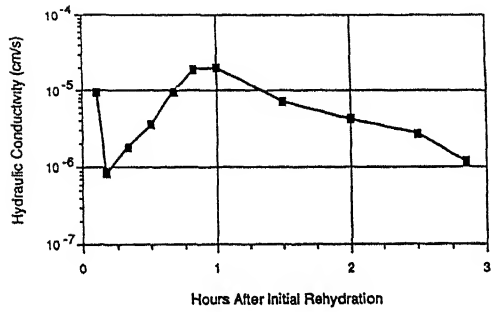

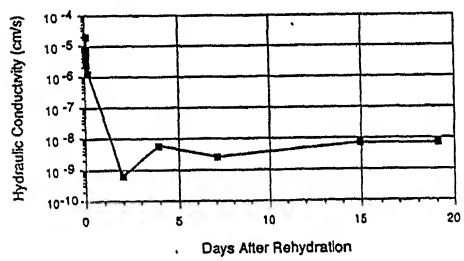

Figure 2.3: Variation of Long-Term Hydraulic Conductivity with Time (after Broadman)

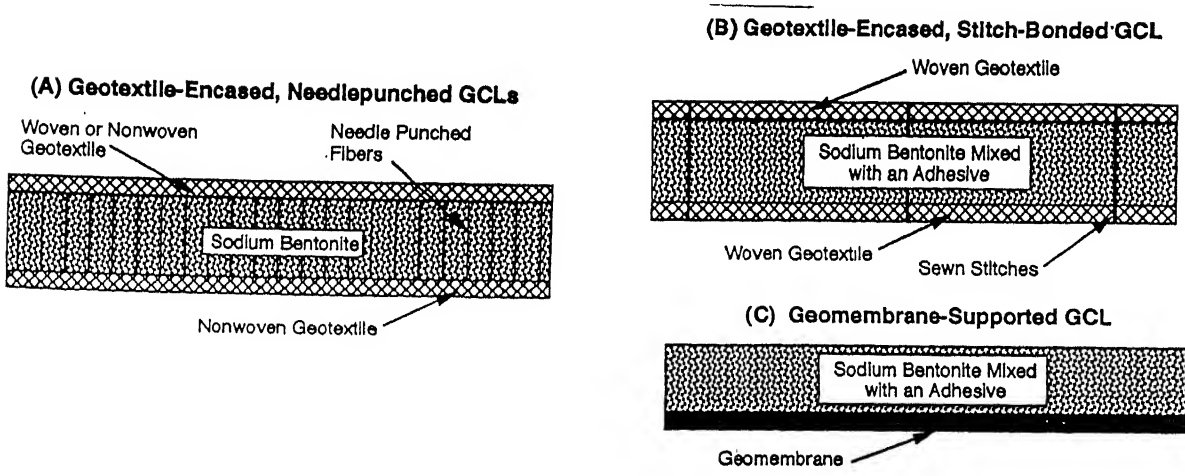

Figure 2.4: Typical Cross-sections of GCLs (after Daniel *et al.*)

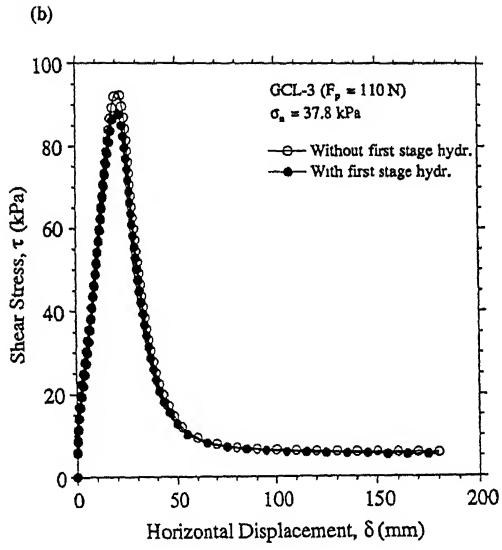

Figure 2.5: Shear Stress-Displacement Curves for GCL Interfaces (after Fox *et al.*)

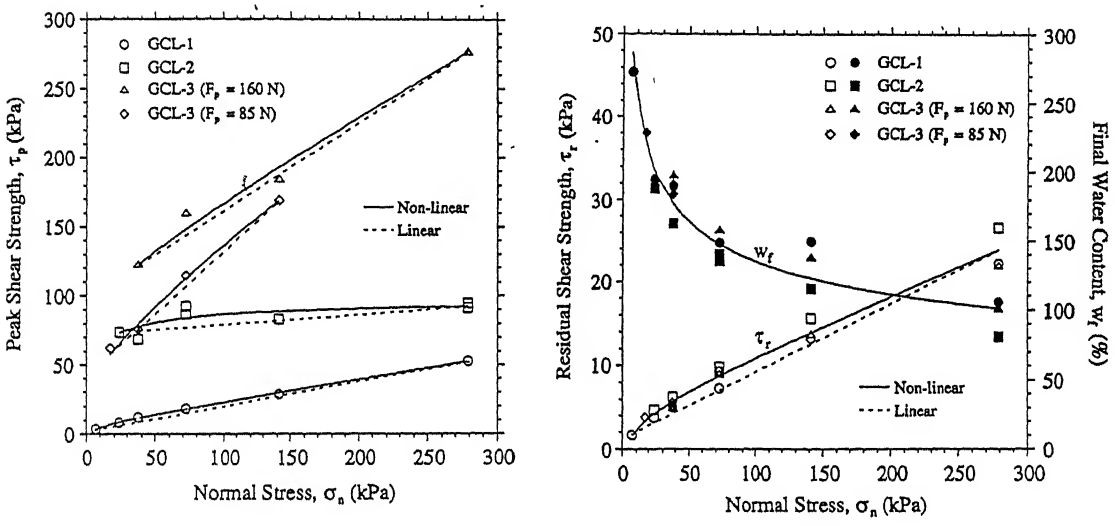

Figure 2.6: Failure Envelopes for GCLs (after Fox *et al.*)

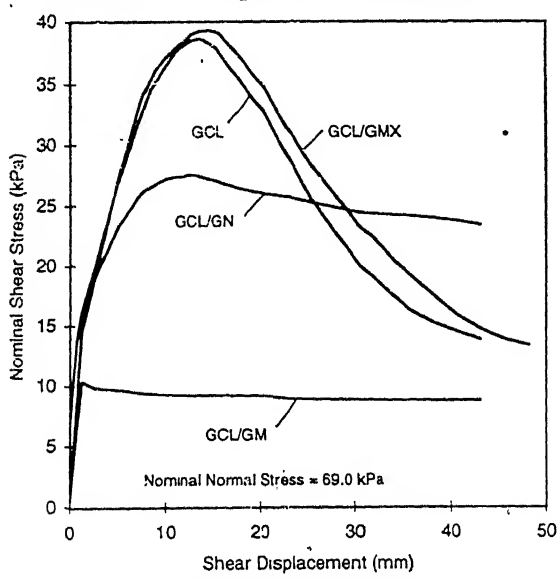

Figure 2.7: Shear Stress-Displacement Profile for GCLs (after Gilbert)

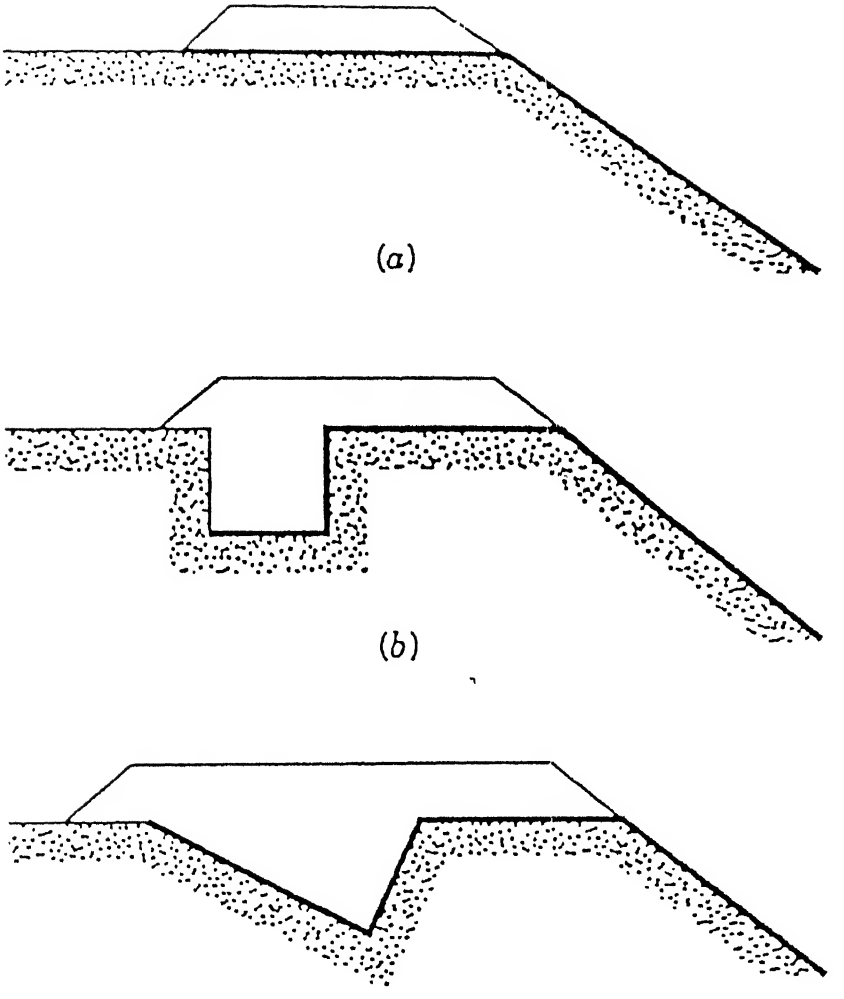

Figure 2.8: Various Types of Anchor Trenches (after Sharma and Lewis)

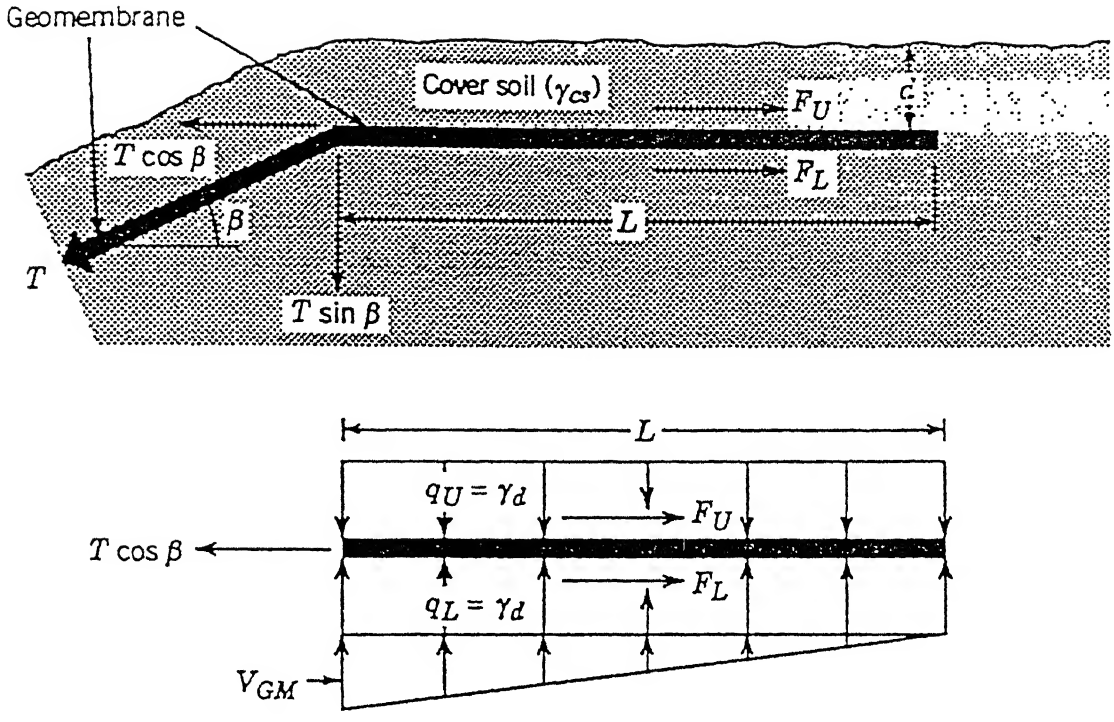

$F_U = q_U \tan \delta_U (L)$ (neglected since cover soil moves with geomembrane)

$$F_L = q_L + 0.5\, v_{GM} \tan \delta_L (L)$$

$$= \left[q_U + 0.5 \left(\frac{2\, T \sin \beta}{L} \right) \right] \tan \delta_L (L)$$

$$T \cos \beta = q_L \tan \delta_L (L) + T \sin \beta \tan \delta_L$$

$$L = \frac{T \cos \beta - T \sin \beta \tan \delta_L}{\gamma_d \tan \delta_L}$$

Figure 2.9: Evaluation of Holding Capacity of Anchors (after Sharma and Lewis)

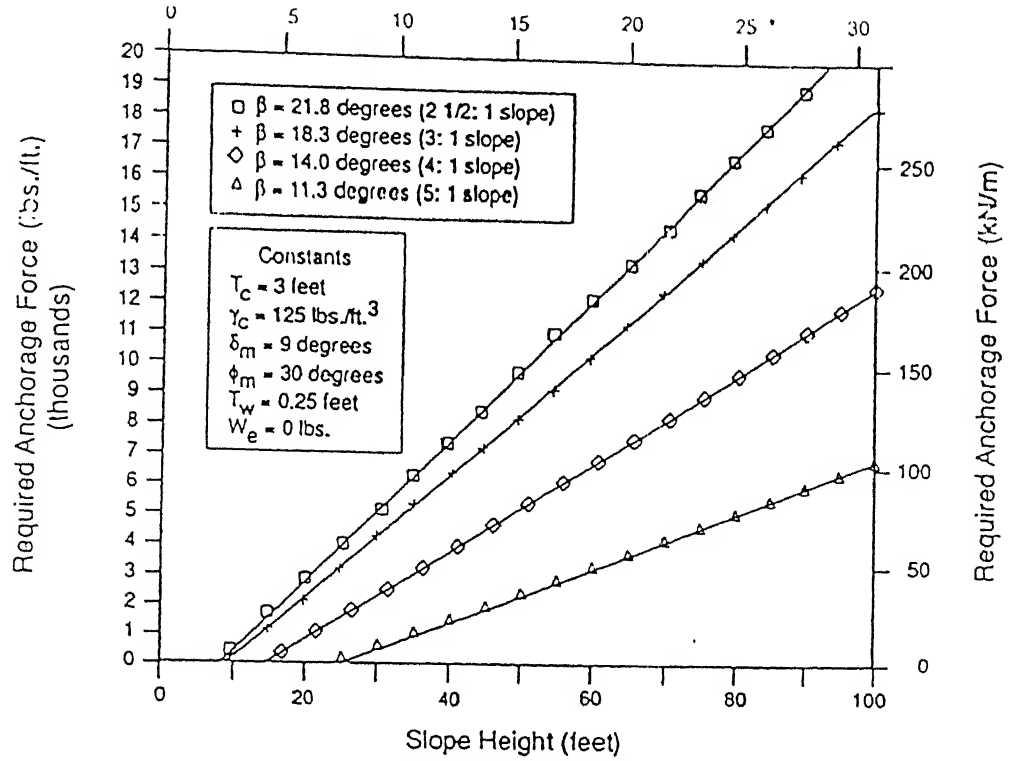

Figure 2.10: Required Anchorage Force for Slopes with 9° Inclination

(after Sharma and Lewis)

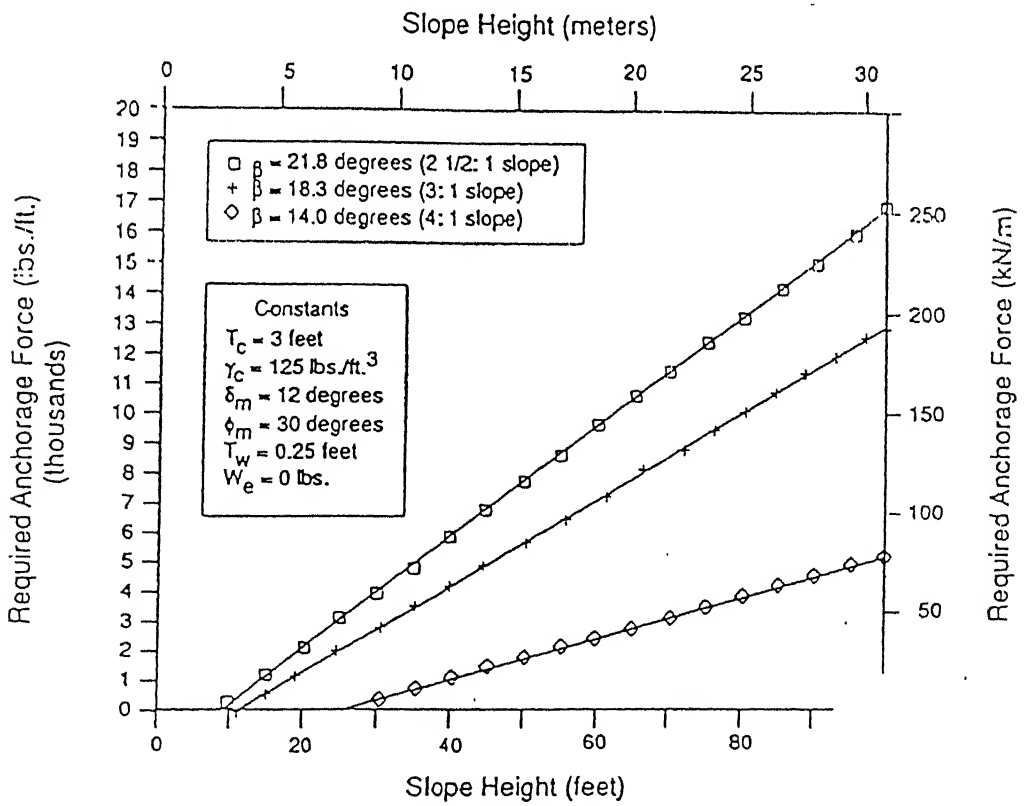

Figure 2.11: Required Anchorage Force for Slopes with 12° Inclination

(after Sharma and Lewis)

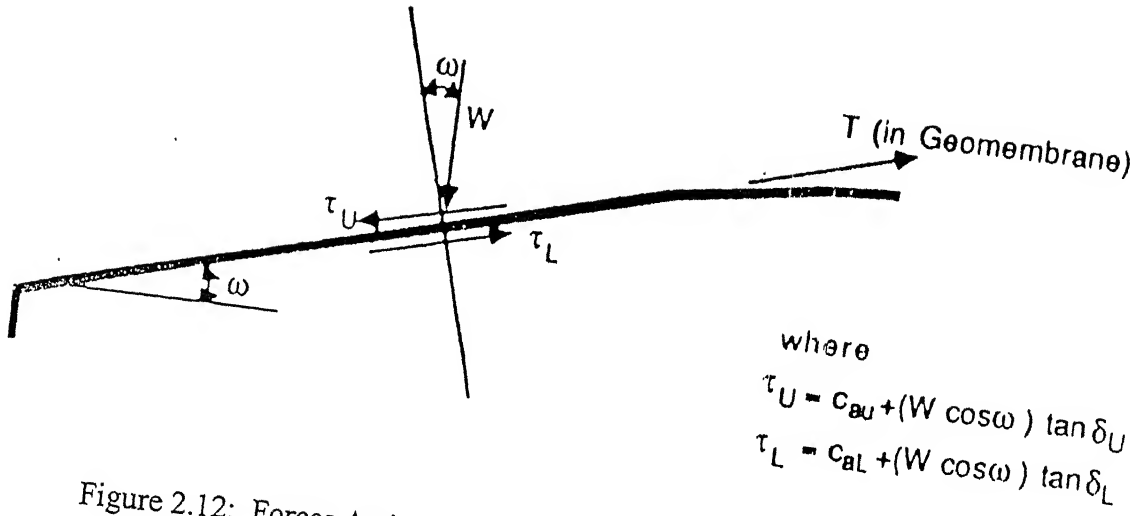

Figure 2.12: Forces Acting on the Geomembrane (after Koerner and Hwu)

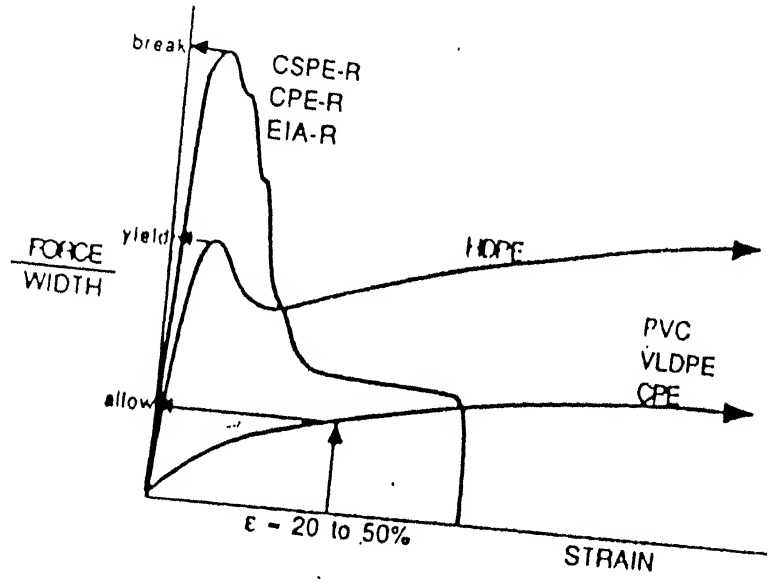

Figure 2.13: Tensile Behaviour of Various Geomembranes (after Koerner and Hwu)

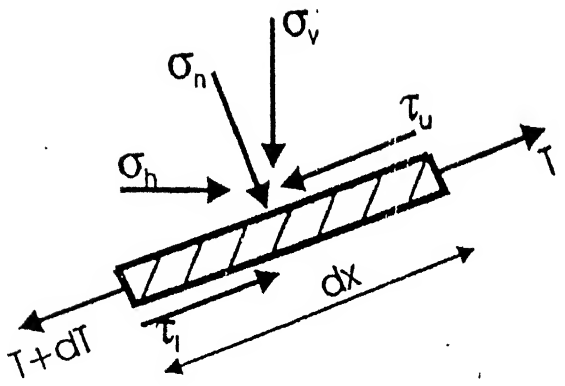

Figure 2.14: Equilibrium of a Small Element (after Kodikara)

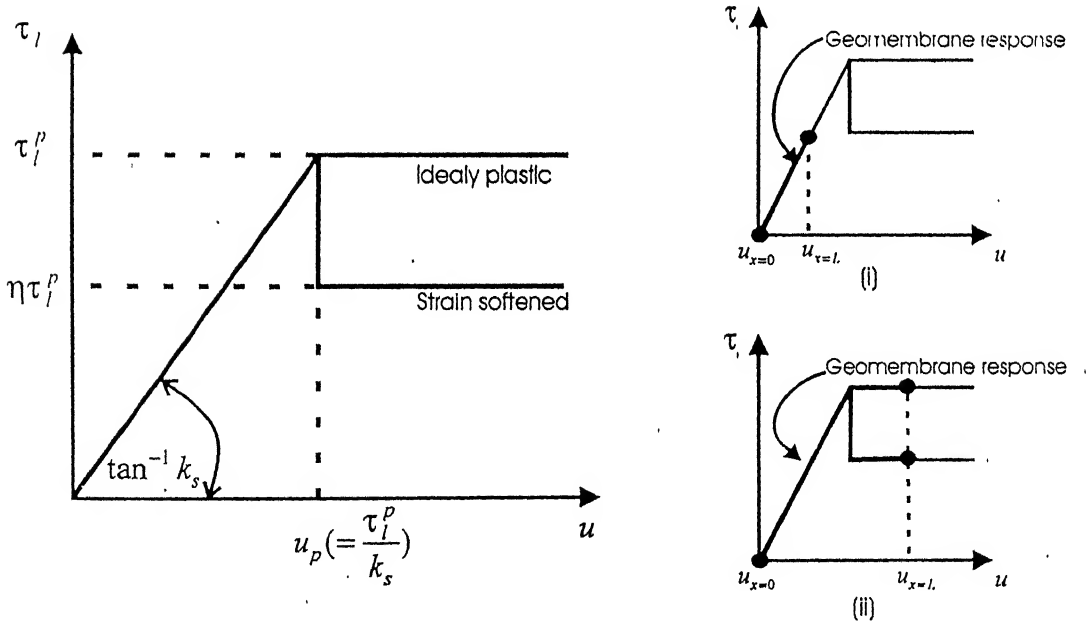

Figure 2.15: Assumed Shear Stress-Displacement Interface Response (after Kodikara)

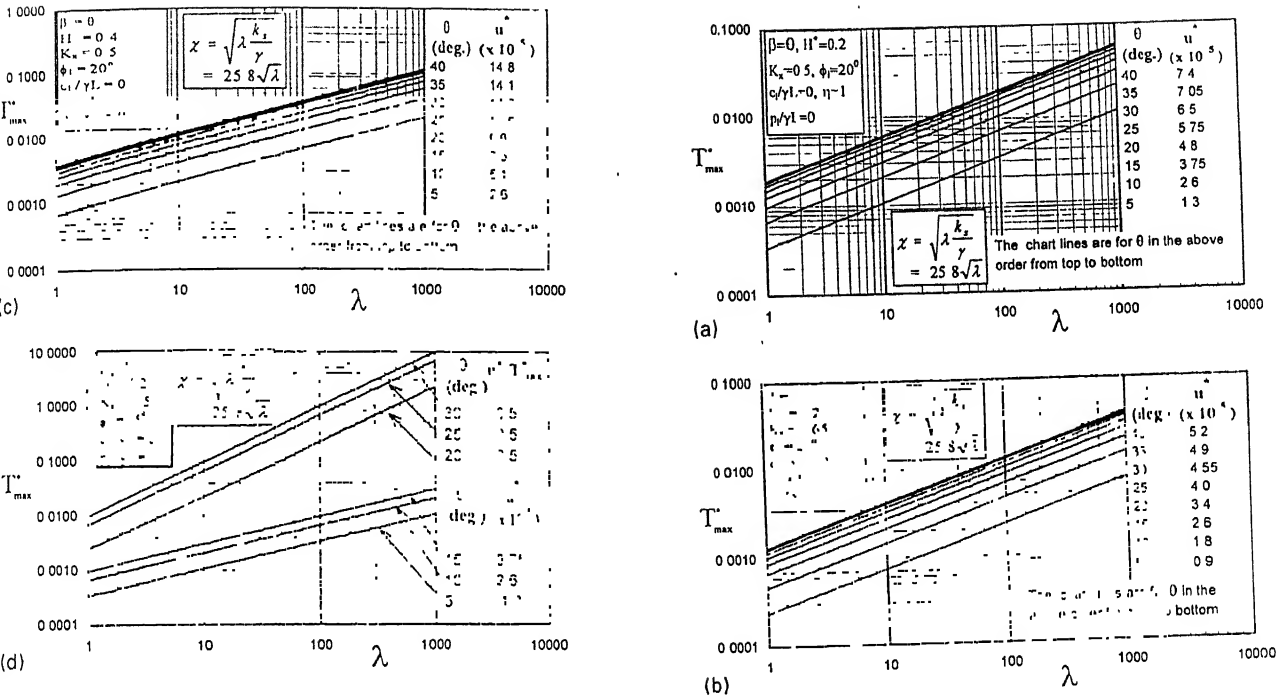

Figure 2.16: Design Charts for Evaluation of Tension (after Kodikara)

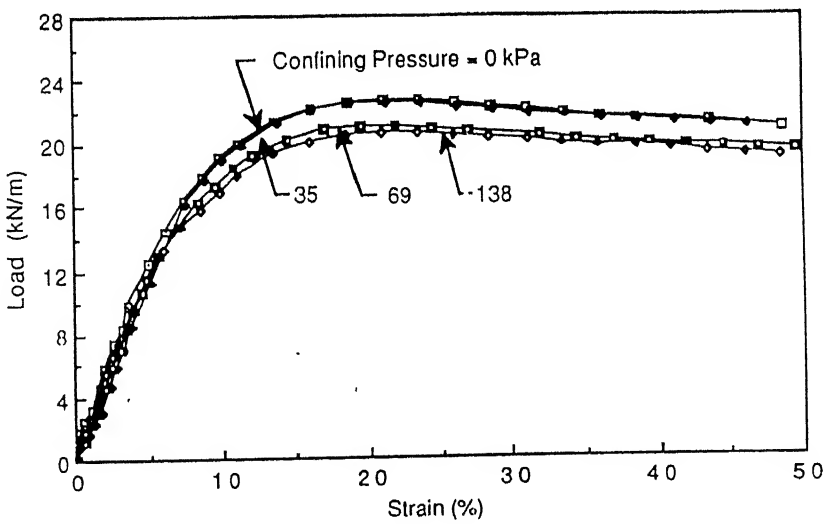

Figure 2.17: Stress-Strain Response for Geomembranes (after Koerner)

CHAPTER 3

STATEMENT OF THE PROBLEM

3.1 Introduction

In most of the present day landfills, liner systems with geomembranes are adopted. Since the landfills generally involve filling of a natural or man-made depression, liners are provided at the sides and bases of the landfills to form an effective barrier to migration of leachate and foul gases. This work focuses on the geomembranes placed on side slopes with anchorage at the crest level. The common practice is to construct compacted clay liners on the slopes of natural ground and then place the geomembrane liners on the surface. Subsequent construction of landfill includes placement of soil cover and waste layers up to the design height. Because of the soil and waste material that are placed on these liners, tension is induced in these liners due to shear stresses from the overlying overburden and waste material. As the geosynthetics have limited tensile capacity, the tension that they are being subjected to must be predicted accurately.

As discussed in Chapter 2, there are various factors that may effect the tension induced in the geomembrane and should be considered while predicting tension. Attempt has been made to include the effects of all these factors like the stress-strain behavior of the geosynthetics, the geosynthetic – clay interface, etc. The problem of estimating the tension induced by assuming a hyperbolic shear stress-displacement response for the geosynthetic-clay interface has been discussed in section 3.2 and the same problem with the strain softening phenomenon of the geosynthetic-clay interface has been discussed in section 3.3. The assumption of a bilinear stress-strain behavior of the geosynthetics and the effect of this assumption on the tension induced has been taken up in section 3.4. In order to study the variation of tension with settlements in the clay liner, an attempt has been made to model the problem using a three parameter mathematical model. The problem and the methodology adopted are discussed in Section 3.5.

3.2 Estimation of Tension with Hyperbolic Shear-Displacement Response at the Geosynthetic-Clay Interface

3.2.1 Statement of the Problem

Landfill slopes may be formed in several benches with berms providing anchorage for individual geomemebrane lining segments used for these benches. Subsequent construction procedure involves filling in stages, successively covering each bench. In this process, the weight of the overburden materials above a particular geomembrane liner is transferred to the underlying clay base through the interfaces of various layers (such as waste, soil, geomembranes etc.) and lastly through the geomembrane-clay interface. This results in substantial down slope shear being applied on the upper interface of the geomembrane. This down slope shear results in tension being induced in the geomembrane. For the sake of simplicity in the analysis, a single material representing all the overburden materials above the geomembrane and an idealised model featuring a single bench situation is considered as shown in Figure 3.2.1.

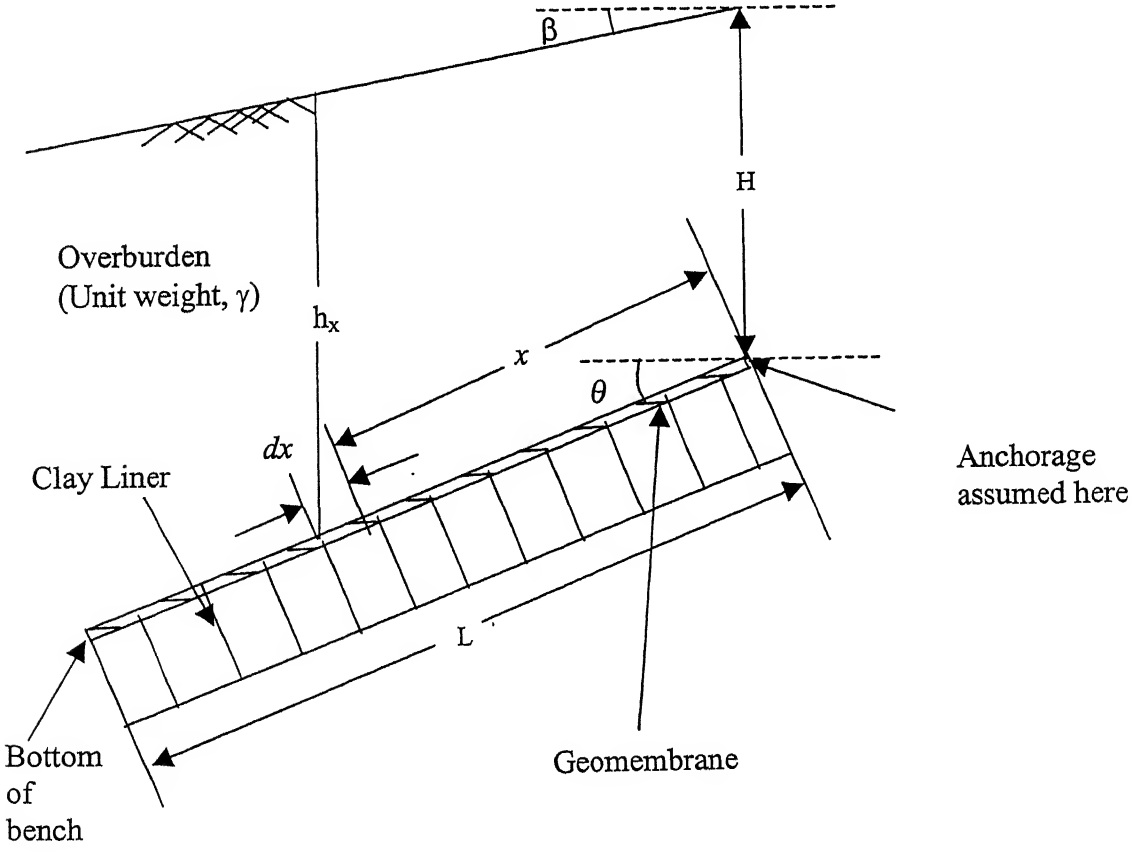

Figure 3.2.

In the above figure,

L is the total length of the geomembrane,

H is the height of overburden near the anchorage,

θ and β are the angles of inclination of the geomembrane and top of the landfill with the horizontal respectively,

γ is the unit weight of the overburden and

u is the displacement of geomembrane at a point distance x from anchorage.

As the amount of tension induced in the geomembrane depends mainly on the shear stresses at the upper and lower interfaces, it is essential to study the shear stress characteristics of the geomembrane-clay interface. It has been assumed that the slip takes place at the lower interface of the geomembrane. As discussed in Chapter 2, most of the geomembrane-clay interfaces have a hyperbolic shear stress-displacement response. The shear stress-displacement response at the lower interface has been assumed to be a hyperbola (Figure 3.2.2) with an initial slope of k_τ, of the shear stress, τ, versus displacement, u, curve and τ_l^P is the maximum shear stress.

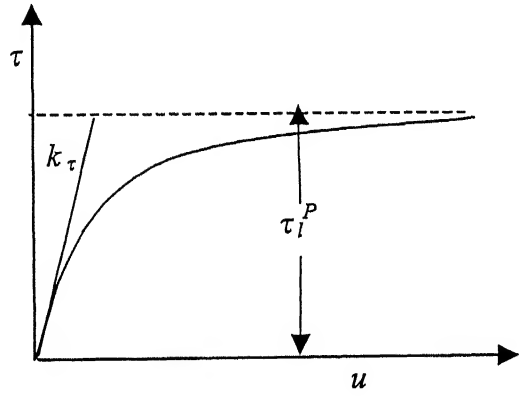

Figure 3.2.2: Hyperbolic Interface Response in Present Study

The assumed curve is defined by the following equation:

$$\tau_l = \frac{k_\tau u}{1 + \frac{k_\tau}{\tau_l^P} u} \qquad (3.2.1)$$

where k_τ is initial slope and

τ_l^P is the maximum shear stress.

τ_l^P is given by

$$\tau_l^P = (\sigma_n - p_l)\tan\delta_l + c_{al} \qquad (3.2.2)$$

where p_l is the pore water pressure at the lower interface,

δ_l is the angle of intrinsic friction at the lower interface and

c_{al} is the adhesion between the geomembrane and clay at the interface.

While it has been assumed that the slip takes place at the lower interface, the shear stress at the upper interface has been evaluated by the principle of Mohr's circle.

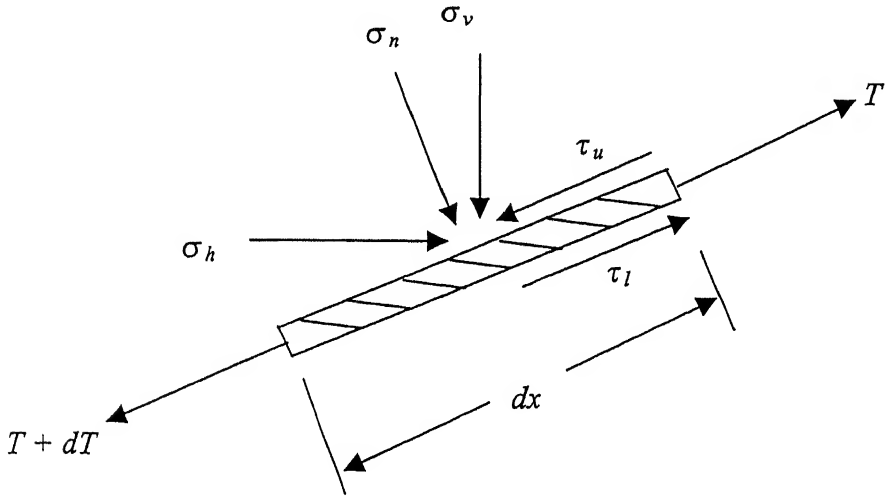

Figure 3.2.3: Equilibrium of an Infinitesimal Element

Considering the force equilibrium of a small element of the geomembrane (Figure 3.2.3), and analysing it, one obtains the governing equation for the problem.

$$\frac{d^2u}{dx^2} - \frac{1}{tE}\left[\frac{k_\tau u}{1+\dfrac{k_\tau u}{(\sigma_n - p_l)\tan\delta_l + c_{al}}}\right] = -\frac{1}{tE}\left[\frac{1}{2}(1-K_x)(H + x\sin\theta - x\cos\theta\tan\beta)\times\gamma\times\sin 2\theta\right] \qquad (3.2.3)$$

where

u is the displacement of the geomembrane at a distance x from the anchorage,

t is the thickness of the geomembrane,

E is the modulus of deformation of the geomembrane,

k_τ is the initial slope of the shear stress-displacement curve,

σ_n is the normal stress acting on the geomembrane at a distance x from the anchorage,

c_{al} is the adhesion between the geomembrane and clay at the lower interface,

δ_l is the angle of wall friction at the lower interface,

p_l is the pore water pressure at the lower interface,

K_x is the coefficient of subgrade modulus for the waste material,

θ and β are the angles of inclination of the liner system and the top of the landfill (Figure 3.2.1),

H is the height of overburden at the anchorage and

γ is the unit weight of the overburden material.

The derivation of equation 3.2.3 has been presented in Appendix – A1. The non-dimensional form of equation 3.2.3 is 3.2.4, which has been solved by the Finite Difference Technique to obtain displacement and tension at various points.

$$\frac{d^2U}{dx^{*2}} - \chi^2 \left[\frac{U}{1 + \frac{\chi^2 U / \lambda}{\left[\left(f(X, H^*) - P_l \right) \tan \delta_l + C_l \right]}} \right] = -\lambda \left[\frac{1}{2} (1 - K_x) \sin 2\theta \left[H^* + X \sin\theta - X \cos\theta \tan\beta \right] \right] \tag{3.2.4}$$

where,

$$\chi = \sqrt{k_\tau L^2 / tE},\ \lambda = \gamma L^2 / tE,\ H^* = H/L,\ C_l = c_{al}/\gamma L,\ P_l = p_l/\gamma L,\ X = x/L,\ U = u/L$$

and $f(X, H^*) = [K_x \cos^2\theta + \sin^2\theta][H^* + X \sin\theta - X \cos\theta \tan\beta]\gamma$

The boundary conditions are:

(i) at $x = 0$, $u = 0$ (no displacement); and

(ii) at $x = L$, $T = 0$ (no tension).

3.2.3 Method of Solution

To obtain displacements and tension at various points, equation 3.2.4 has been solved using the Finite Difference Method. Firstly the number of elements, n, into which the liner was discretised for the numerical procedure, was varied from 10 to 100. No further increase in accuracy was achieved for n values greater than 100. Hence, n equal to 100 was adopted for further analysis.

A parametric study is carried out for the following ranges of parameters:
Unit weight of overburden material, γ, varies from 12 to 18 kN/m^3,
Adhesion between the geomembrane and clay, c_a, varies from 0 to 20 kPa,
Pore water pressure at the interface, p_l, varies from 0 to 20 kPa,
Angle of wall friction between the geomembrane and clay, δ_1, varies from 10° to 25°,
Angle of inclination of the geomembrane with the horizontal, θ, varies from 5° to 30°,
Angle of inclination of the top of the landfill with the horizontal, β, varies from –20° to 30°,
Height of overburden near the anchorage, H, varies from 0 to 10 m,
Length of the geomembrane, L, varies from 1 to 100 m,
Thickness of the geomembrane, t, varies from 0.5 to 5 mm,
Modulus of deformation of the geomembrane, E, varies from 100 to 500 MPa,
Coefficient of lateral earth pressure, K_x, varies from 0.3 to 0.6 and
Initial slope of the interface response, k_τ, varies from 10^3 to 10^5 KPa.

The ranges of the non-dimensional parameters were calculated from the ranges of the parameters as given above. To validate the solutions obtained by the present approach, the results for one set of non-dimensional parameters (χ = 183; λ =.50; H^* = 0.2; $\theta = \beta = \phi_1 = 30°$; $C_a = 0$; $P_1 = 0$ and $K_x = 0.5$) are compared with those of Kodikara (1996) and verified to be in good agreement (Appendix B). To study the effect of various parameters, the non-dimensional parameters were varied within the feasible range of parameters. The results achieved have been presented and discussed in Chapter 4.

3.3 Estimation of Tension – Effect of Strain Softening in the Geomembrane-Clay Interface

3.3.1 Statement of the Problem

As discussed in Chapter 2, some geomembrane-clay interfaces undergo strain softening. The interfaces attain shear stress for a given displacement and undergo strain softening if the horizontal displacement is further increased. The response curve

in these cases is as shown in Figure 3.3.1. In general, the residual shear stresses are around 60% of the peak shear stresses.

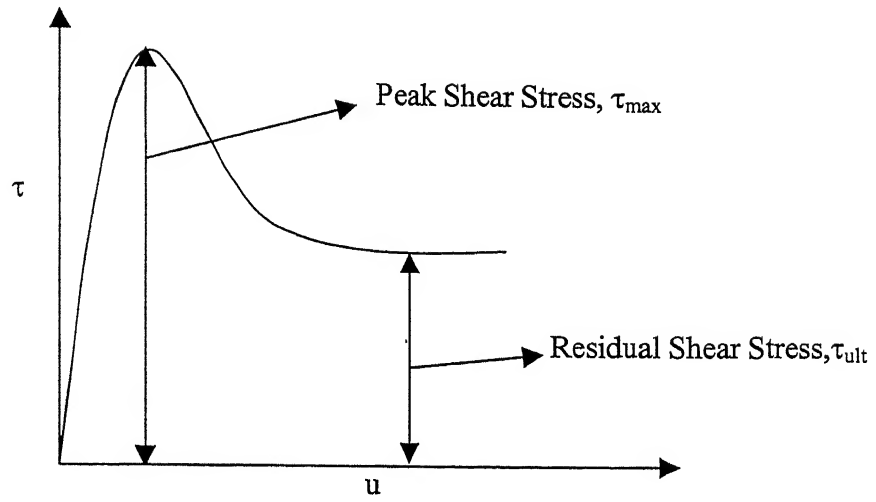

Figure 3.3.1: Shear Stress-Displacement Curve for Strain Softening Case

As the tension induced in a geomembrane depends mainly on the shear stress induced at the top and the bottom interfaces, it would be entirely different if geomembrane-clay interface undergoes strain softening. In order to study the effect of strain softening on the tension induced, the shear stress-displacement response at the lower interface has been assumed as shown in Figure 3.3.2. As shown in the figure, the response curve is assumed to be represented by three straight lines.

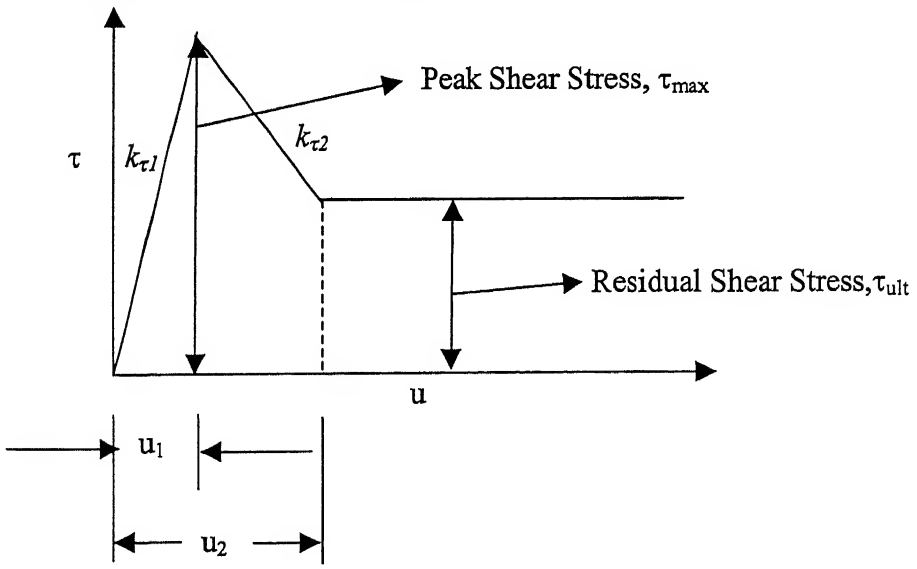

Figure 3.3.2: Assumed Shear Stress-Displacement Curve for Strain Softening Case

In the assumed shear stress-displacement profile, the shear stress linearly increases from 0 to peak shear stress, τ_{max} for $0 < u < u_1$, where u_1 is the displacement corresponding to peak shear stress, τ_{max}; the shear stress linearly decreases from peak shear stress, τ_{max} to residual shear stress, τ_{ult} for $u_1 < u < u_2$, where u_2 is the displacement corresponding to the point where the residual shear stress is mobilised; the shear stress remains unchanged and is equal to residual shear stress, τ_{ult} for $u > u_2$. The assumed response is defined by the following equations:

$$\begin{aligned} \tau_l &= k_{\tau 1} u \quad \text{if} \quad u \le u_1 \\ \tau_l &= k_{\tau 1} u_1 - k_{\tau 2}(u - u_1) \quad \text{if} \quad u_1 < u \le u_2 \\ \tau_l &= \tau_{ult} \quad \text{if} \quad u > u_2 \end{aligned} \tag{3.3.1}$$

where

τ_l is the shear stress acting on the lower interface,

u is the displacement at the lower interface,

u_1 and u_2 are displacements respectively corresponding to the peak shear stress and the point where the residual shear stress is mobilised,

$k_{\tau 1}$ and $k_{\tau 2}$ are the slope of the assumed shear stress-displacement response for $u < u_1$ and $u_1 < u < u_2$ respectively, and

τ_{ult} is the residual shear stress.

Similar to the previous case, the slip is assumed to take place at the lower interface. The shear stress at the upper interface of the geomembrane has been evaluated as before. Considering the equilibrium of a small element as shown in Figure 3.2.3, one gets the governing equation of the problem which is given by

$$\frac{d^2u}{dx^2} = \frac{1}{tE}\left[k_{\tau 1} u - \left[\tfrac{1}{2}(1 - k_x)(H + x\sin\theta - x\cos\theta\tan\beta)\times\gamma\times\sin 2\theta\right]\right] \quad \text{for} \quad u < u_1$$

$$\frac{d^2u}{dx^2} = \frac{1}{tE}\left[\begin{array}{l}(k_{\tau 1} u_1 - k_{\tau 2}(u - u_1)) \\ -\left(\tfrac{1}{2}(1 - k_x)(H + x\sin\theta - x\cos\theta\tan\beta)\times\gamma\times\sin 2\theta\right)\end{array}\right] \quad \text{for} \quad u_1 < u < u_2$$

$$\frac{d^2u}{dx^2} = \frac{1}{tE}\left[\tau_{ult} - \left[\tfrac{1}{2}(1 - k_x)(H + x\sin\theta - x\cos\theta\tan\beta)\times\gamma\times\sin 2\theta\right]\right] \quad \text{for} \quad u > u_2$$

(3.3.2)

where

t is the thickness of the geomembrane,

E is the modulus of deformation of the geomembrane,

k_x is the coefficient if lateral earth pressure,

H is the height of the overburden at the anchorage,

θ and β are angles of inclination of the geomembrane and the top of the landfill respectively,

γ is the unit weight of the overburden material.

Details of derivation of the above equation are given in Appendix A2.

The non-dimensional form of equations 3.3.2 are given by

$$\frac{d^2U}{dX^2} = \left[\chi_1^2 U - \frac{\lambda}{2}\left[(1-k_x)(H^* + X^*\sin\theta - X^*\cos\theta\tan\beta)\times\sin 2\theta\right]\right] \quad if \quad u < u_1$$

$$\frac{d^2U}{dX^2} = \left[\chi_1^2 U_1 - \chi_2^2(U-U_1)\right] - \left[\tfrac{1}{2}\times\lambda(1-k_x)(H^* + X^*\sin\theta - X^*\cos\theta\tan\beta)\times\sin 2\theta\right] \quad if \quad u_1 < u < u_2$$

$$\frac{d^2U}{dX^2} = \lambda\left[\begin{array}{l}\left((\sigma_n^* - p_l^*)\tan\delta_l + C_l\right) \\ \quad -\tfrac{1}{2}(1-k_x)(H^* + X^*\sin\theta - X^*\cos\theta\tan\beta)\times\sin 2\theta\end{array}\right] \quad if \quad u > u_2 \qquad (3.3.3)$$

where

$$\chi_1 = \sqrt{k_{\tau 1}L^2/tE},\ \chi_2 = \sqrt{k_{\tau 2}L^2/tE},\ \lambda = \gamma L^2/tE,\ H^* = H/L,\ C_l = c_{al}/\gamma L,\ P_l = p_l/\gamma L,$$

$$X = x/L,\ U = u/L$$

χ_1, χ_2, λ, H^*, C_l, P_l, X and U are non-dimensional parameters as defined above.

The boundary conditions that are:

(iii) at $x = 0$, $u = 0$ (no displacement); and

(iv) at $x = L$, $T = 0$ (no tension).

3.3.2 Method of Solution

The solutions were obtained by solving equation 3.3.3 using the Finite Difference Method. Desired accuracy was achieved by dividing the geomembrane into 100 elements. For achieving the solutions, one needs to know the values of

displacement at various points. This becomes necessary because the governing equation changes depending on displacements at various points. For calculating the initial displacements, the strain-displacement response is assumed to be hyperbolic. Once the displacements were calculated, appropriate equation was applied depending on the values of displacements. The equations and the conditions of their application are given by equation 3.3.3. To validate the results, solutions were obtained for a given set of parameters and by taking a very high value of u_1, so that the shear stress-displacement response remains within elastic limits. The results were compared with those of the previous method and were found to be in good agreement. The effect of strain softening is signified mainly by three parameters. Results were obtained by varying these three parameters within feasible ranges. The results are presented and discussed in Chapter 4.

3.4 Estimation of Tension – Effect of Bi-linear Stress-Strain Behavior of the Geomembrane

3.4.1 Statement of the Problem

Tension induced at various points in a geomembrane is a function of the strain level at those points. As the tension induced depends on the stress-strain characteristics of the geosynthetic, it is essential to study the stress-strain characteristics of various geosynthetics and to include these aspects in the analyses. As discussed in Chapter 2, most of the geosynthetics have a non-linear stress-strain response as shown in Figure 3.4.1. As shown in the figure, the stress-strain response is initially non-linear but tends to be linear after a certain strain level, ε_o. The reason for this could be that in most of the geosynthetics that are subjected to tensile strains, at low strain levels the fibers which are slack, align themselves in the direction of strain resulting in low values of modulus of deformation at low strain levels. However, after all the fibers in the geosynthetic are aligned in the direction of strain, the modulus of deformation increases and remains constant. In most of the analyses presented till date over the problem of estimating tension, the stress-strain response has been assumed to be linear from zero strain (shown by discontinuous line in Figure 3.4.1)

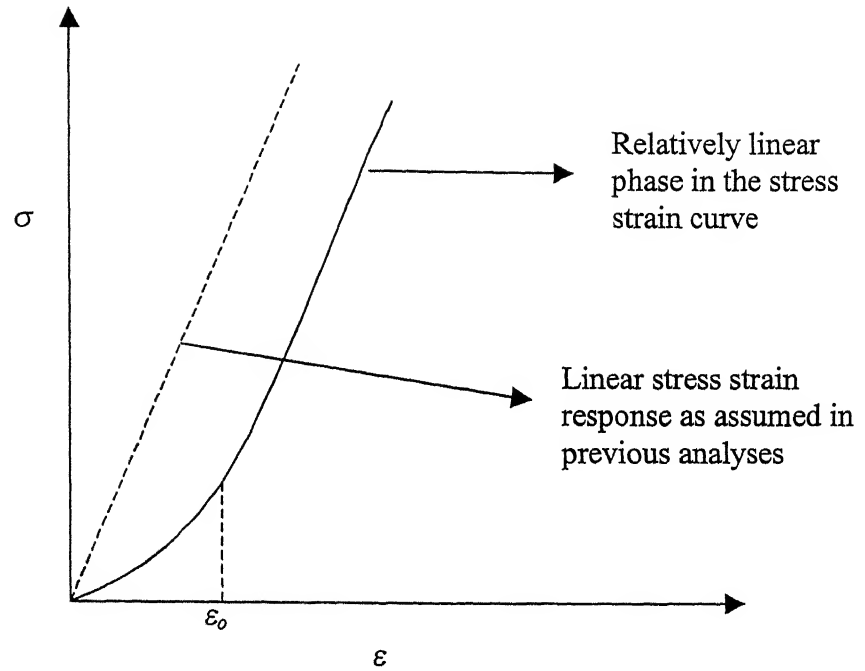

Figure 3.4.1: Stress-Strain Characteristics of Geosynthetics

To study the influence of non-linear stress-strain characteristics of geosynthetics on the amount of tension induced in the geomembrane, the stress-strain curve has been assumed to be bilinear as shown in Figure 3.4.2

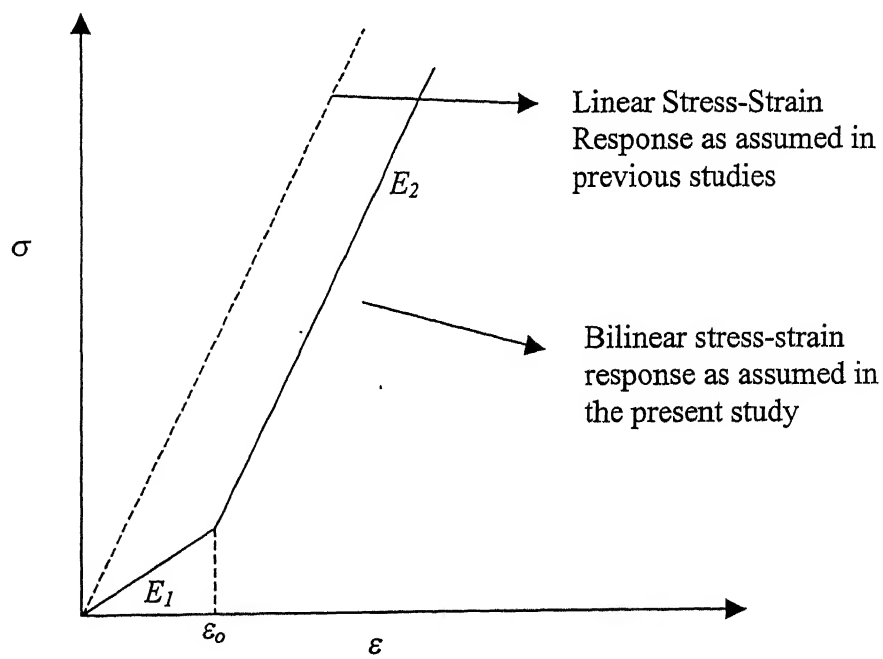

Figure 3.4.2: Assumed Stress-Strain Characteristics of the Geosynthetic

In the above Figure,

σ and ε are respectively the tensile stress and strain in the geosynthetic,

ε_o is the strain at which the modulus of deformation of the geosynthetic has a transition,

E_1 and E_2 are the modulus of deformation for $\varepsilon < \varepsilon_o$ and $\varepsilon \geq \varepsilon_o$ respectively.

The assumed stress-strain characteristic response is represented by the following equations:

$$\begin{aligned} \sigma &= E_1 \varepsilon \quad if \quad \varepsilon < \varepsilon_o \\ \sigma &= \sigma_1 + E_2(\varepsilon - \varepsilon_o) \quad if \quad \varepsilon > \varepsilon_o \end{aligned} \tag{3.4.1}$$

where

σ and ε are the tensile stress and strain in the geosynthetic respectively,

σ_1 ($= E_1 \varepsilon_0$) is the stress corresponding to the strain level at the transition, and

E_1 and E_2 are the modulus of deformation for $\varepsilon < \varepsilon_o$ and $\varepsilon \geq \varepsilon_o$ respectively.

The tensile stress, σ and strain, ε at any point in a geomembrane are given by

$$\sigma = \frac{T}{t} \; and \; \varepsilon = \frac{du}{dx} \tag{3.4.2}$$

where

T is the tension induced in the geomembrane per unit width at any point at a distance x from the anchorage,

t is the thickness of the geomembrane and

u is the displacement at that point.

Considering the equilibrium of a small element of length dx as shown in Figure 3.2.3, the governing equations of the problem are is given by

$$\frac{d^2u}{dx^2} - \frac{1}{tE_2}\left[\frac{k_\tau u}{1 + \dfrac{k_\tau u}{(\sigma_n - p_l)\tan\delta_l + c_{al}}}\right] = -\frac{1}{tE_2}\left[\frac{1}{2}(1 - K_x)(H + x\sin\theta - x\cos\theta\tan\beta) \times \gamma \times \sin 2\theta\right] \; for \; \varepsilon > \varepsilon_o$$

$$\frac{d^2u}{dx^2} - M_R \frac{1}{tE}\left[\frac{k_\tau u}{1+\dfrac{k_\tau u}{(\sigma_n - p_l)\tan\delta_l + c_{al}}}\right]$$
$$= -M_R \frac{1}{tE_2}\left[\frac{1}{2}(1-K_x)(H + x\sin\theta - x\cos\theta\tan\beta)\times\gamma\times\sin 2\theta\right] \quad for\ \varepsilon < \varepsilon_o \tag{3.4.3}$$

where

$$M_R = \frac{E_2}{E_1}$$

The details of the derivation of the above equation are given in Appendix A3.

The non-dimensional form of the above equations are

$$\frac{d^2U}{dx^{*2}} - \chi^2\left[\frac{U}{\chi^2 U/\lambda + \left[(f(X,H^*) - P_l)\tan\delta_l + C_l\right]}\right]$$
$$= -\lambda\left[\frac{1}{2}(1-K_x)\sin 2\theta\left[H^* + X\sin\theta - X\cos\theta\tan\beta\right]\right] \quad if\ \varepsilon > \varepsilon_o$$

$$\frac{d^2U}{dx^{*2}} - M_R\chi^2\left[\frac{U}{\chi^2 U/\lambda + \left[(f(X,H^*) - P_l)\tan\delta_l + C_l\right]}\right]$$
$$= -M_R\lambda\left[\frac{1}{2}(1-K_x)\sin 2\theta\left[H^* + X\sin\theta - X\cos\theta\tan\beta\right]\right] \quad if\ \varepsilon < \varepsilon_o \tag{3.4.4}$$

where

χ, λ, H^*, C_l, P_l, X and U are non-dimensional parameters defined as

$$\chi = \sqrt{k_\tau L^2/tE},\ \lambda = \gamma L^2/tE,\ H^* = H/L,\ C_l = c_{al}/\gamma L,\ P_l = P_l/\gamma L,\ X = x/L,\ U = u/L$$

and $f(X, H^*) = [K_x\cos^2\theta + \sin^2\theta][H^* + X\sin\theta - X\cos\theta\tan\beta]\gamma$.

The boundary conditions are:

(v) at $x = 0$, $u = 0$ (no displacement); and

(vi) at $x = L$, $T = 0$ (no tension).

3.4.2 Method of Solution

Equation 3.4.4 was solved using the Finite Difference Method. Desired accuracy was achieved by discretising the geomembrane into 100 elements, as before. As mentioned in equation 3.4.4, one of the two equations is applicable depending on the strain level in the geomembrane. Thus, the first step towards the solution is to calculate strain at various points. For calculating strain at various points, equation 3.4.4 was first solved with $M_R > 1.0$ and $\varepsilon_o > 0$. Then, from the resulting displacements, strains at various points have been calculated. Then, the appropriate equation is selected depending on the strain levels at various points and the displacements were recalculated. While calculating the tension induced in the geomembrane, equation 3.4.1 and 3.4.2 were applied appropriately.

The effect of a bilinear stress-strain response on tension induced in the geomembrane is mainly influenced by two parameters. They are, the ratio of the two moduli of deformation, M_R, and the strain at which the modulus of deformation has a transition, ε_o. A parametric study was carried out for a range of these parameters. The ranges of these parameters are:

M_R varies from 1.0 to 100 and

ε_o varies from 0 to 0.1.

From Figure 3.4.2, it is clear that if $\varepsilon_o = 0$ or if $M_R = 1.0$, the bilinear stress-strain characteristic curve reduces to a linear stress-strain relation. That is, if $\varepsilon_o = 0$ or if $M_R = 1.0$, the solutions achieved through the present analysis should match with those of the previous analysis. Thus to validate the solutions, values of ε_o and M_R were taken to be 0 and 1 respectively. The results achieved were then compared with those of the previous method and were found to be in good agreement. The values of M_R and ε_o were then varied within their feasible range of existence and the results for the selected values of parameters were obtained. The results are presented and discussed in Chapter 4.

3.5 Estimation of Tension – Effect of Settlement of the Clay Layer

3.5.1 Statement of the Problem

While constructing a landfill liner system, geomembranes are placed on compacted clay liners and are subsequently covered with soil. When the construction of the liner system is finished, the next step is filling the landfill with waste and soil as per design specifications. Though most of the clay liners are made of compacted clays and are generally stiff, because of the overburden in the form of wastes and soil, some settlement in the clay liner is inevitable. To study the effect of this settlement on the tension induced in the geomembrane, the problem has been modeled by a three parameter model (originally proposed by Madhav and Pooroshasb (1989)) as shown in Figure 3.5.1.

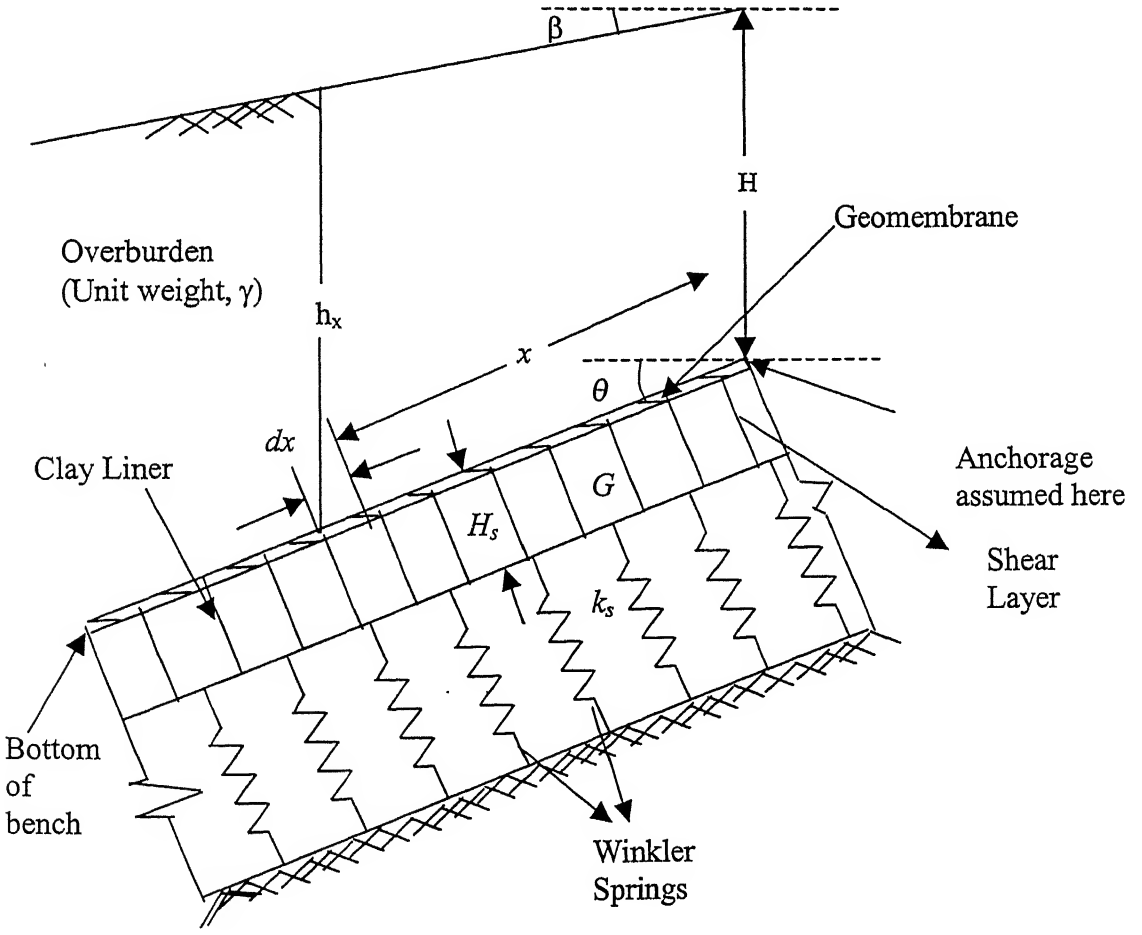

Figure 3.5.1: Modeling of the Problem for Prediction of Tension due to Settlement

where

θ and β are angles of inclination of the geomembrane and the top of the landfill respectively,

H_s is the height of the shear layer,

G is the shear modulus of the shear layer,

k_s is the stiffness of Winkler springs,

H is the height of overburden at the anchorage,

γ is the unit weight of the overburden material.

The horizontal and vertical force equilibrium of an infinitesimally small element of the geomembrane at a distance x from the anchorage, as shown in Figure 3.5.2, was considered. Unlike the previous analyses, it is assumed that slip is taking place at both the upper and lower interfaces of the geomembrane and so the full shear strengths are completely mobilised at both the interfaces. The resulting equations governing the problem, are given as equations 3.5.1 and 3.5.2.

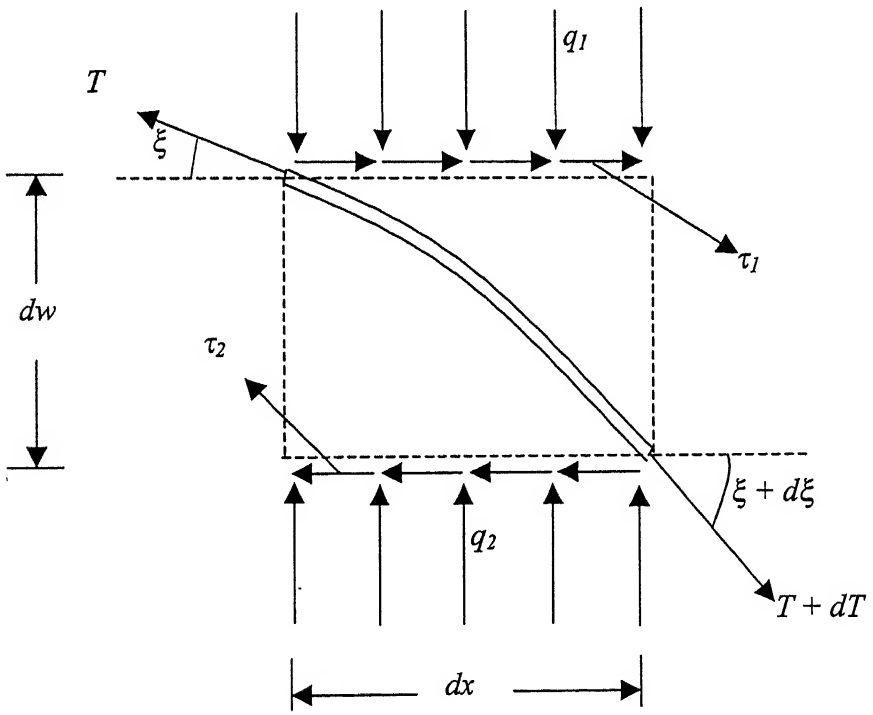

Figure 3.5.2: Forces acting on a Small Element of the Geomembrane

where

ξ is the inclination of the geomembrane at a distance x from anchorage,

q_1 and q_2 are the normal stresses on the upper and lower interfaces of the geomembrane respectively,

τ_1 and τ_2 are the shear stresses acting on the upper and lower interfaces of the geomembrane respectively,

dx is the length of the element,

dw is the settlement in a small element at a distance x from the anchorage, and

T is the tension induced in the geomembrane at a distance x from the anchorage.

$$\frac{d^2w}{dx^2}\left[T\cos^2\xi + GH_s\cos\xi - \mu_2 GH_s\sin\xi\right] = w\left[k_s\cos\xi - \mu_2 k_s\sin\xi\right] + \left[\mu_1 q_1\sin\xi - q_1\cos\xi\right] - \left[c_{a2} - c_{a1}\right]\sin\xi \tag{3.5.1}$$

$$\frac{dT}{dx} = \left[\mu_2 k_s\cos\xi + k_s\sin\xi\right]w - \left[\mu_2 GH_s\cos\xi + GH_s\sin\xi\right]\frac{d^2w}{dx^2} - \left[\mu_1 q_1\cos\xi + q_1\sin\xi\right] + \left[ca_2 - c_{a1}\right]\cos\xi \tag{3.5.2}$$

where

w is the settlement in the geomembrane at a distance x from the anchorage,

μ_1 and μ_2 are the coefficients of friction at the upper and lower interface and are defined as

$\mu_1 = \tan\phi_1$ and $\mu_2 = \tan\phi_2$, where ϕ_1 and ϕ_2 are the interface friction angles

q_1 is the normal stress acting at any point and is given by

$$q_1 = \left(k_x\cos^2\theta + \sin^2\theta\right)\left(H + x\sin\theta - x\cos\theta\tan\beta\right)\gamma$$

where

k_x is the coefficient of subgrade modulus,

θ is the angle of inclination of the geomembrane with horizontal,

β is the angle of inclination of the top of the landfill with the horizontal and

γ is the unit weight of the overburden material.

The non-dimensional form of equations 3.5.1 and 3.5.2 are

$$\frac{d^2W}{dX^2}\left[T^*\cos^2\xi + G^*\cos\xi - \mu_2 G^*\sin\xi\right] = W\left[\cos\xi - \mu_2\sin\xi\right] + \left[\mu_1 q_1^*\sin\xi - q_1^*\cos\xi\right] - \left[C_2 - C_1\right]\sin\xi \tag{3.5.3}$$

$$\frac{dT^*}{dX} = W\left[\mu_2 \cos\xi + \sin\xi\right] - \left[\mu_2 G^* \cos\xi + G^* \sin\xi\right]\frac{d^2W}{dX^2} - \left[\mu_1 q_1^* \cos\xi + q_1^* \sin\xi\right] + \left[C_2 - C_1\right]\cos\xi \quad (3.5.4)$$

where T^*, W, G^*, X, q_1^*, C_2 and C_1 are non-dimensional parameters, defined as

$$T^* = T/k_s L^2, W = w/L, G^* = GH/k_s L^2, X = x/L, q_1^* = q_1/k_s L, C_2 = c_{a2}/k_s L, C_1 = c_{a1}/k_s L.$$

The non-dimensional parameter, q_1^* is given by

$$q_1 = \left(k_x \cos^2\theta + \sin^2\theta\right)\left(H^* + x^* \sin\theta - x^* \cos\theta \tan\beta\right)\gamma^*$$

where

H^*, γ^* and x^* are non-dimensional parameters and are given by

$$H^* = \frac{H}{L}, x^* = \frac{x}{L} \text{ and } \gamma^* = \frac{\gamma}{k_s L}.$$

The boundary conditions are

(i) at $x = 0$ and at $x = L$, $\frac{dw}{dx} = 0$ (no shear);

(ii) at $x = L$, $T = 0$ (no tension).

3.5.2 Method of Solution

Equations 3.5.3 and 3.5.4 have been solved using the Finite Difference Method. A parametric study was carried out for a range of the parameters. Solutions were obtained by varying the non-dimensional parameters within their feasible ranges. To validate the solutions, uniformly distributed normal load was applied on the model by equating θ and β to 0. The calculated settlements at every point were found to be the same and were in good agreement with those of Ghosh and Madhav (1991). The results obtained from the parametric study are presented and discussed in Chapter 4.

CHAPTER 4
RESULTS AND DISCUSSION

4.1 Introduction

One of the present day solutions for proper management of waste is disposal in engineered landfills. The most important component of a landfill is the liner system which acts as a barrier to the percolating leachate. Construction of a landfill involves placement of waste above the liner system. This overburden material on the liner system induces tension in the geomembrane of the liner system. For proper design of the liner system, tension induced in the geomembrane of a liner system should be estimated accurately and it is imperative to establish the tension induced as a design parameter. Efforts have been made to estimate the tension induced in the geomembrane of a present day liner system. The analyses for the same have been presented in section 3.2.

As discussed in Chapter 2, the tension induced is effected by some aspects like, the stress-strain behavior of the geomembrane material, shear stress-displacement characteristics of the geomembrane-clay interface, etc. An attempt has been made to include these factors in the analyses and to study their effects on the tension induced. In all, five such aspects have been studied. The analyses of all the four cases have been presented in Chapter 3. This Chapter presents the results obtained and discussions of the results.

Results obtained by assuming a hyperbolic shear stress-displacement interface response have been presented and discussed in section 4.2, while section 4.3 deals with results arrived at by assuming the same interface with strain softening. The results from the incorporation of a bilinear stress-strain response for geomembrane material have been presented and discussed in section 4.4. The effect of a cavity between the geomembrane and clay at the lower interface was also studied and the results presented and discussed in section 4.5. To study the effect of settlement on the tension induced, the problem was modeled and the results presented and discussed in section 4.5.

4.2 Hyperbolic Interface Response

Experiments on the geomembrane-clay interface reveal that in most of the cases, the shear stress-displacement response of the interface takes the shape of a hyperbola. This aspect has been included in the analyses. Results were obtained by varying every single parameter within the feasible range, while keeping other parameters constant. The results obtained are presented in Figures 4.2.1 to 4.2.16.

Figure 4.2.1 shows the variation of normalised tension, $T^*(= T/tE)$ and normalised displacement, $U(= u/L)$ with normalised distance from the anchorage, X(= x/L) for a set of parameters. The non-dimensional parameter, $\lambda(= \gamma L^2/tE)$, represents the unit weight of the overburden), has been varied from 80 to 1500. From the results, it can be noticed that the normalised tension decreases from a maximum value of 0.067 at the anchorage to 0.003 at a normalised distance of 0.04 from the anchorage, when λ is equal to 1500. The value remains nearly the same over remaining part of the geomembrane. However, for λ = 80, the tension decreases uniformly from the maximum value of 0.003 at the anchorage to 0.0001 at a normalised distance of 0.04 from the anchorage. It can be noticed that as the value of λ increases, the tension induced in the geomembrane also increases, because λ is directly proportional to the unit weight of the overburden and the length of the landfill. Thus one can conclude that larger the landfill and more the unit weight of the overburden, more is the tension induced in the geomembrane. One can notice from the variation of normalised displacement with the normalised distance from anchorage that the gradient of displacement is very high near the anchorage. The slope or gradient of the curve remains constant beyond a normalised distance 0.04 from the anchorage. The displacement is maximum for λ = 1500 and reduces with λ.

Results achieved by varying the angle of inclination of the geomembrane with the horizontal, θ, are presented in Figure 4.2.2. A maximum value of tension induced in the geomembrane is 0.0165 for $\theta = 35^\circ$. The tension reduces with distance from the anchorage. The minimum tension is 0.0015 at the anchorage for $\theta = 10^\circ$. The variation in the values of maximum tension with θ is less than that of λ. The reason for decreasing normalised tension with decreasing θ could be because as θ decreases,

the rate of loading also decreases which results in lesser tension.The variation of normalised displacement with distance is gradual from the anchorage to a normalised distance of 0.12 from the anchorage beyond which the variation of normalised displacement with distance is close to linear.

Figure 4.2.3 shows the variations of normalised tension and displacement for various values of non-dimensional parameter, χ (= $\sqrt{k_\tau L^2 / tE}$, which depends on the initial slope of the interface response, k_τ). The normalised tension decreases from a value of 0.0087 for χ = 200 at the anchorage to a much lower value at a normalised distance of 0.09 from the anchorage. The values of maximum normalised tension decrease with increasing values of χ. The non-dimensional parameter, χ, is directly proportional the initial slope of the shear stress-displacement curve, k_τ. Thus, a high value of χ means higher initial slope for which higher resisting shear stresses are mobilised at the lower interface. Thus lesser normalised tensions would be induced at the lower interface. However, the variation in maximum normalised tension with χ is lesser than that with λ. From the profile of variation of normalised displacements, one can notice that the gradient of displacements is very high near the anchorage. The gradient decreases and remains linear from a normalised distance of 0.09 from anchorage to the free end.

The angle of inclination of the top of the landfill with the horizontal, β, has been varied from -10° to 25° and the profiles of variations of the normalised tension and displacement are shown in Figure 4.2.4. Form the figure, one can notice very small variation in the values of maximum normalised tension with β. The maximum values tend to decrease with increasing β. The maximum normalised tension decreases from a value of 0.0051 to 0.0046 as β increases from -10° to 25°. The displacement profile flattens increasing values of β. The gradient of displacement profile is seen to be very high near the anchorage but reduces with distance from the anchorage. The gradient remains fairly constant from a normalised distance of 0.05 from the anchorage to the free end. As increasing value of β implies decreased rate of loading on the geomembrane, and lesser tensions are induced as β increases.

The variation of normalised displacement with normalised distance from anchorage, for a range of normalised adhesion, C_{aL} values, is depicted in Figure 4.3.5. In the absence of adhesion, i.e. $C_{aL} = 0$, the displacement increases very sharply near the anchor point and only marginally with distance for $X > 0.2$. The maximum normalised displacement value is close to 0.0003. The significant influence of adhesion on the liner response can be noted from the figure. For low values of C_{aL} (= 0.01), the rate of increase of U with X is still high near the anchorage, the displacement values tend to become asymptotic closer to the anchor point and attain considerably smaller values of displacement. For $C_a = 0.2$, the maximum value of U is only 4×10^{-5}. Similar trends in the variation of normalised tension with distance can be seen. The tension is maximum near the anchor point and decreases rapidly with the distance. Larger interface shear resistances are mobilised farther from the anchor point because of larger liner displacements, thus leading to a decrease in tension values. The maximum tension value decrease from 0.0083 for $C_a = 0$ to 0.0033 for $C_a = 0.2$. Similar results are obtained with variations in interfacial friction angle, δ_l. The results are as shown in Figure 4.2.6.

The variations of normalised tension and normalised displacements with normalised distance, for a range of H^*(=H/L, depends on the height of overburden at the anchorage) are shown in Figure 4.2.7. The normalised tension decreases from a maximum value of 0.014 at the anchorage to 0.0002 at a normalised distance of 0.09 from the anchorage for $H^* = 0.3$. The values of normalised tension decrease very steeply from the point of anchorage. Maximum normalised tension decreases from 0.014 for $H^* = 0.3$ to 0.0025 for $H^* = 0$. From the variations of normalised displacement, all the profiles are parallel after a distance of 0.07 from the anchorage. The gradients of the profiles of normalised displacement are steep near the anchorage. The gradients in all the profiles converge to more or less the same value after a normalised distance of 0.07 from the anchorage. As H^* is a non-dimensional parameter that is directly proportional to the height of overburden near the anchorage, H and is inversely proportional to the length of the landfill, a high value of H^* means higher overburden height which would result in more shear stress being applied to the upper interface of the geomembrane. This is the reason for a proportional increase in the normalised tension with increase in H^*.

Figure 4.2.8 shows the variations in normalised displacement and normalised tension with normalised distance from the anchorage for various values of the coefficient of lateral earth pressure, k_x. The tension induced decreases from a maximum value of 0.00456 for $k_x = 0.5$ to 0.00035 for $k_x = 1$. The tension decreases very steeply from its maximum value at the anchorage with increasing distance from the anchorage upto a normalised distance of 0.05. Beyond this point, tension remains fairly constant. From the profile of normalised displacements, one can notice that the normalised displacements increase sharply from the anchorage to a distance of 0.05 from the anchorage. The maximum normalised displacements decrease with increasing values of k_x. A higher value of k_x would mean lesser shear stress being induced at the upper interface of the geomembrane. As lesser disturbing shear stresses are induced with increasing values of k_x, lesser normalised tension and displacements can be noticed as k_x increases.

Using these results, design charts for the estimation of maximum tension with the same set of parameters as shown in Figures 4.2.9 to 4.2.12 are developed. Design charts for a different set of parameters can be easily developed by the same procedure. The tension induced in the geomembrane directly be found out corresponding to the relevant set of parameters with the help of these design charts.

4.3 Strain Softening in the Geomembrane-Clay Interface

Experiments reveal that some of the geomembrane-clay interfaces undergo strain softening in the post-peak range. As the tension induced in the geomembrane depends mainly on the shear stresses induced at the upper and lower interfaces, it was attempted to include this property of the interface while estimating tension induced in the geomembrane. The statement of the problem and the analysis have been given in section 3.3. In the assumed shear stress-displacement response curve, the main factor that may signify the effect of strain softening is the slope of the curve beyond the peak shear stress. Thus, the non-dimensional parameter, $\chi_2 (= \sqrt{k_{\tau 2} L^2 / tE}$, which depends on the slope of the curve beyond peak shear stress, $k_{\tau 2}$), was varied within a feasible range. Results obtained are as presented in Figure 4.3.1.

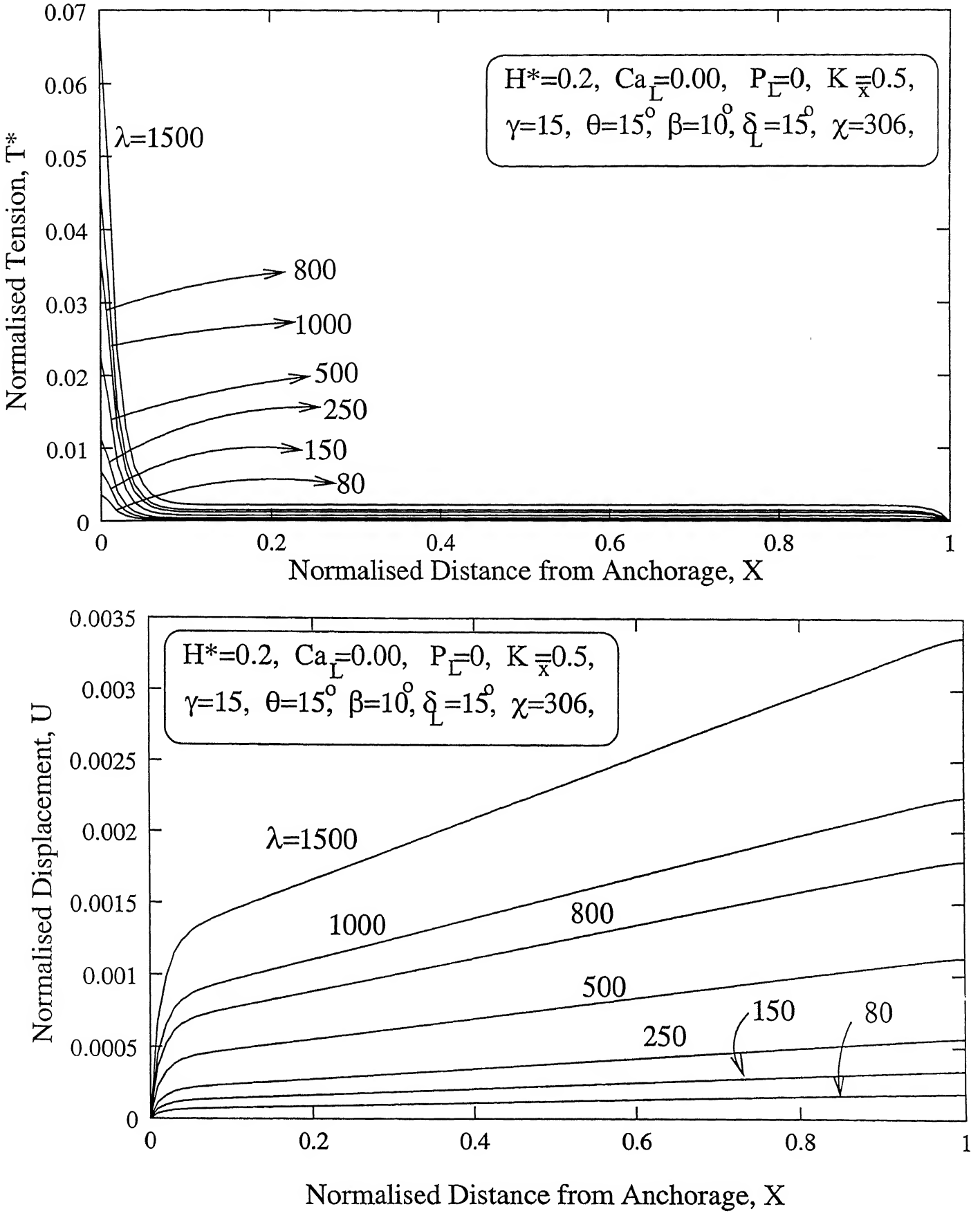

Figure 4.2.1: Variation of (a) Normalised Tension and (b) Normalised Displacement for various values of λ

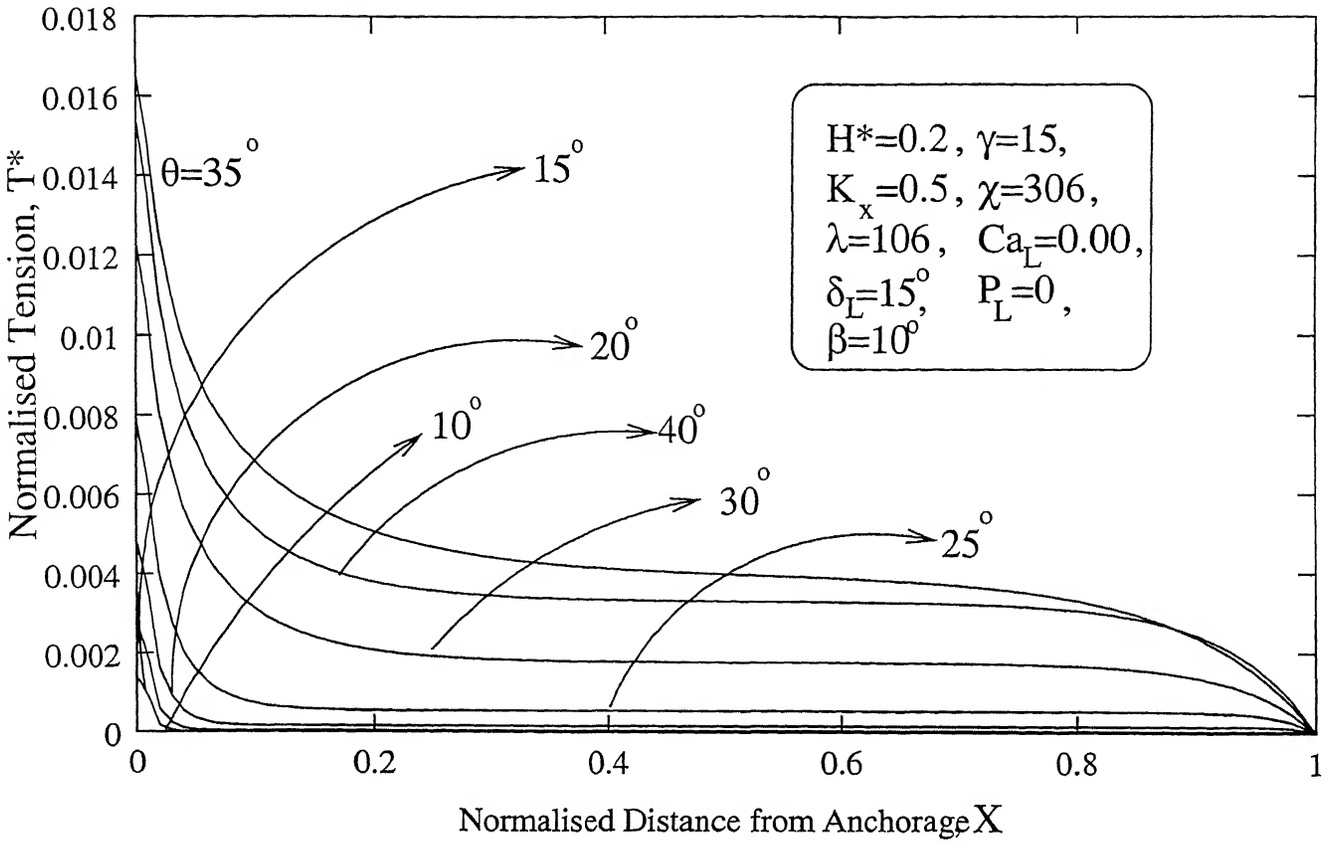

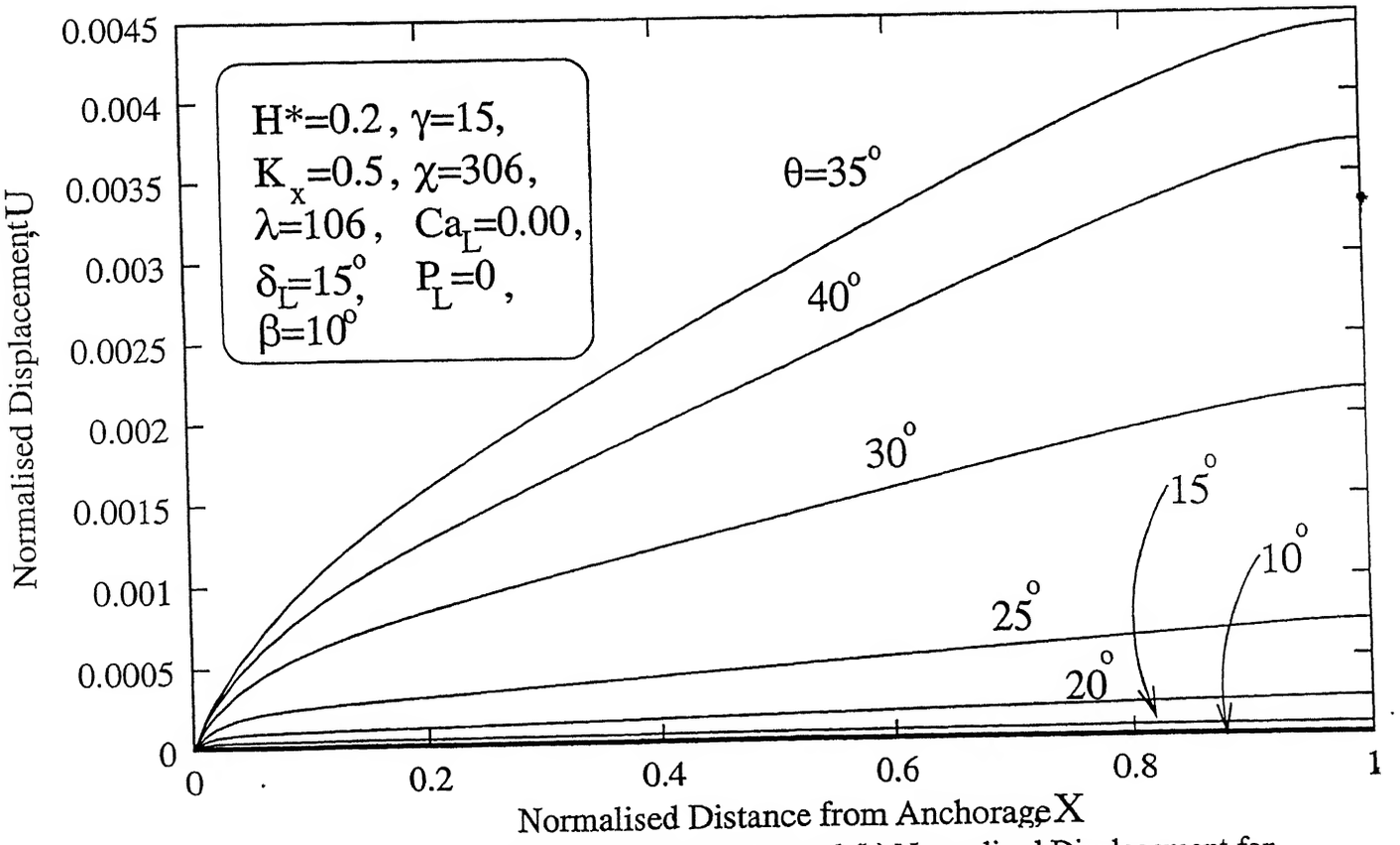

Figure 4.2.2: Variation of (a) Normalised Tension and (b) Normalised Displacement for various values of θ

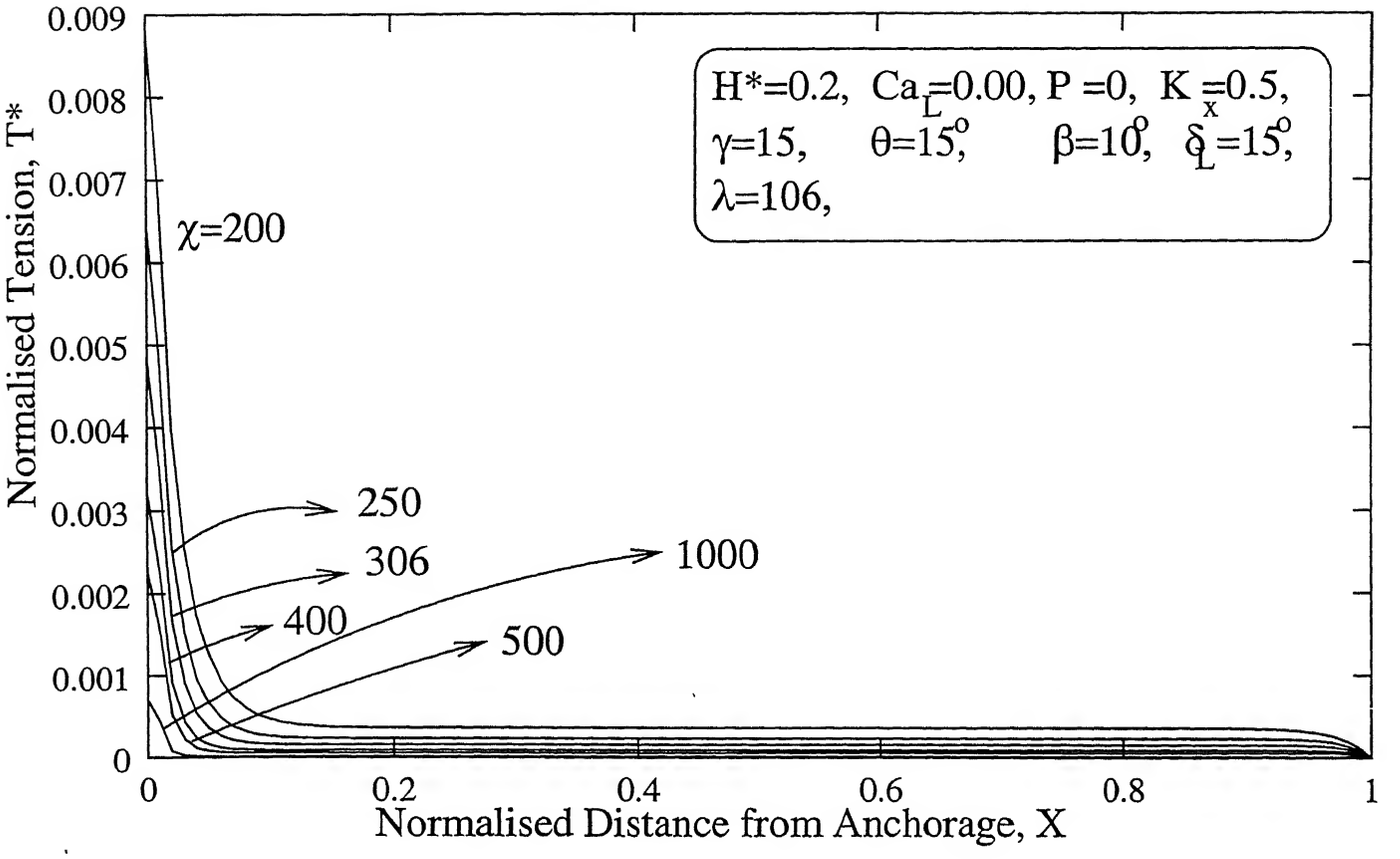

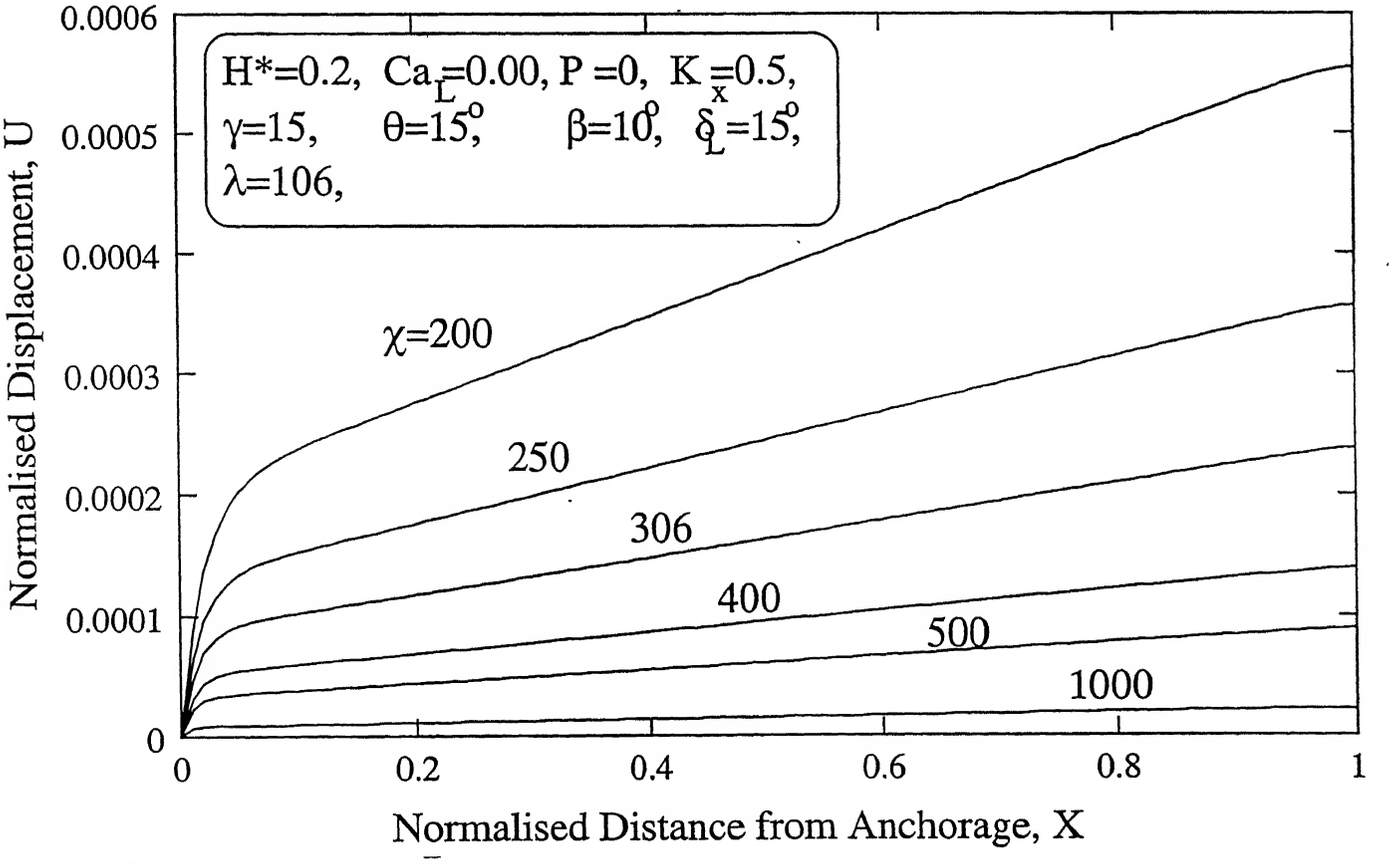

Figure 4.2.3: Variation of (a) Normalised Tension and (b) Normalised Displacement for various values of χ

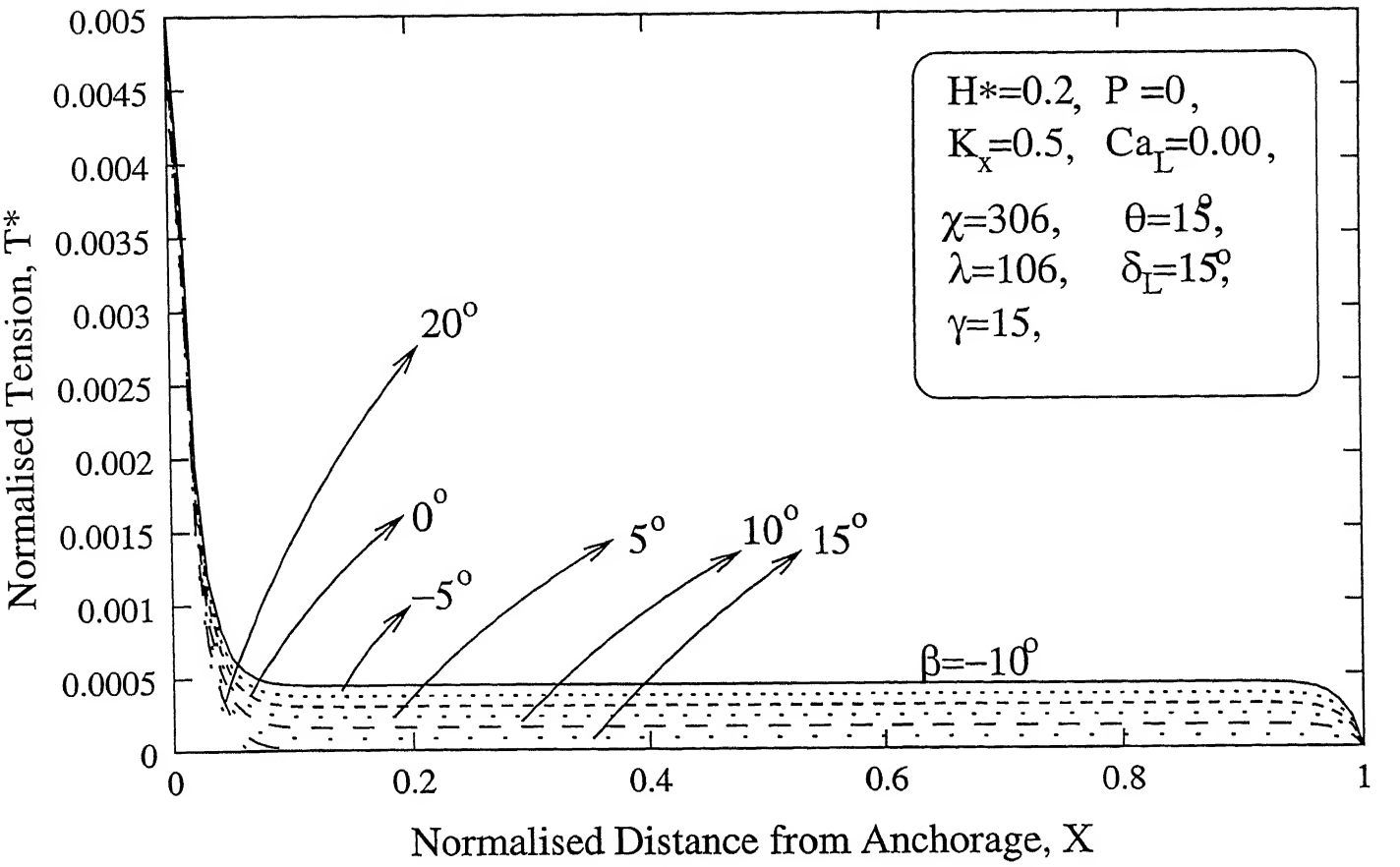

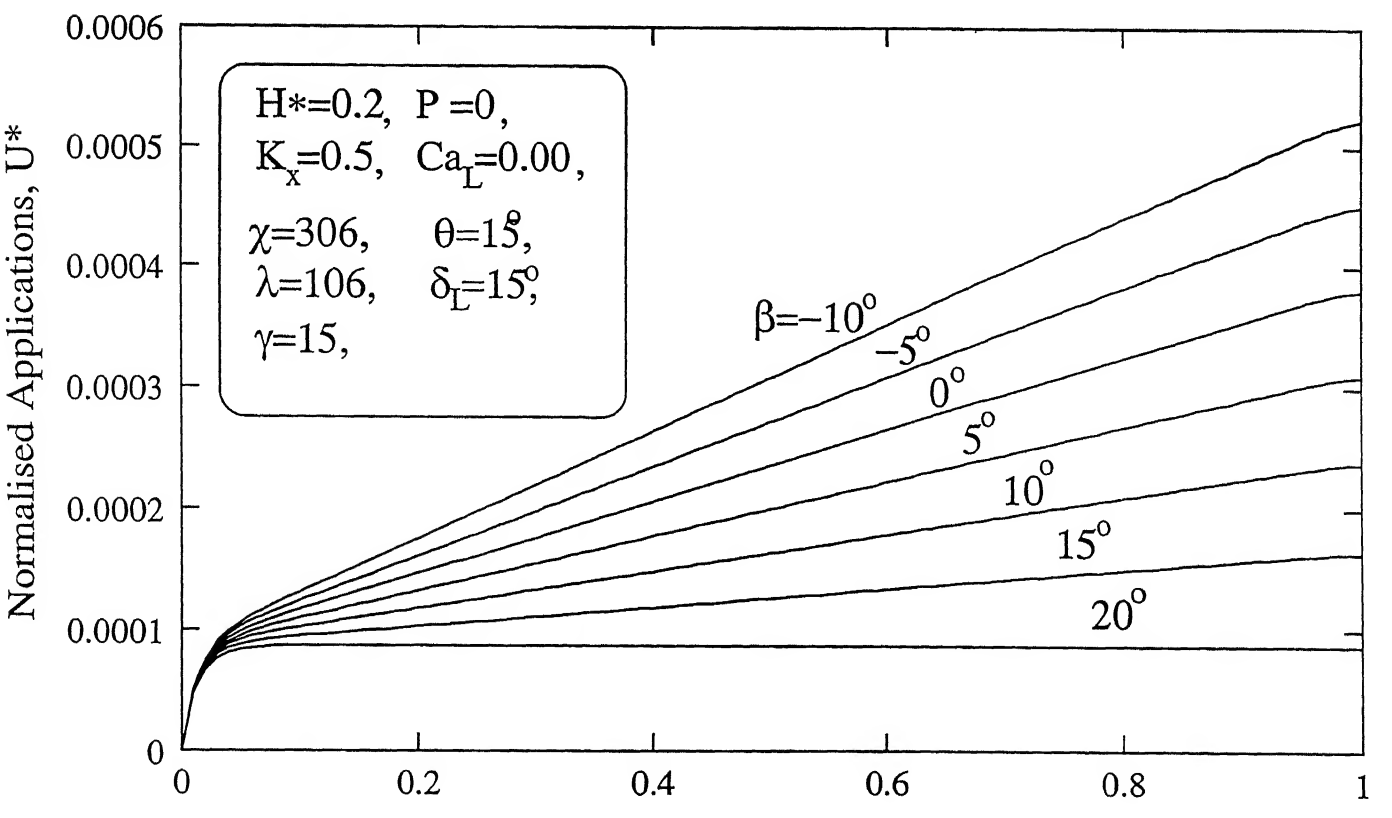

Figure 4.2.4: Variation of (a) Normalised Tension and (b) Normalised Displacement for various values of β

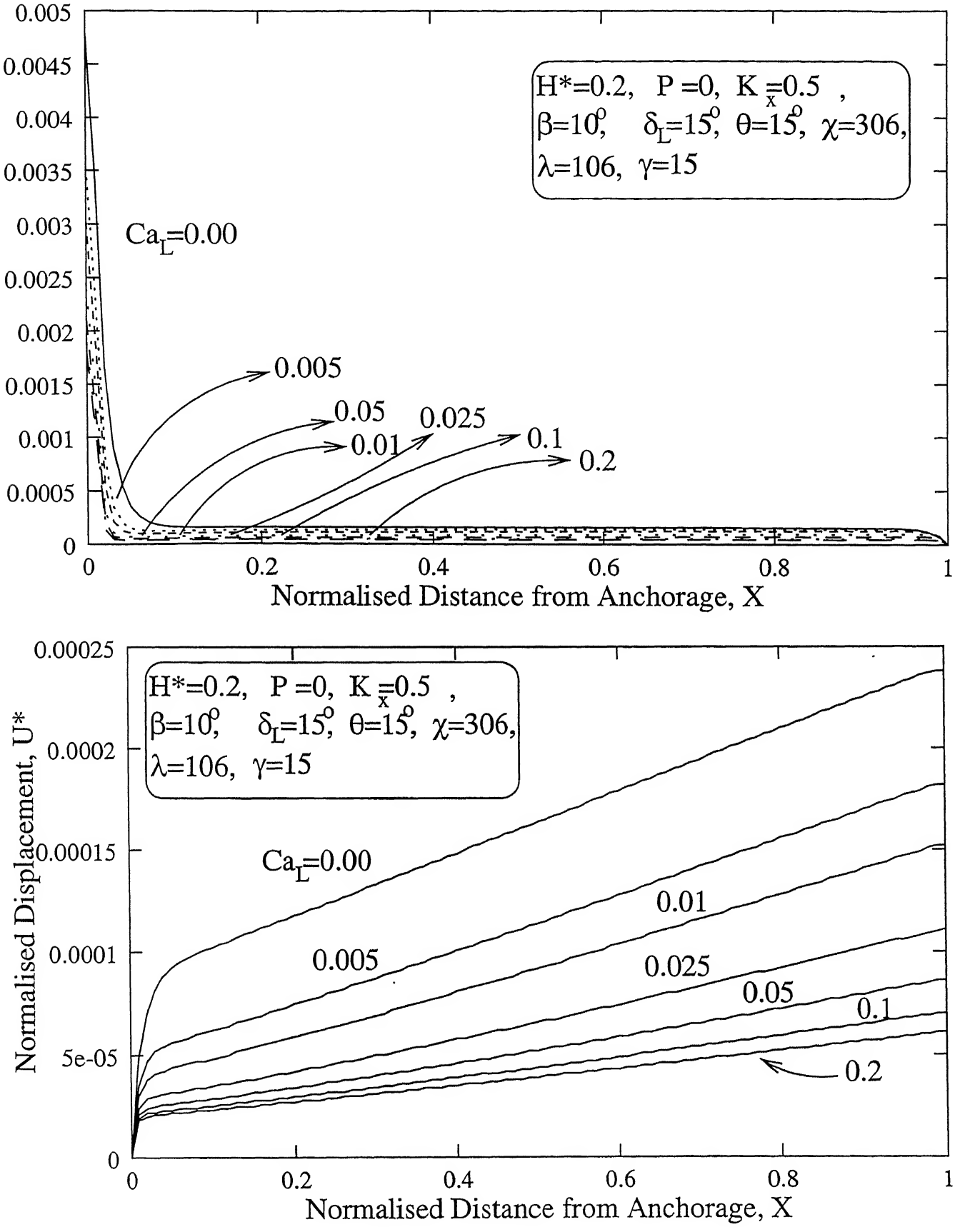

Figure 4.2.5: Variation of (a) Normalised Tension and (b) Normalised Displacement for various values of C_{aL}

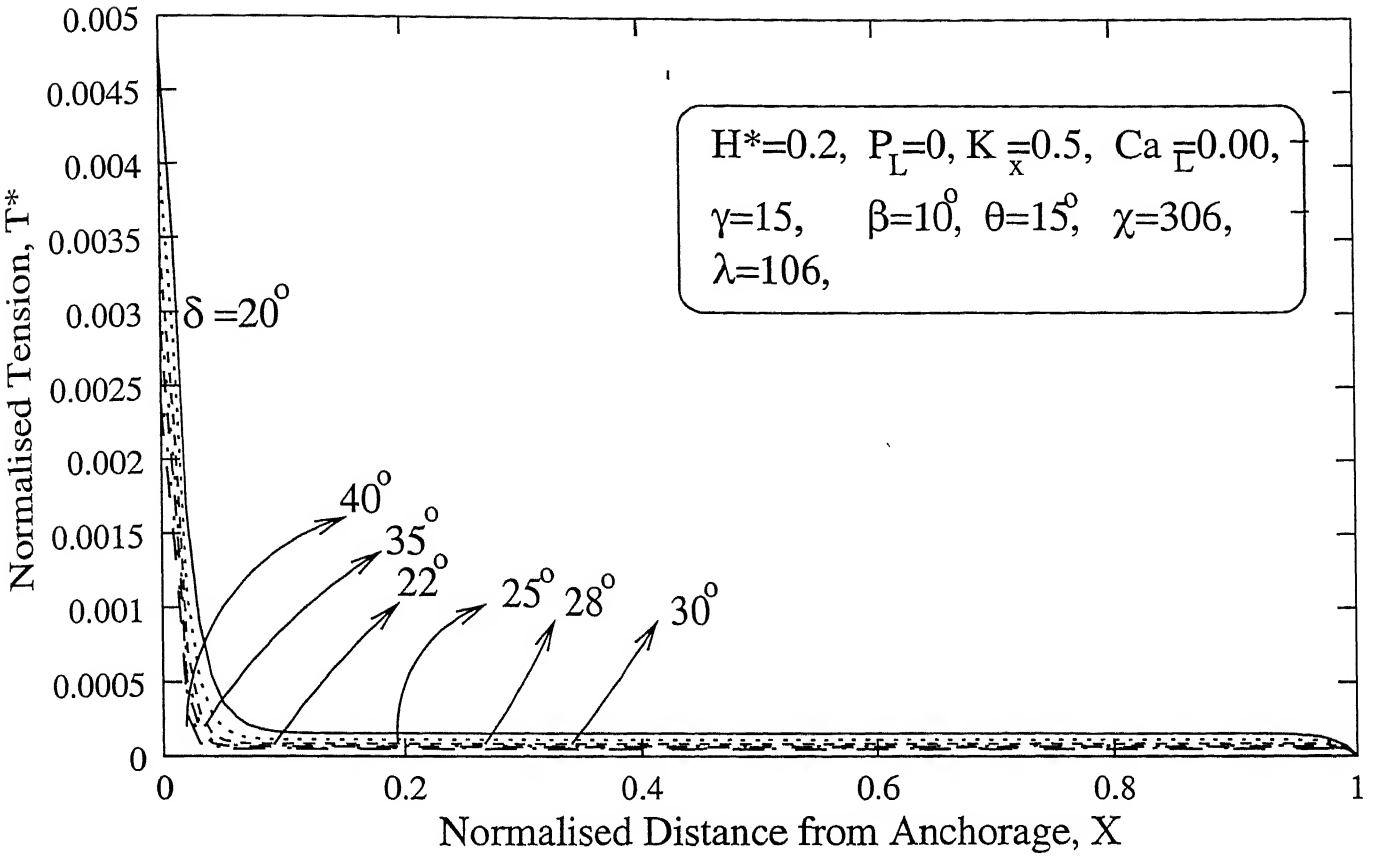

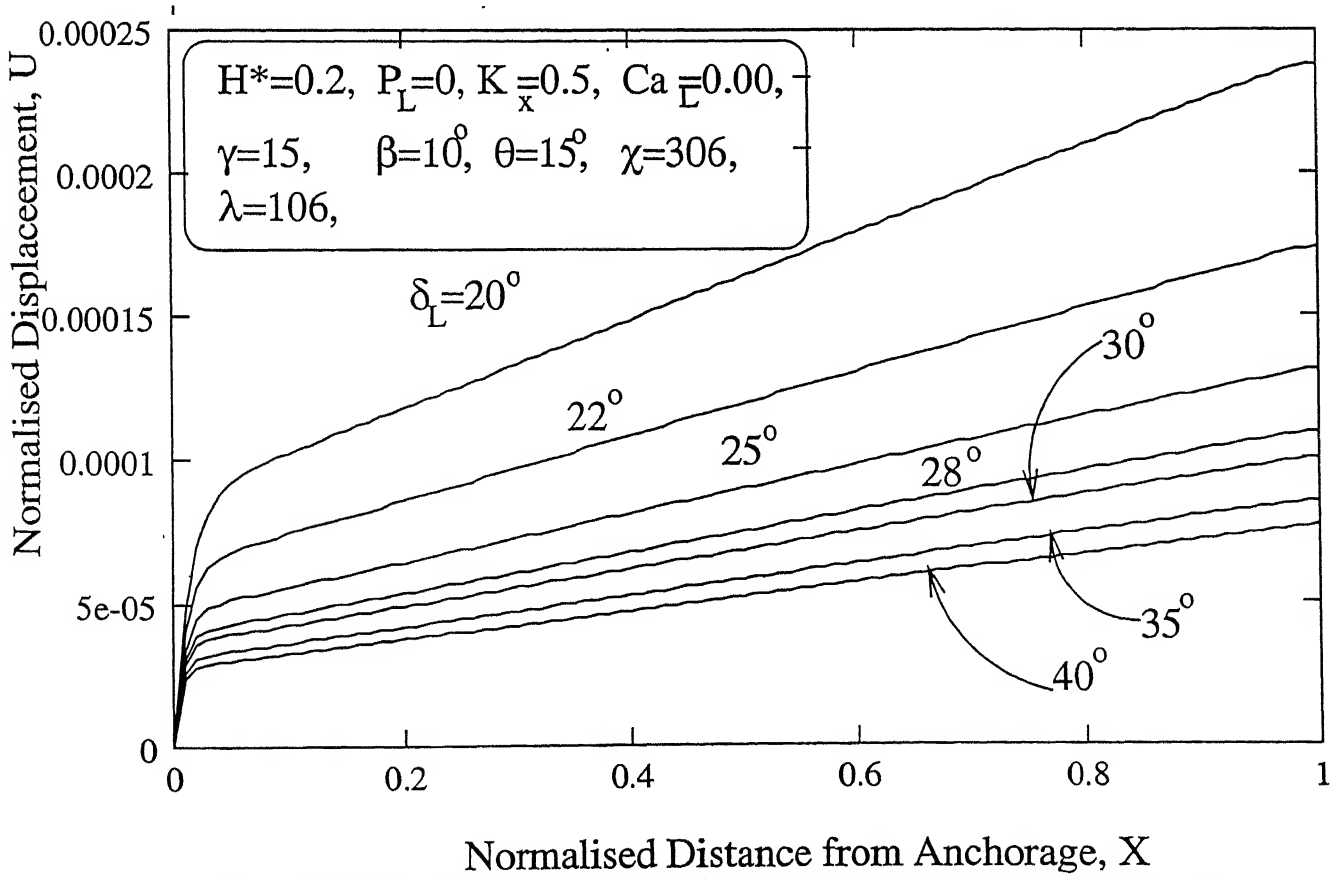

Figure 4.2.6: Variation of (a) Normalised Tension and (b) Normalised Displacement for various values of δ_L

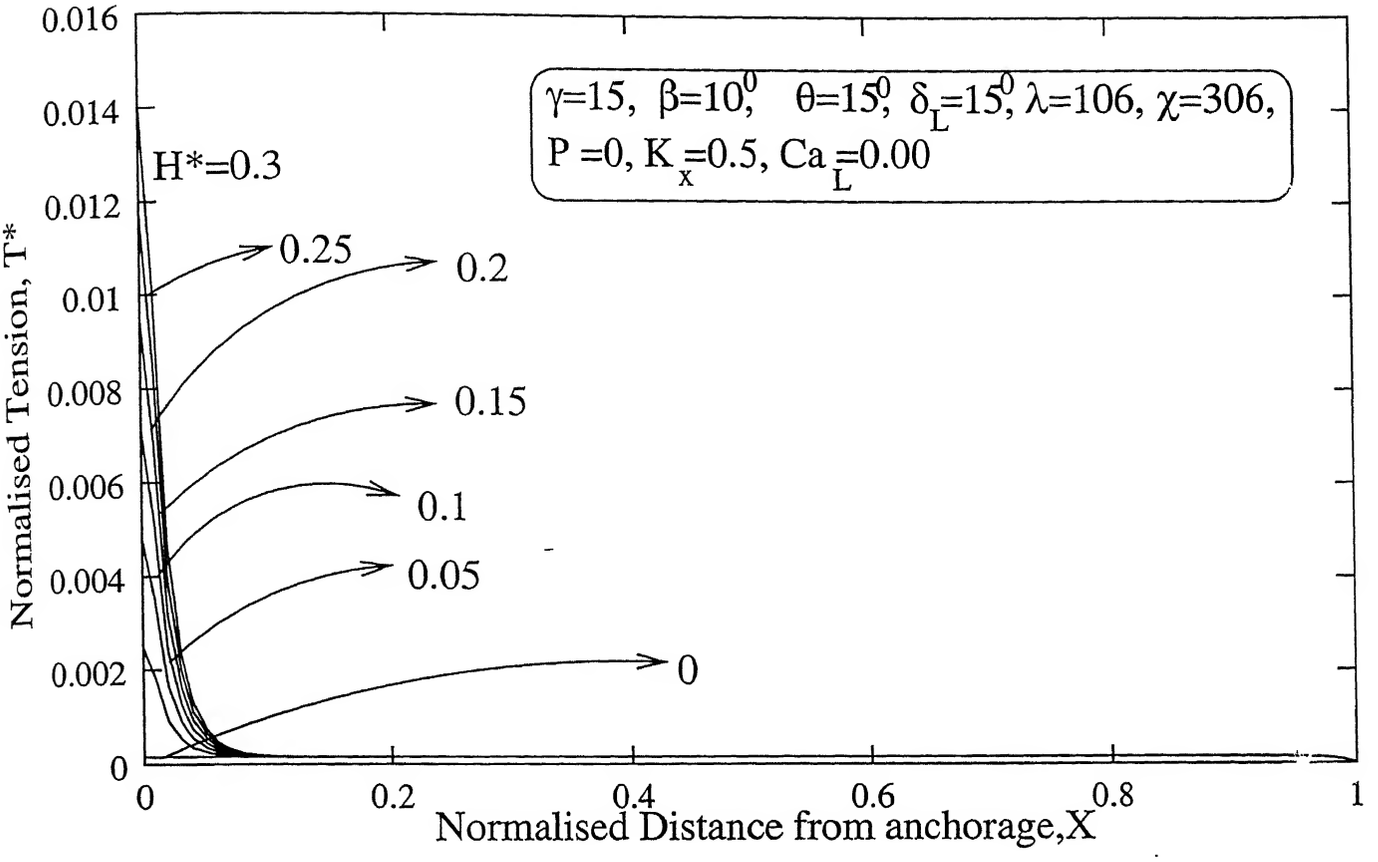

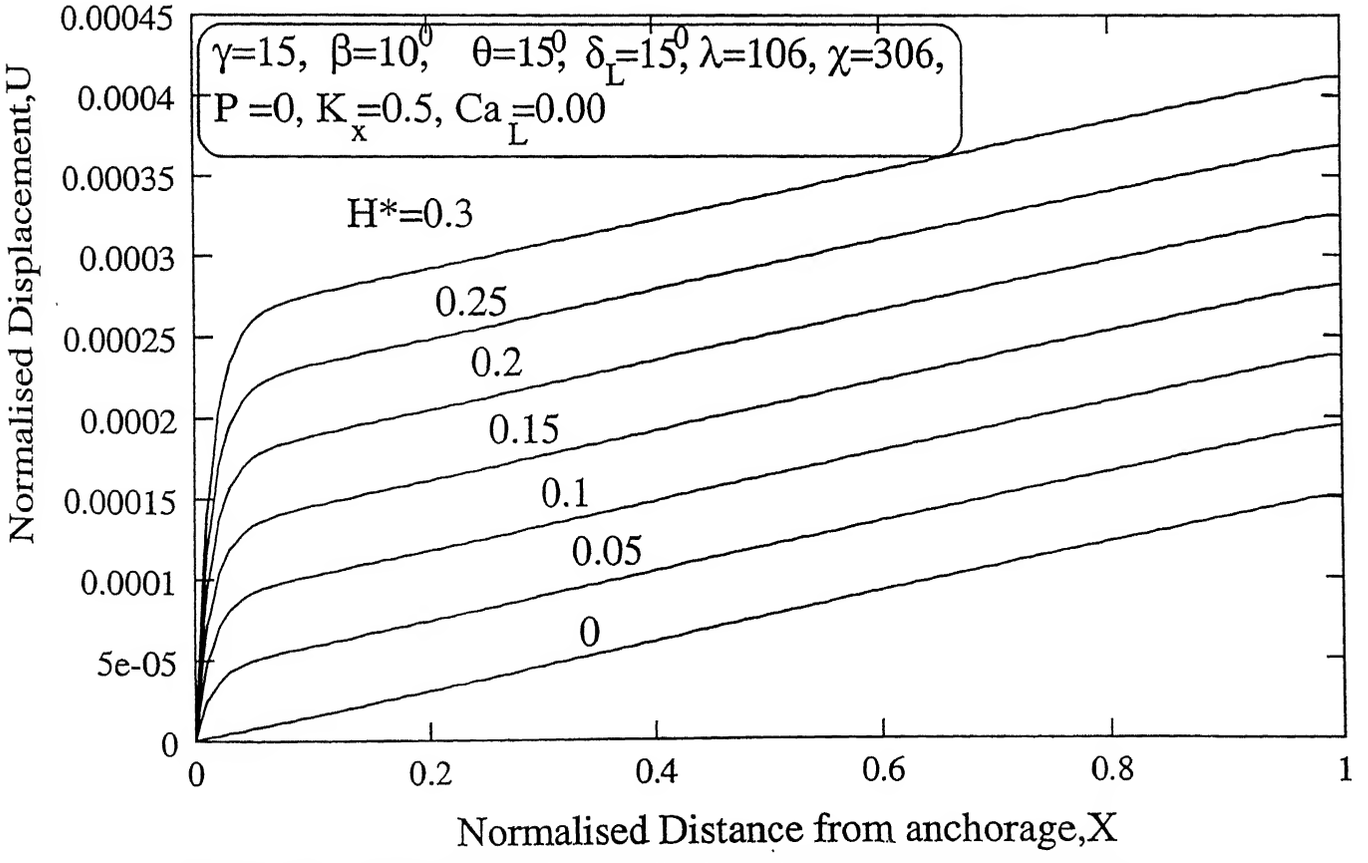

Figure 4.2.7: Variation of (a) Normalised Tension and (b) Normalised Displacement for various values of H^*

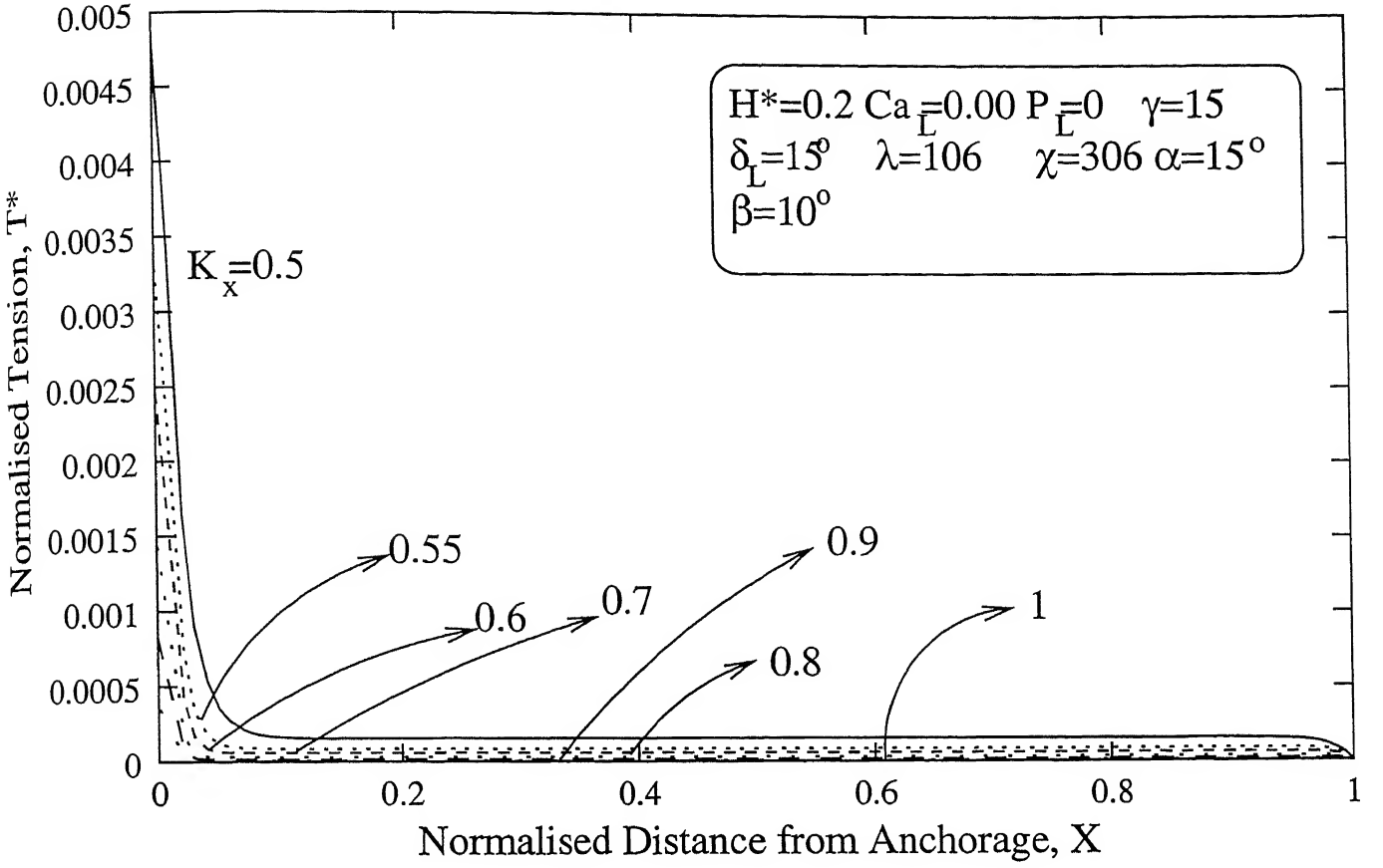

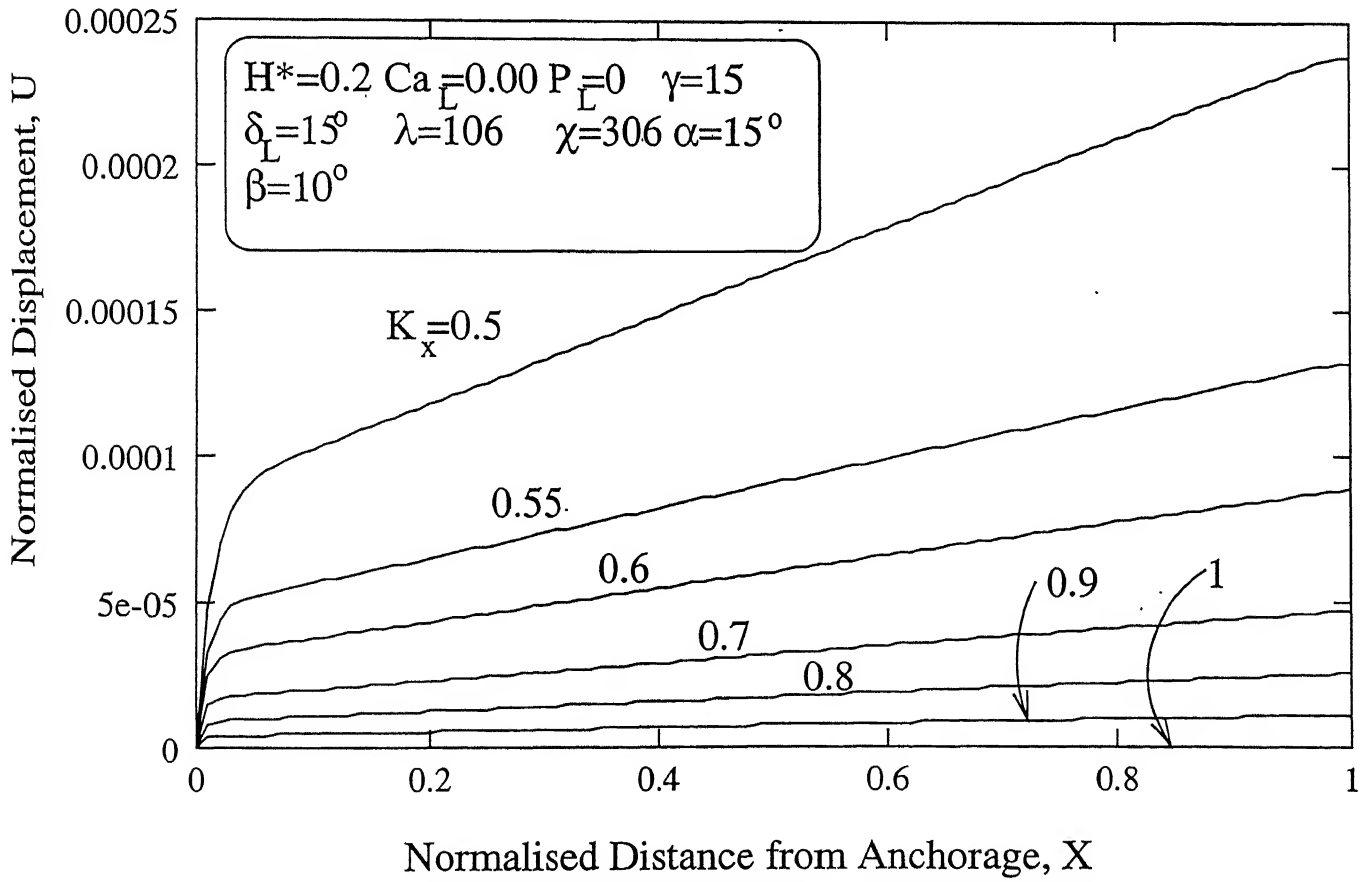

Figure 4.2.8: Variation of (a) Normalised Tension and (b) Normalised Displacement for various values of k_x

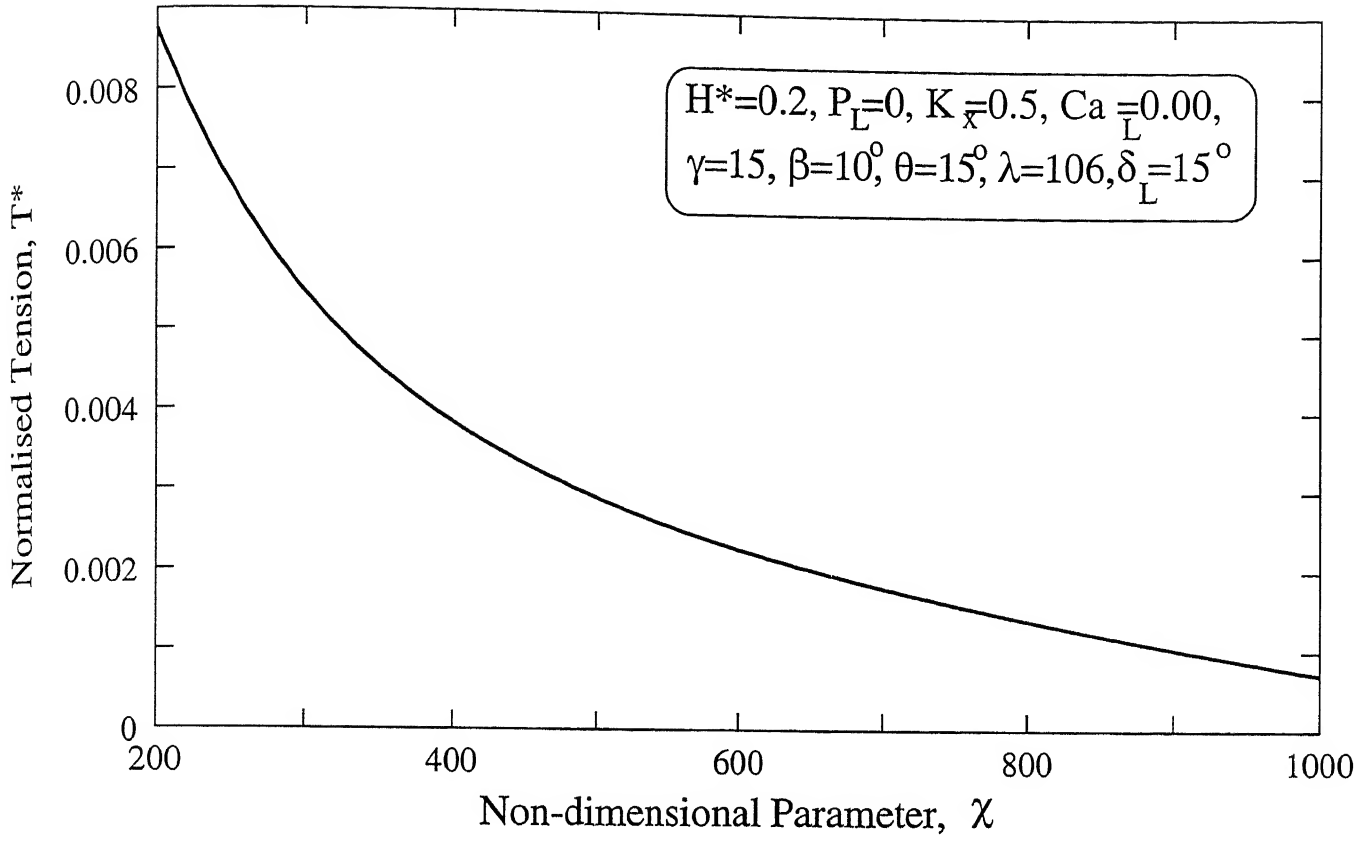

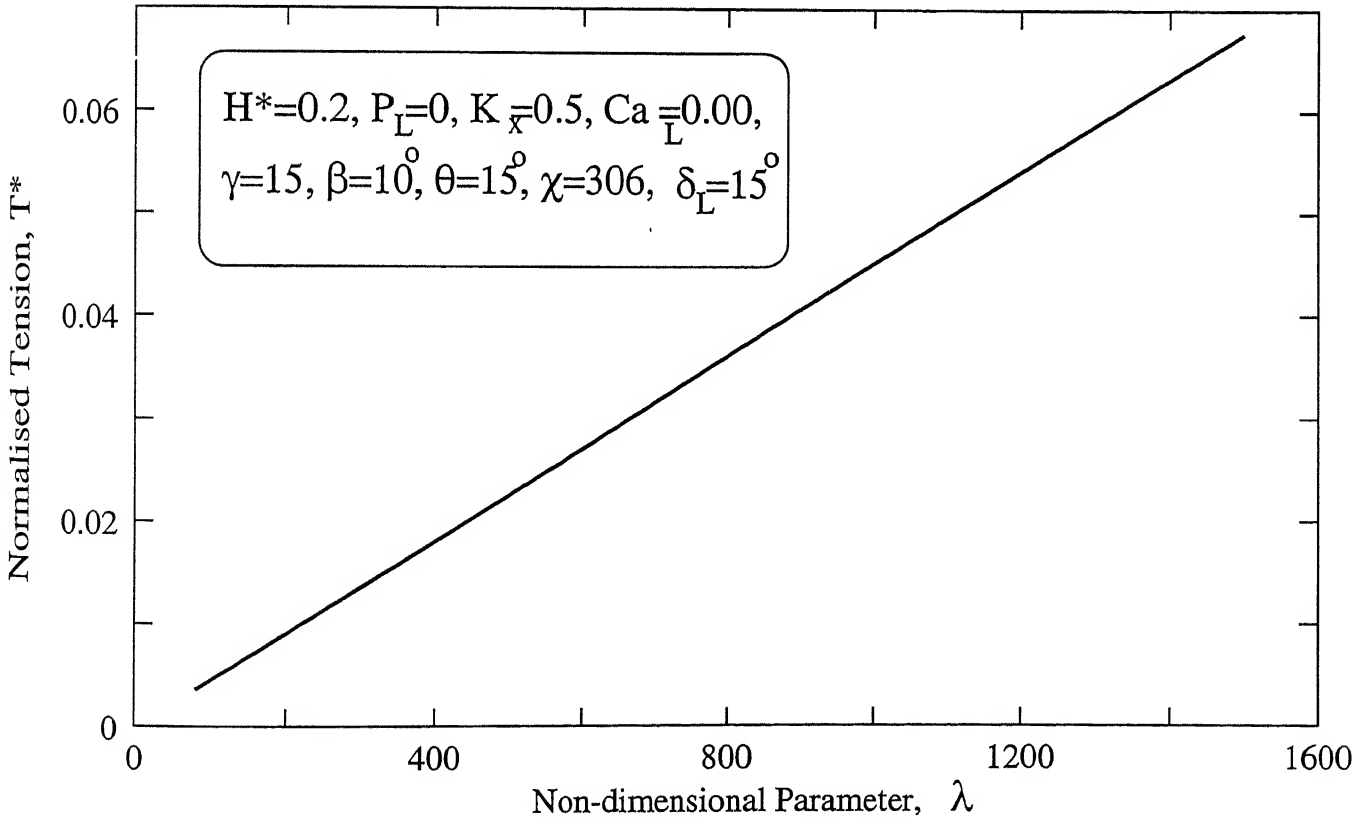

Figure 4.2.9: Design Charts with respect to (a) χ and (b) λ

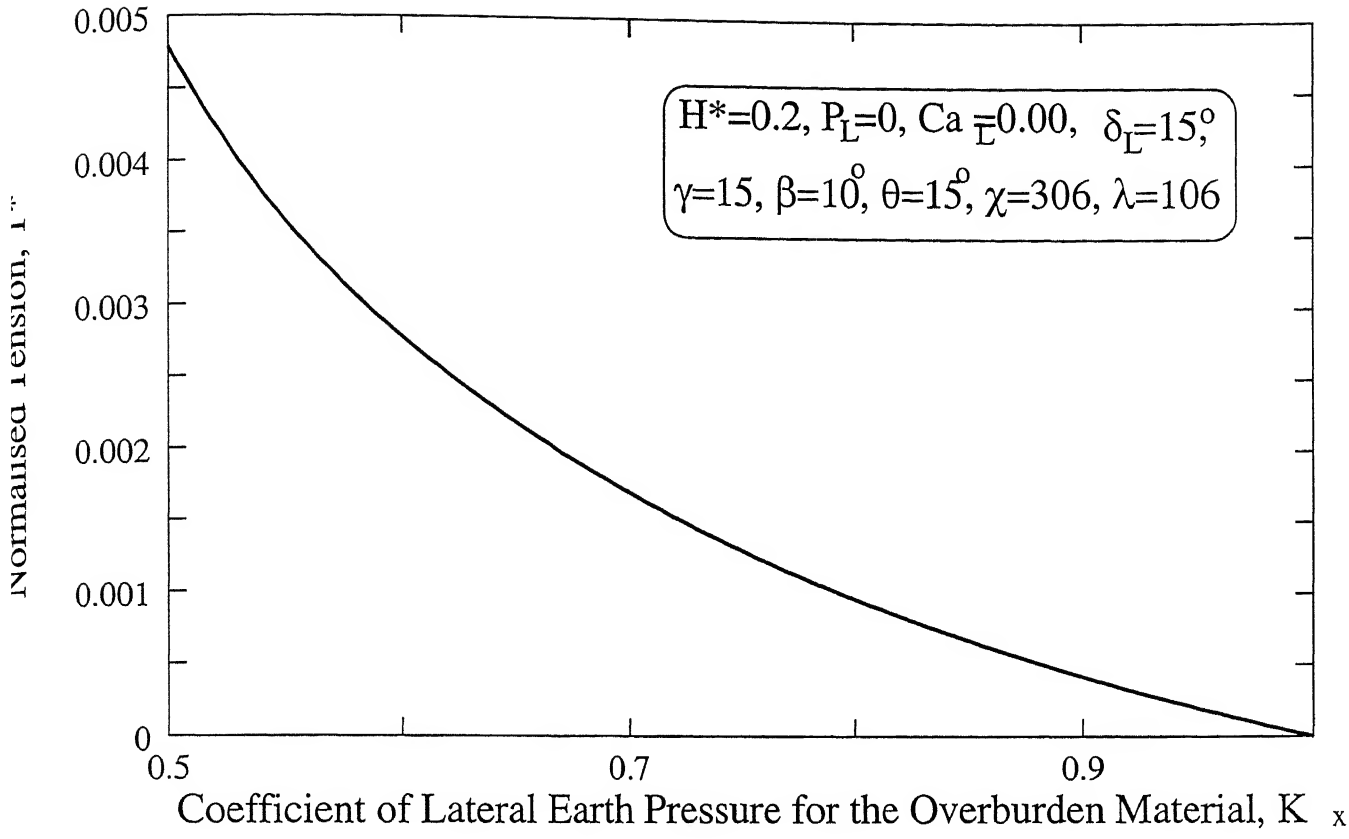

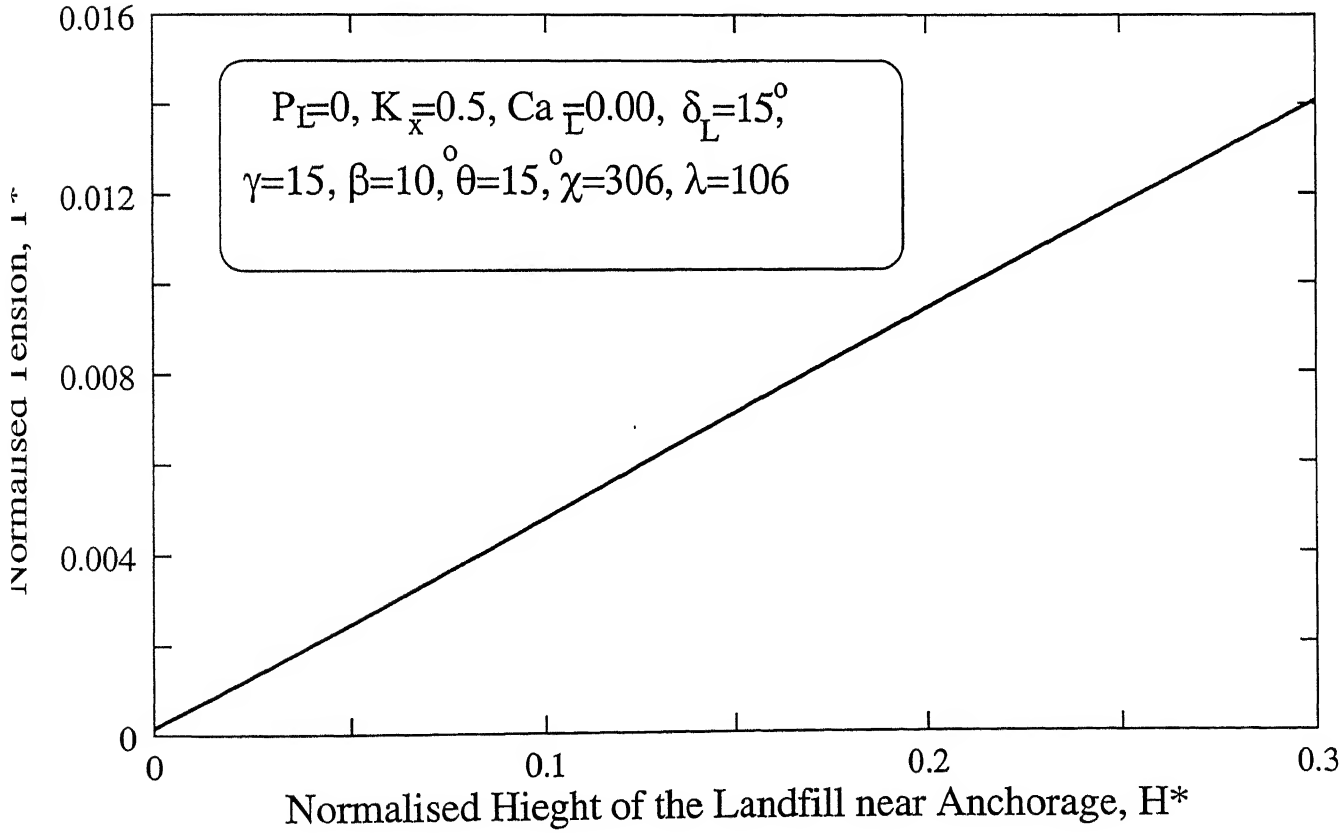

Figure 4.2.10: Design Charts with respect to (a) k_x and (b) H^*

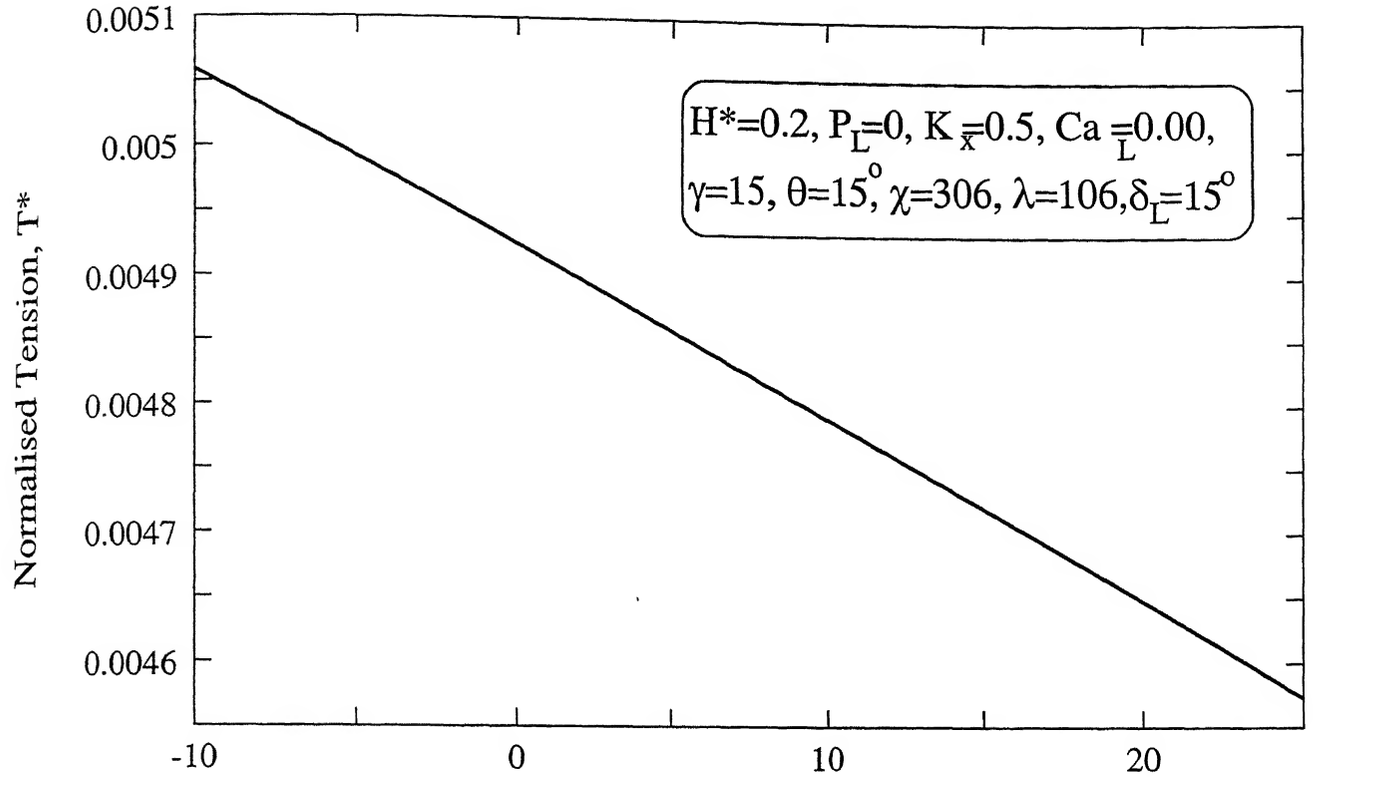

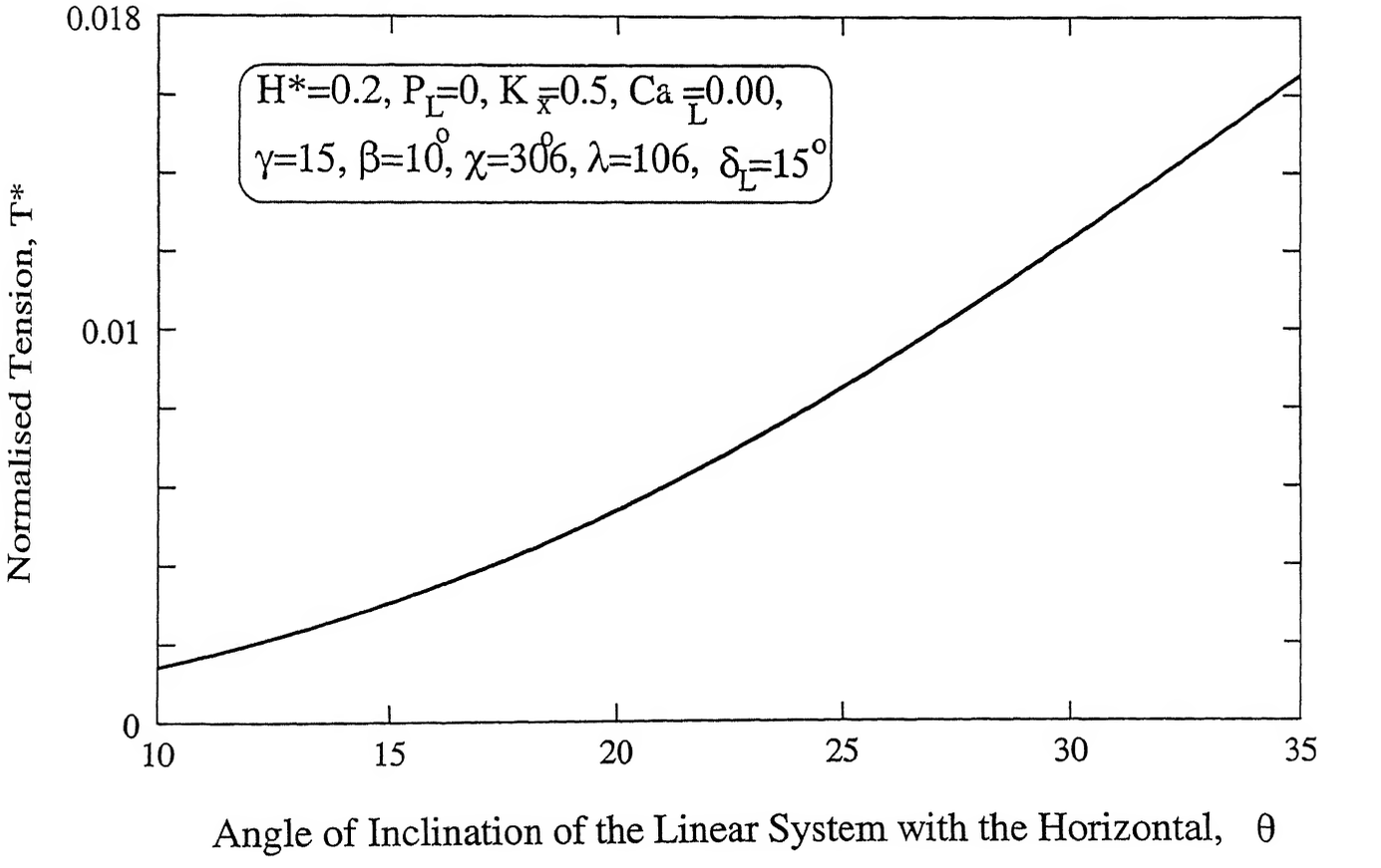

Figure 4.2.11: Design Charts with respect to (a) β and (b) θ

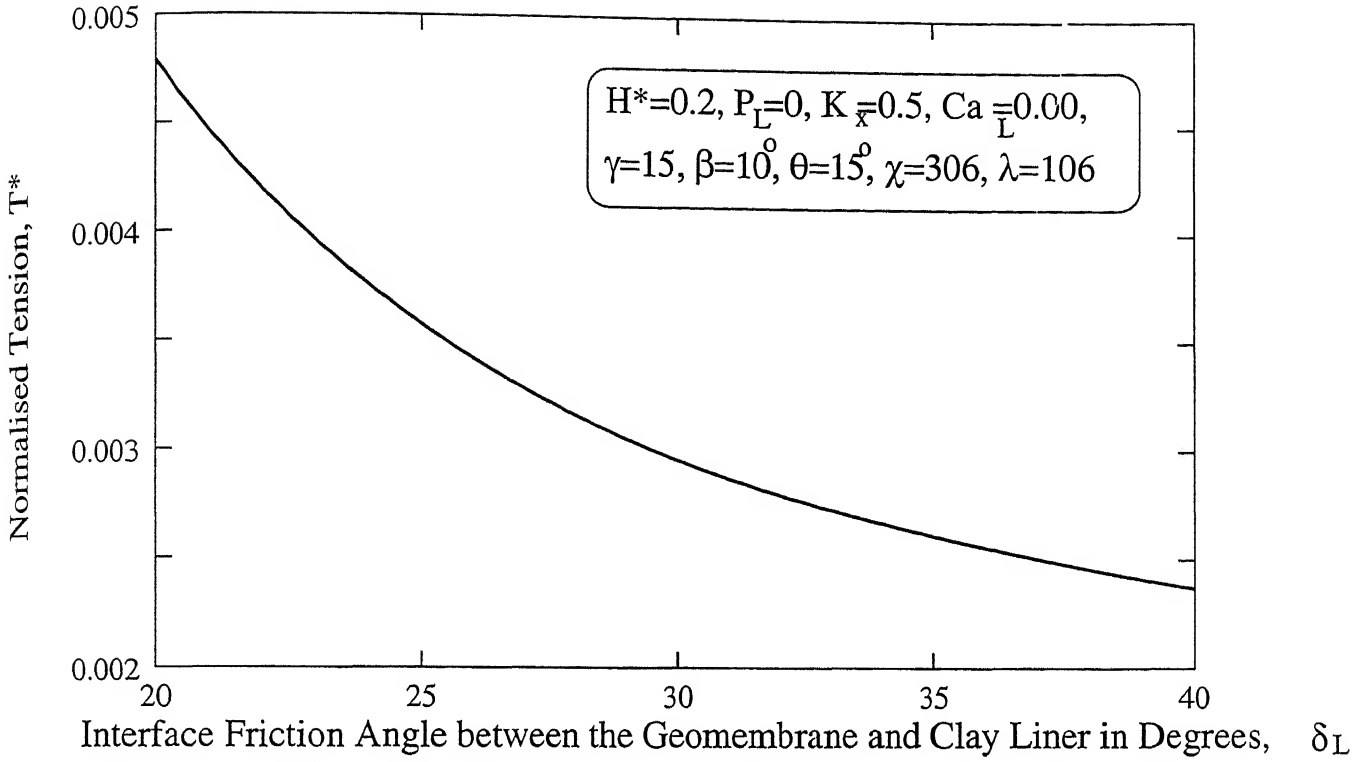

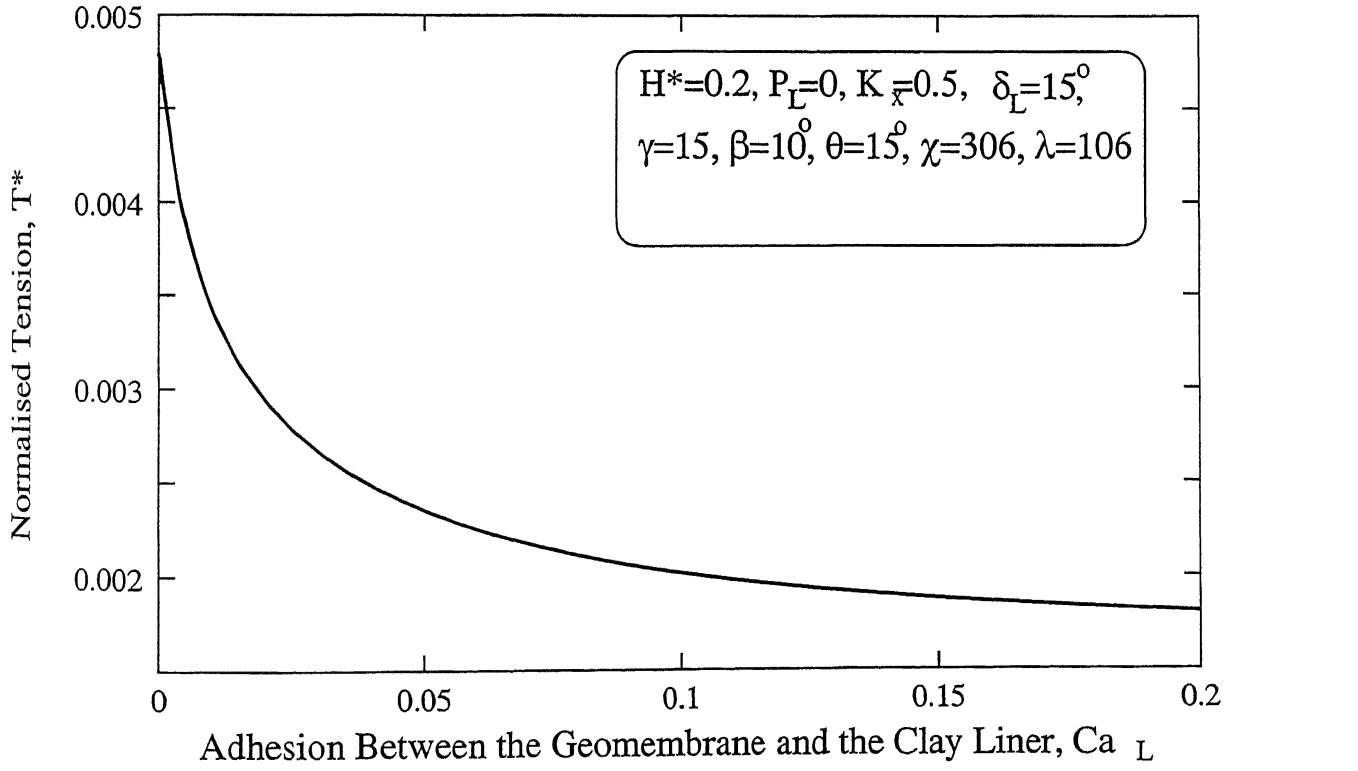

Figure 4.2.12: Design Charts with respect to (a) δ_L and (b) C_{aL}

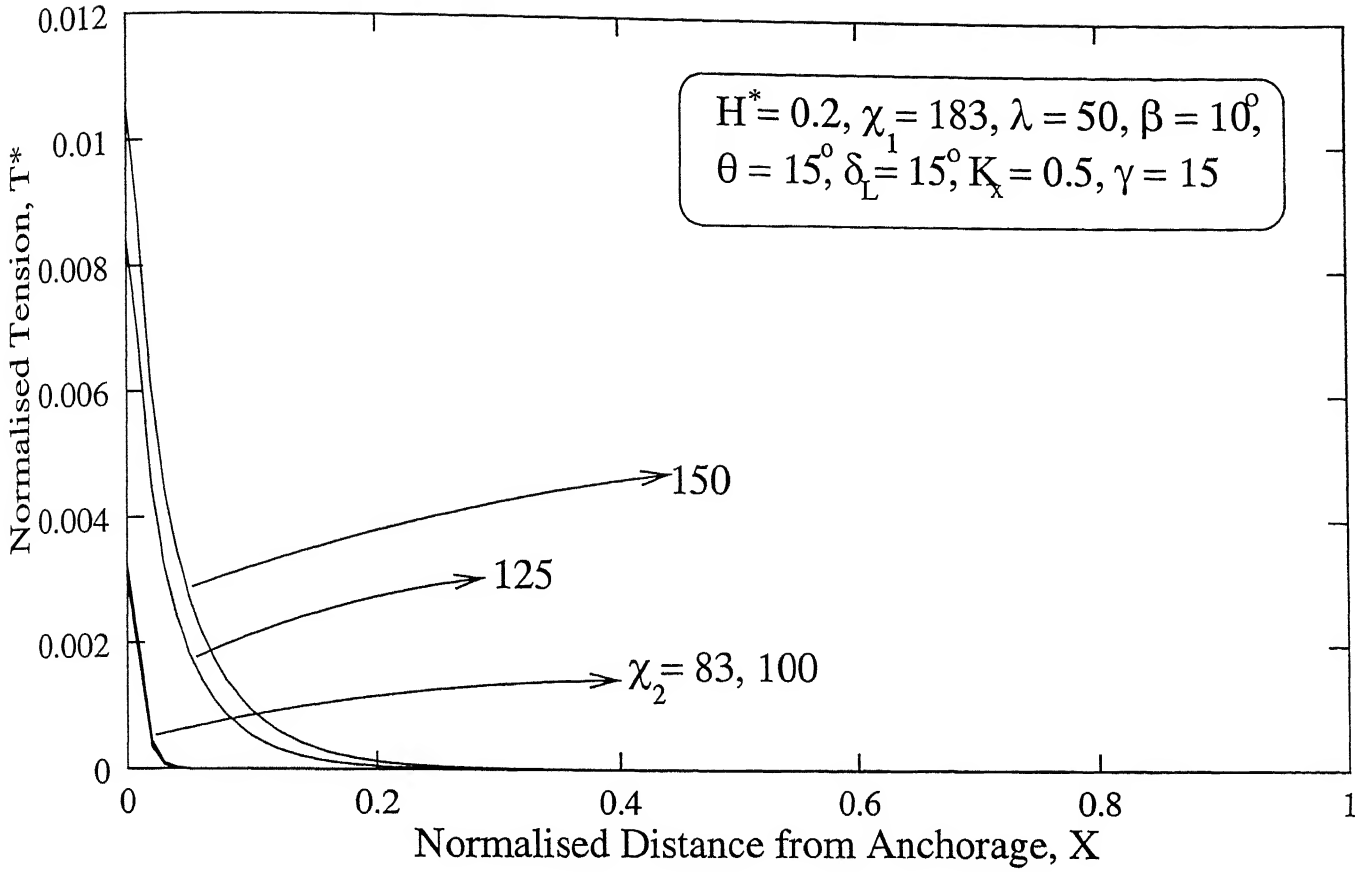

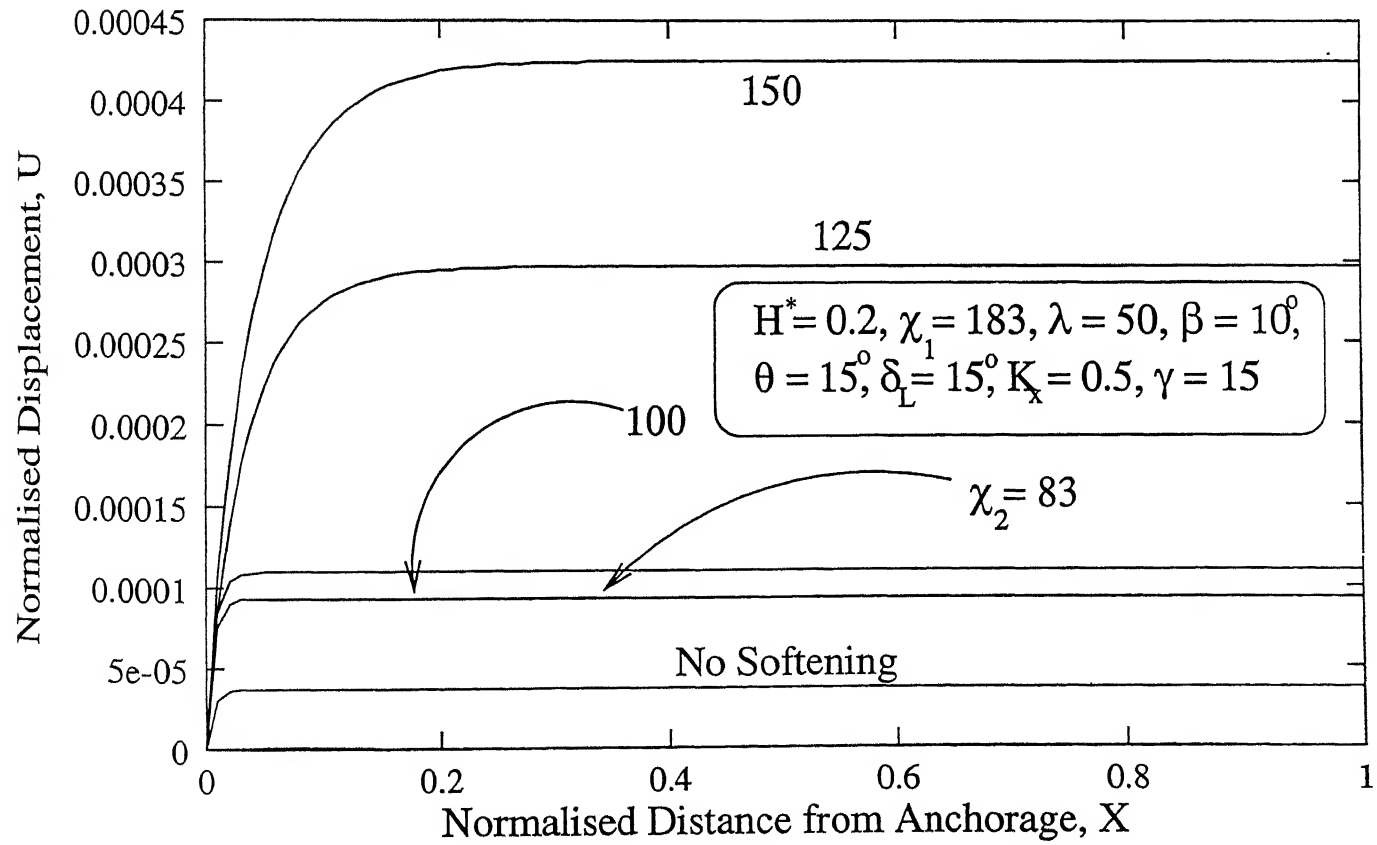

Figure 4.3.1: Effect of Strain Softening on (a) Normalised Tension and (b) Normalised Displacement

The variation of normalised tension with normalised distance is very steep near the anchorage. This variation decreases to zero from a normalised distance of 0.11 from the anchorage. The tension induced in the geomembrane increases drastically as χ_2 is increased. An increased value of χ_2 implies a steeper slope of the shear stress-displacement curve in the post-peak range. As the strain levels are nearly the same in all the cases, a steeper slope would mean lesser residual shear stresses being induced at the lower interface. As the strain levels are larger than the strain corrosponding to peak shear stress, the shear stresses mobilised at the lower interface tend towards the residual stress at the lower interface. Thus, as χ_2 increases, because of lesser residual stresses, more normalised tension and displacements are induced. From the displacement profile, one can notice that the normalised displacement increases very steeply near the anchorage and remains constant beyond a normalised distance of 0.2 from the anchorage. It can be noted that the normalised tension and displacement increase quite drastically if one considers the strain softening phenomenon. The maximum normalised tension values increase from 0.003 for a hyperbolic case to 0.015 for a strain softening case. Similar trends can be noticed with the profiles of normalised displacement. Thus one can conclude that it is very essential to include the effect of strain softening for proper estimation of tension, particularly if the results from the tests on geomembrane-clay interface indicate the phenomenon of strain softening.

4.4 Bilinear Stress-Strain Characteristics of the Geomembrane

Most of the geomembranes used in the construction of landfill liners have non-linear stress-strain characteristics. To study the effect of this non-linear response, the stress-strain characteristic curve has been assumed to be bilinear as discussed in section 3.4. The problem has been analysed and results obtained by varying the ratio of the final and initial moduli of deformation of the geomembrane, E_2/E_1, and the strain level, ε_0 at which the modulus of deformation of the geomembrane changes. The results are presented in Figures 4.4.1 and 4.4.2.

Figure 4.4.1 shows the variations of normalised tension and displacement with normalised distance from anchorage. The normalised tension decreases drastically

from a maximum value of 0.0086 at the anchorage for $E_2/E_1 = 1$ to a very small value at a normalised distance of 0.1 from the anchorage. Similar trends can be noticed with the profiles of variation of normalised displacement. The variation of displacement with normalised distance from anchorage has a very steep gradient near the anchorage. However, the gradients decrease with distance to a much lower value and remain constant after a normalised distance of 0.1 from the anchorage. However, the ratio of the final to initial moduli of deformation, E_2/E_1 doesn't have any significant effect on the tension profiles. The same can be noticed in the profiles of variation in normalised displacement. If the strain levels are less than 0.001, the normalised tension induced in the geomembrane decreases sharply with increasing values of E_2/E_1. The resulting maximum normalised tension for a linear stress-strain response for the geomembrane is 0.0086 which is greater than resulting tension with the assumption of a bilinear response. The assumption of perfectly linear response would lead to an overestimate of the tension induced in the geomembrane.

Figure 4.4.2 shows the variations of normalised displacement and tension for various values of the strain level, ε_0, at which the modulus of deformation changes. From the figure, it can be noticed that the normalised tension induced in the geomembrane decreases from a maximum value of 0.0077 at the anchorage to a very small value at a normalised distance of 0.11 beyond which it decreases slightly. The maximum normalised tension induced for a perfectly linear response is 0.0077, while it decreases to a value of 0.0047 for the strain parameter, $\varepsilon_0 = 0.01$. The normalised displacements increase steeply near the anchorage. However, the gradient decreases to a much smaller value beyond $X = 0.08$ distance from the anchorage. The maximum tension decreases with increasing ε_0. For very low values of ε_0, the maximum normalised tension induced equals to the normalised tension induced with a perfectly linear response. As the values of ε_0 are decreased, the stress-strain characteristic curve gets closer to perfectly linear one i.e., linear stress-strain characteristics. Similar variations can be noticed in the displacement profiles also. Most of the geomembranes have non-linear stress-strain characteristics, and the value of maximum tension induced vary significantly in case of bilinear response. It is necessary to consider the appropriate stress-strain response of geomembrane for estimating tension induced.

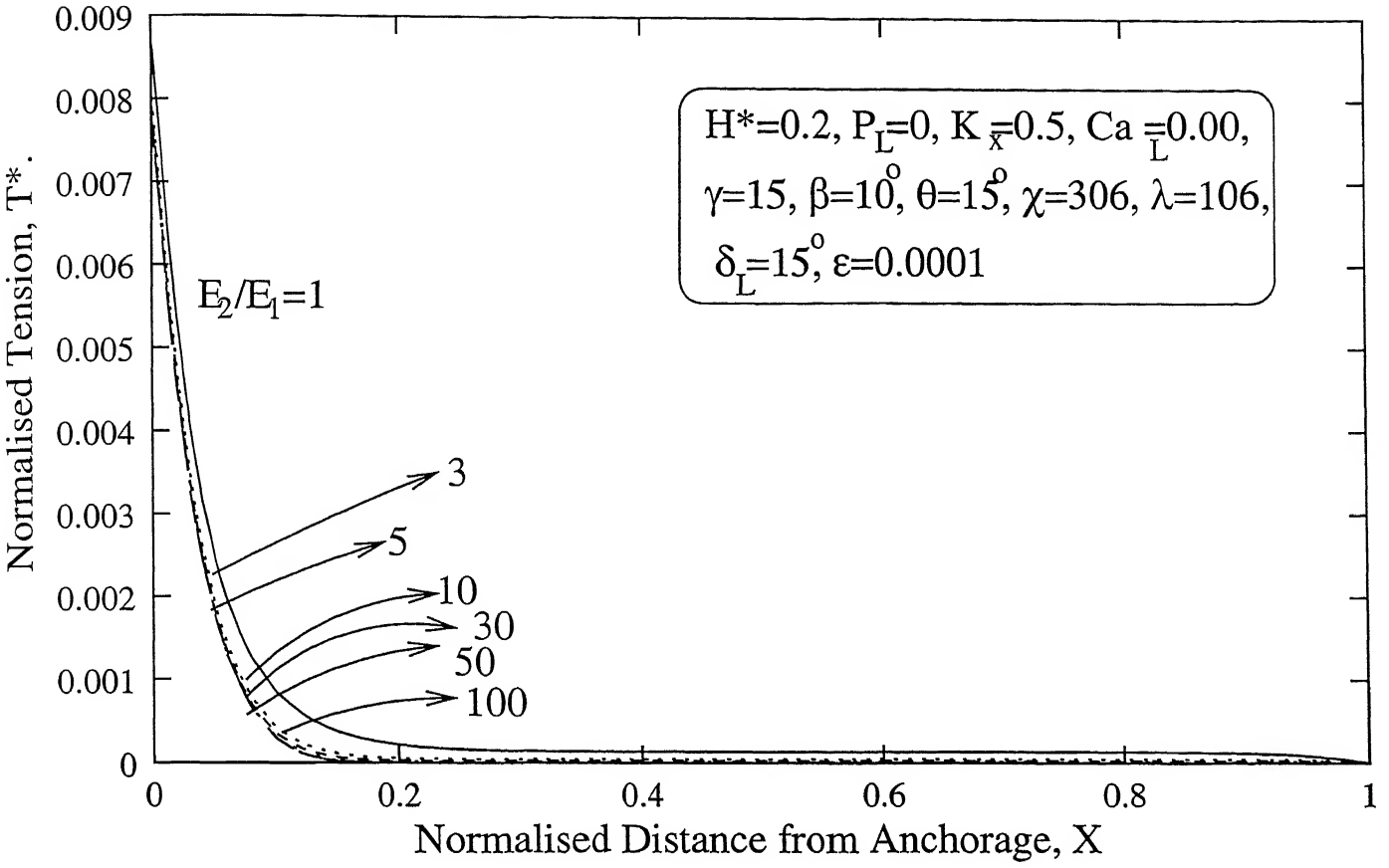

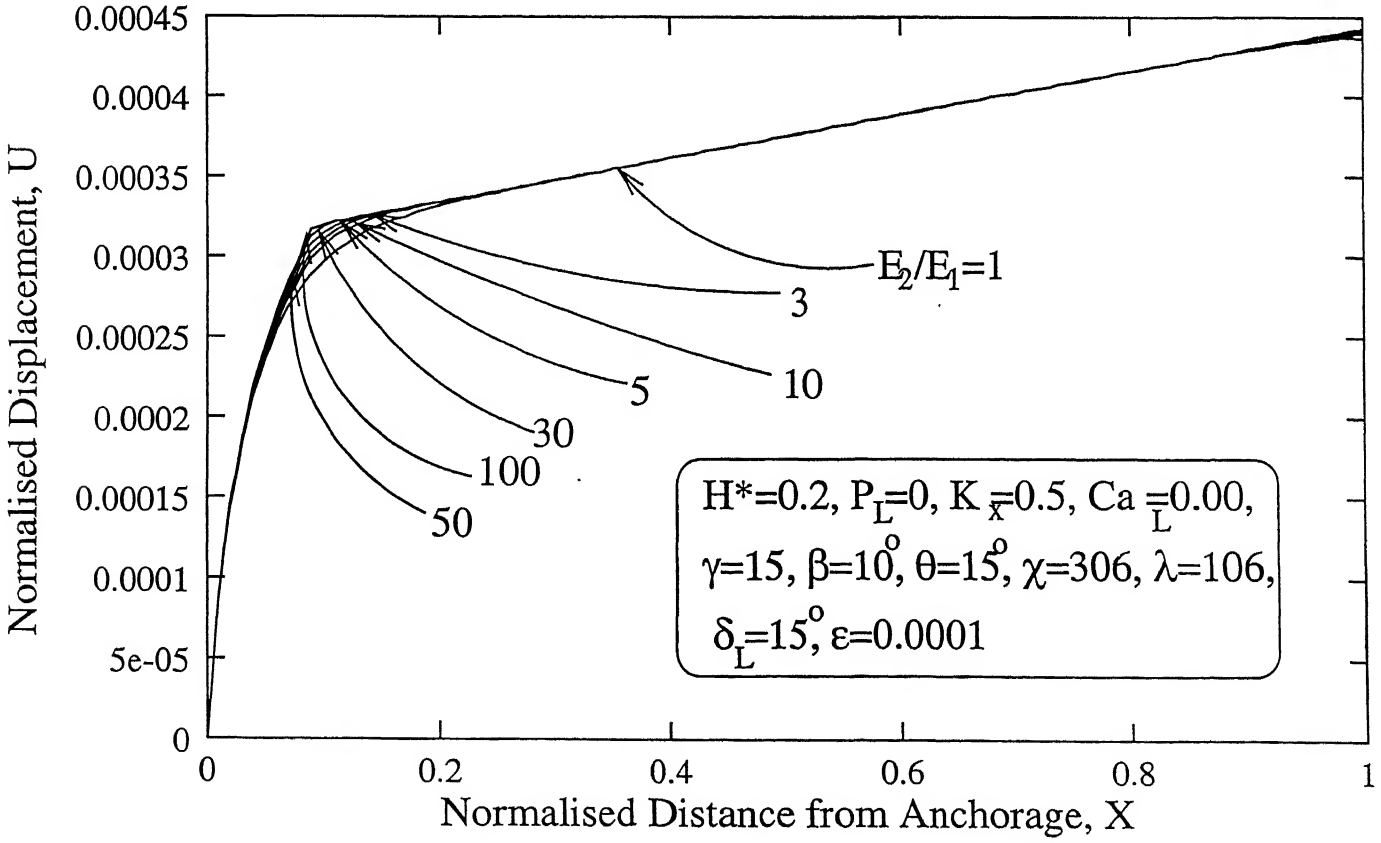

Figure 4.4.1: Effect of Change in Ratio of Moduli of Deformation on (a) Normalised Tension and (b) Normalised Displacement

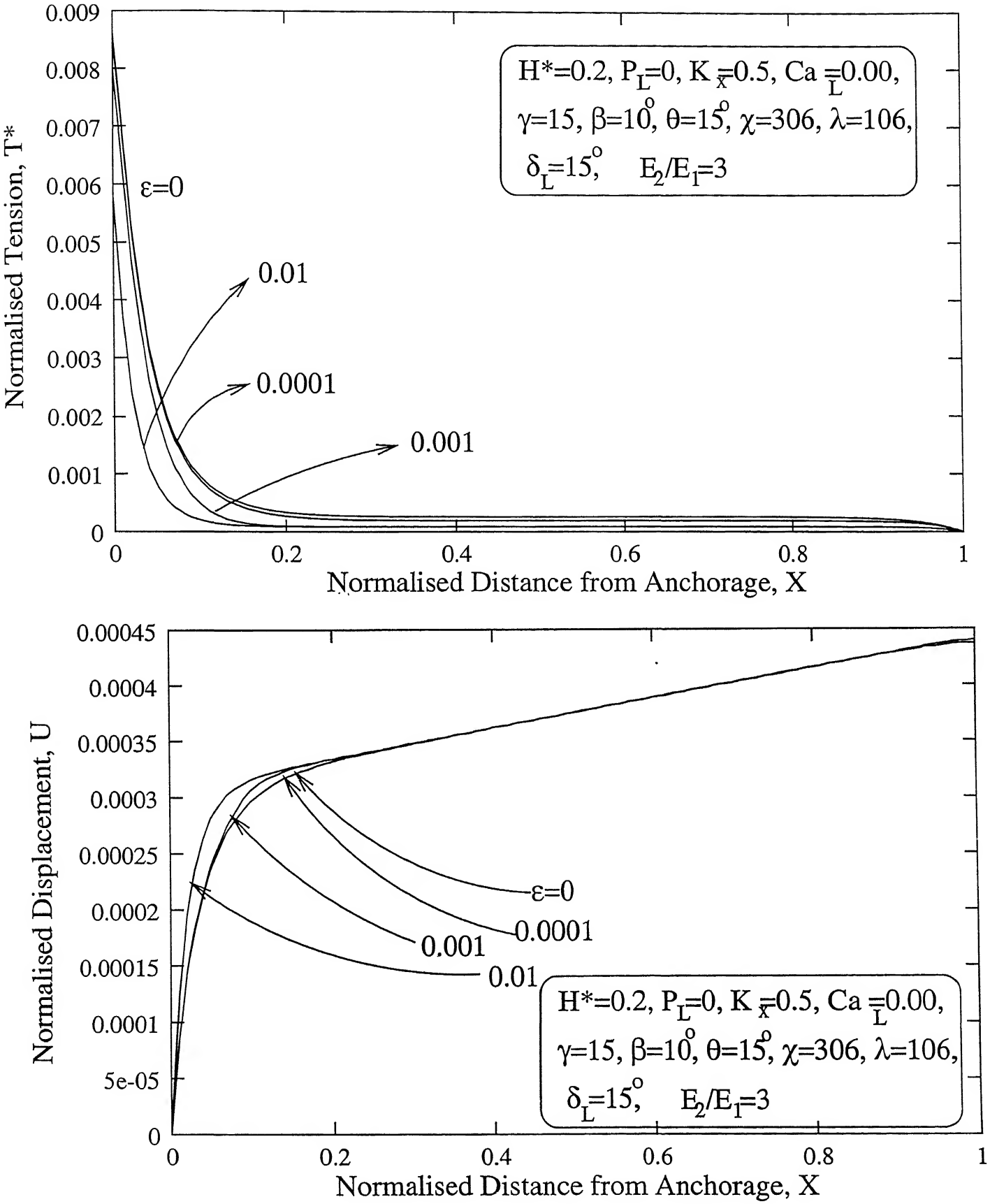

Figure 4.4.2: Effect of Change in Strain level, ε_o, on (a) Normalised Tension and (b) Normalised Displacement

4.5 Effect of Settlement of the Subgrade Soil

To study the effect of settlement of the subgrade soil on the tension induced in the geomembrane, the problem has been modeled by a three parameter model (originally proposed by Madhav and Pooroshasb, 1989). The analysis of the model was presented in Chapter 3. A parametric study carried out for the parameters ranging within appropriate ranges are presented in Figures 4.5.1 to 4.5.9.

The variation of normalised tension and settlement with normalised distance for various values of γ^* (= $\gamma/k_s L$, depends on the unit weight of the overburden material) is shown in figure 4.5.1. Maximum tension is at the anchorage and normalised tension decreases from anchorage to the free end. The variation is gradual. The normalised tension for $\gamma^* = 0.03$ is 0.00084 and decreases with γ^* and is equal to 0.00014 for γ^* equal to 0.005. As γ^* is directly proportional to the unit weight of the overburden material, γ, a higher value of γ^* would represent a much denser overburden, which induces more tension. The normalised settlement increases with normalised distance from anchorage. The slope of the curve increases with increasing values of γ^*. The normalised settlements at every point increase as γ^* increases. As $\gamma^*$is inversely proportional to the coefficient of subgrade modulus, a high value of γ^* represents a much softer subgrade, thus more settlements can be noticed. The maximum settlement for $\gamma^* = 0.03$ is 0.0108 while for $\gamma^* = 0.005$ is 0.0009.

Figure 4.5.2 shows the results obtained by varying the angle of inclination of the top of the landfill, β. For all values of β, the normalised tension decreases from a maximum value at the anchorage to zero at the free end with linear or nearly linear variation with distance. The maximum normalised tension of 0.00069 is induced for β is equal to -20° while the value for $\beta = 15^\circ$ is 0.00027. The value of maximum normalised tension decreases as β increases because a higher angle of inclination of the top of the landfill with the horizontal would mean lesser rate of increase of height of overburden with respect to distance resulting in lesser tension being induced in the geomembrane. The normalised settlements increase with normalised distance from anchorage for all value of β. The gradients of normalised tension and settlement

curves with distance increase as β decreases. The normalised settlements at all points increase with decreasing values of β because as β decreases, the rate of increase of height of overburden increases resulting in more settlements.

Figure 4.5.3 shows the variations of normalised tension and settlement with normalised distance for various values of angle of inclination of the geomembrane, θ. The normalised tension has a maximum value of 0.0012 which decreases to zero at the free end for $\theta = 40^{\circ}$ while the maximum normalised tension is 0.00048 at the anchorage for $\theta = 0^{\circ}$. A value of 0° for θ means that the geomembrane is horizontal. However, tension is induced in this case also as shear stresses are induced at the upper interface because of a linearly increasing loading (as $\beta = -20^{\circ}$). The tension increases with increasing θ. The maximum value of normalised tension for $\theta = 40^{\circ}$ is 0.0012 while it is equal to 0.00048 for $\theta = 0^{\circ}$. The reason could be that as θ increases, the rate of increase in the height of overburden increases and this would result in more tension. From the settlement profile, it can be noticed that the normalised settlement increases from a minimum at the anchorage to a maximum at the free end. Typical values of normalised settlement are 0.0073 and 0.0035 at the anchorage and 0.0162 and 0.006 at the free end respectively for $\theta = 40^{\circ}$ and for $\theta = 0^{\circ}$. The settlement increases uniformly with increase in θ. For $\theta = 40^{\circ}$ and 0°, it is equal to 0.0073 and 0.0035 respectively. As any increase in θ would entail an increase of overburden material, larger settlements result for higher values of θ.

The coefficient of lateral earth pressure, k_x, was varied from 0 to 1.0. The results obtained are presented in Figure 4.5.4. The figure shows the variation of normalised tension and settlement with normalised distance from anchorage. The value of maximum normalised tension for $k_x = 1.0$ and 0 are 0.0013 and 0.0008 respectively. The value of normalised settlement for $k_x = 1.0$ at the anchorage is 0.0086 and increases to 0.00168 at the free end. For $k_x = 0$, the normalised settlement at the free end is 0.001 while it is equal to 0.00168 for $k_x = 1.0$. As the normal stresses increase with increasing k_x, a high value of k_x would means larger settlements. Similarly, the shear stresses at the upper interface of the geomembrane, decrease with increasing k_x. So, the tension induced in the geomembrane decreases with increasing k_x.

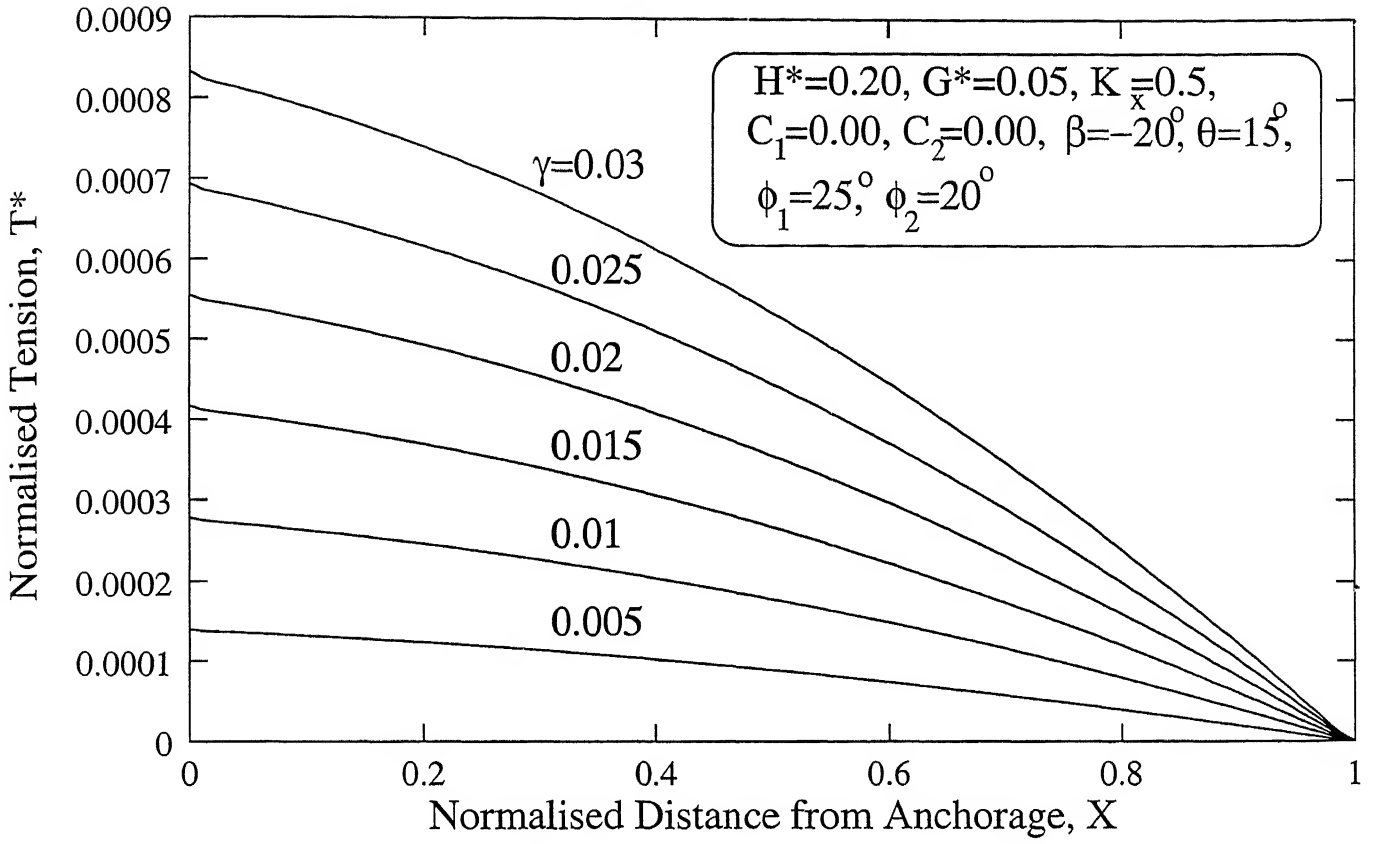

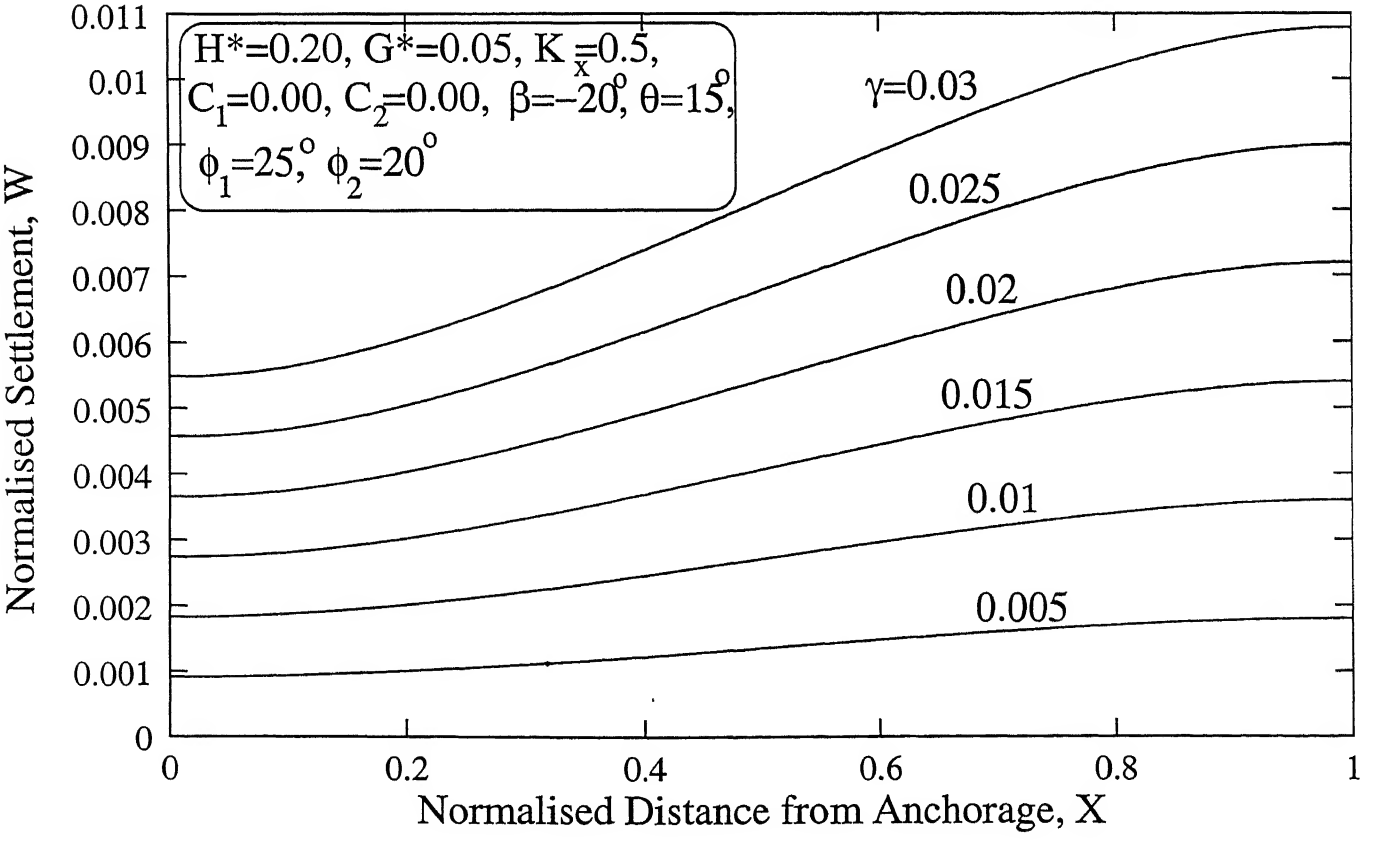

Figure 4.5.1: Variation of (a) Normalised Tension and (b) Normalised Settlement for various values of γ^* (Model Study)

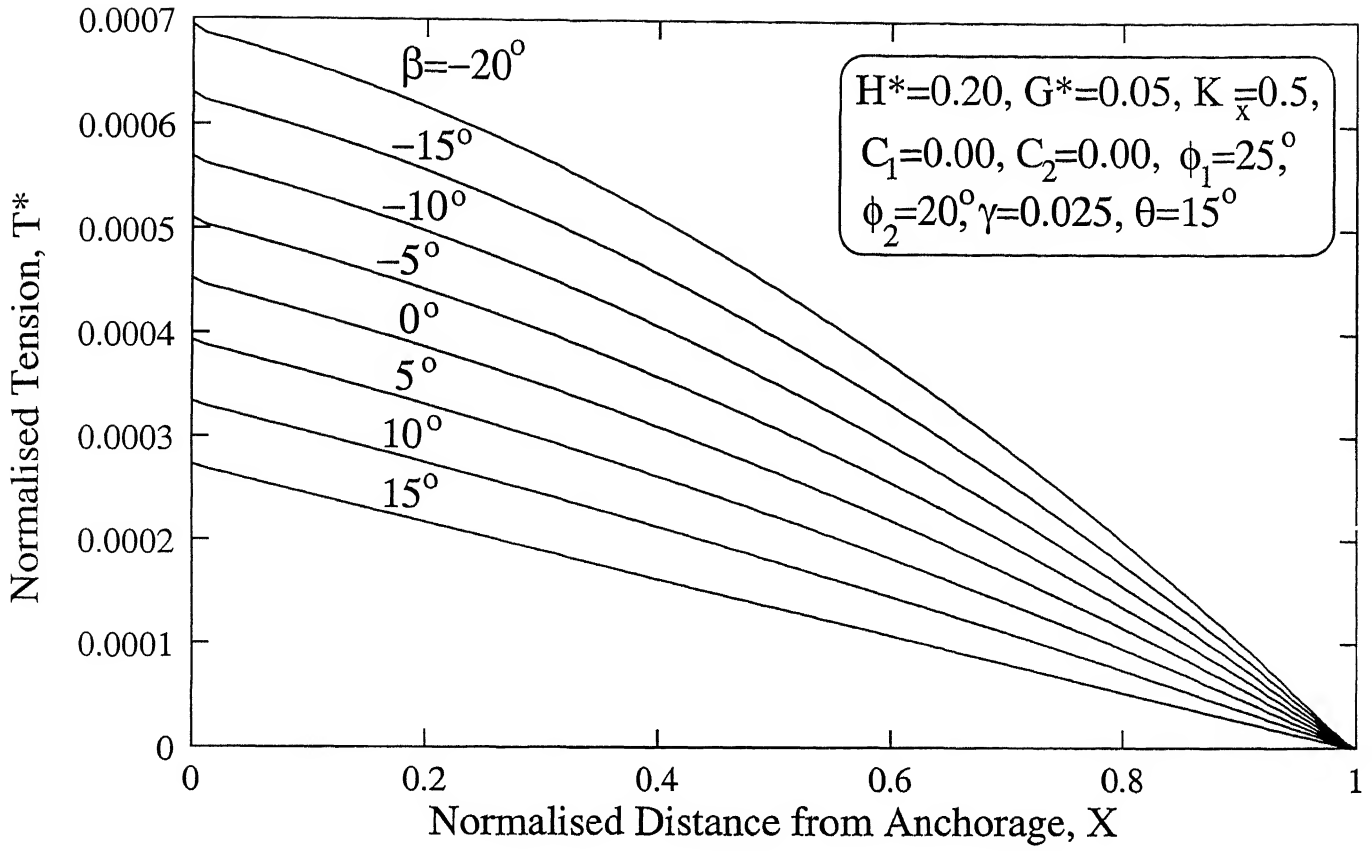

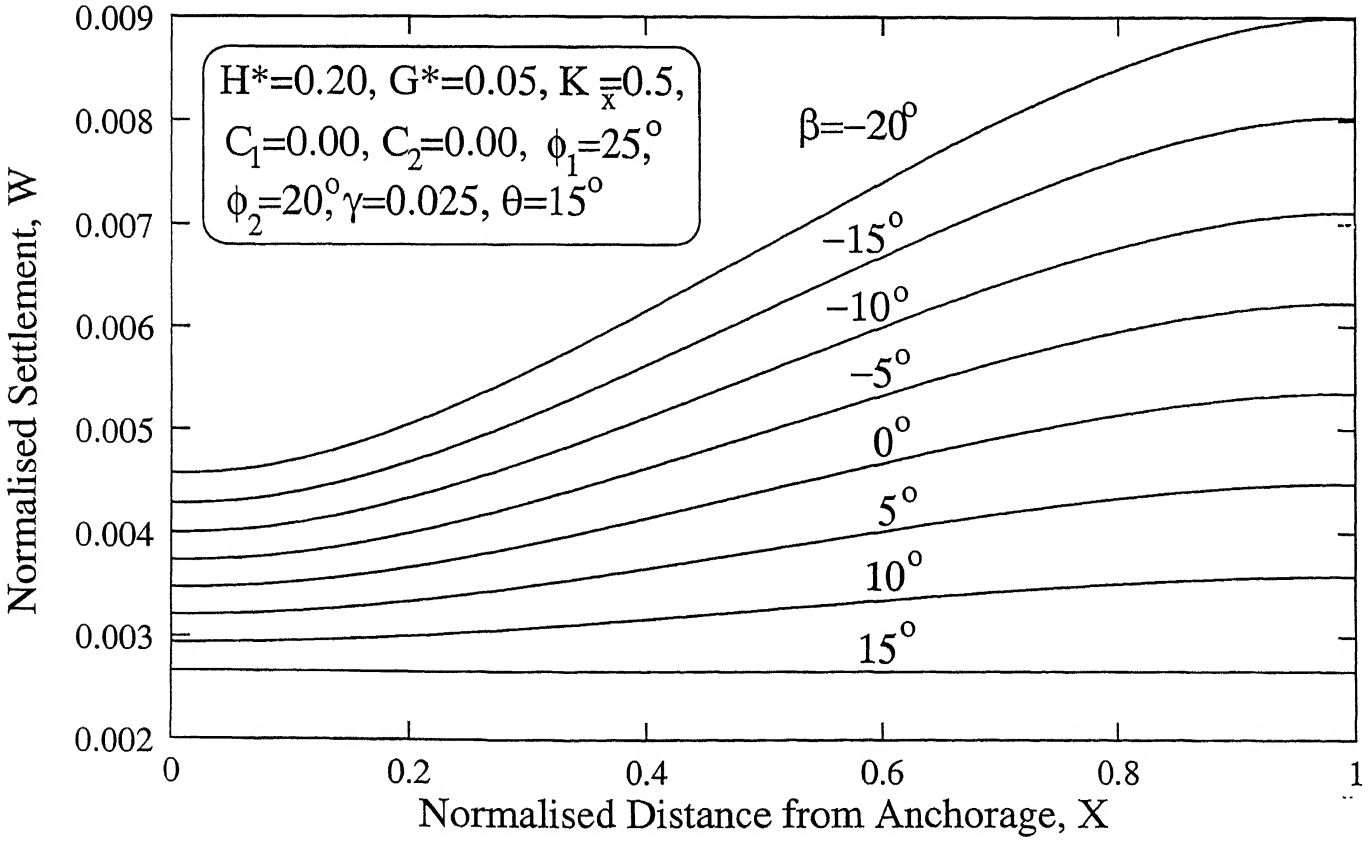

Figure 4.5.2: Variation of (a) Normalised Tension and (b) Normalised Settlement for various values of β (Model Study)

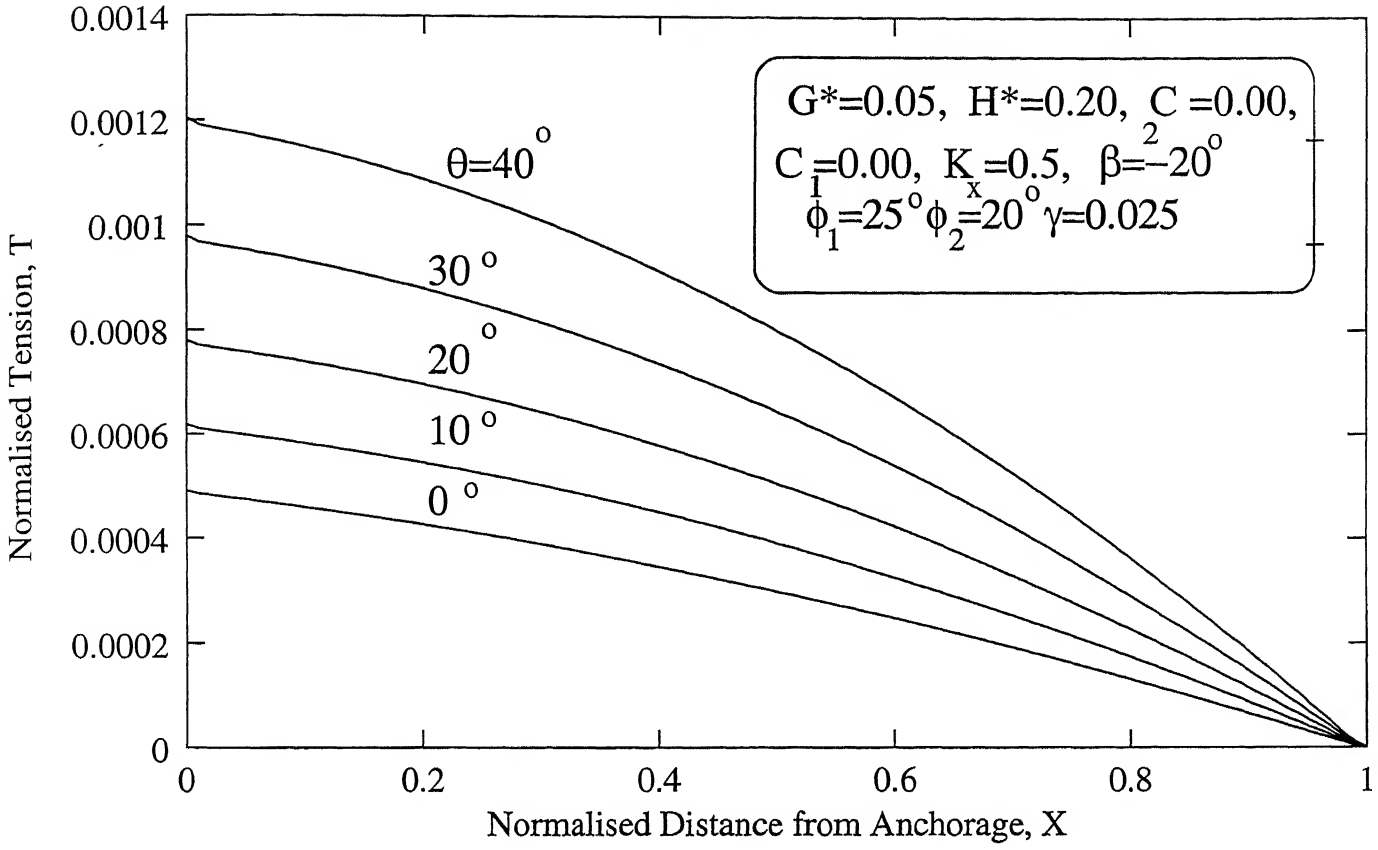

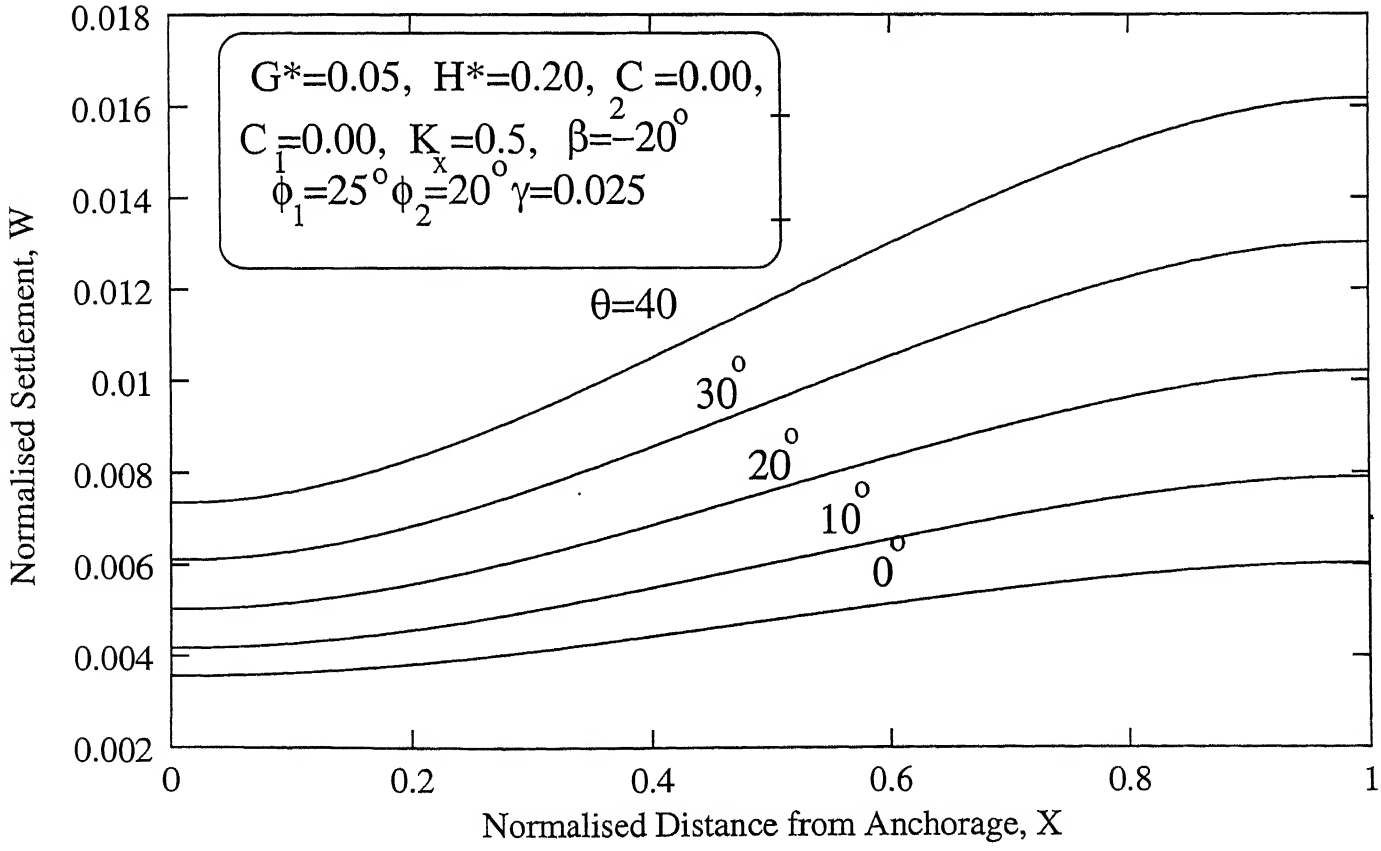

Figure 4.5.3: Variation of (a) Normalised Tension and (b) Normalised Settlement for various values of θ (Model Study)

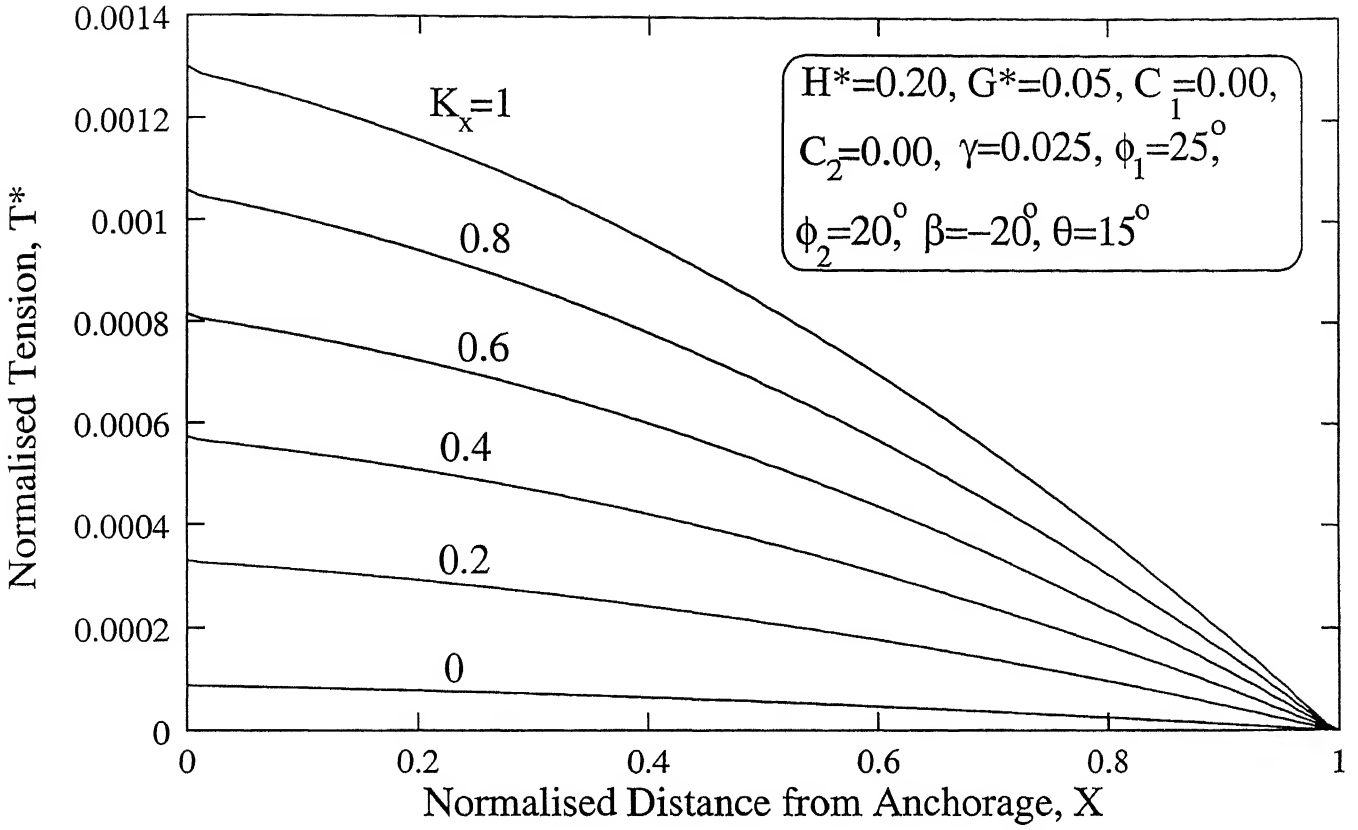

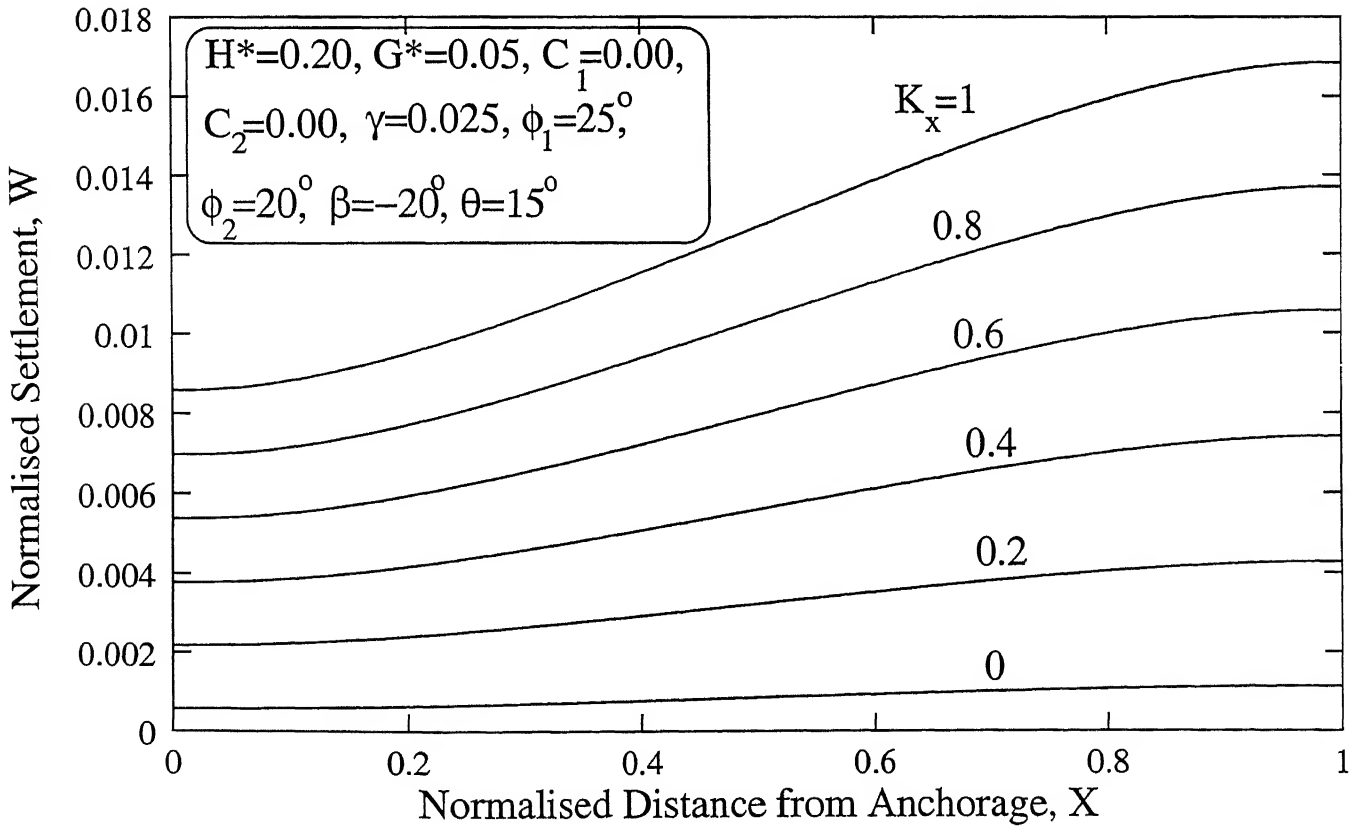

Figure 4.5.4: Variation of (a) Normalised Tension and (b) Normalised Settlement for various values of k_x (Model Study)

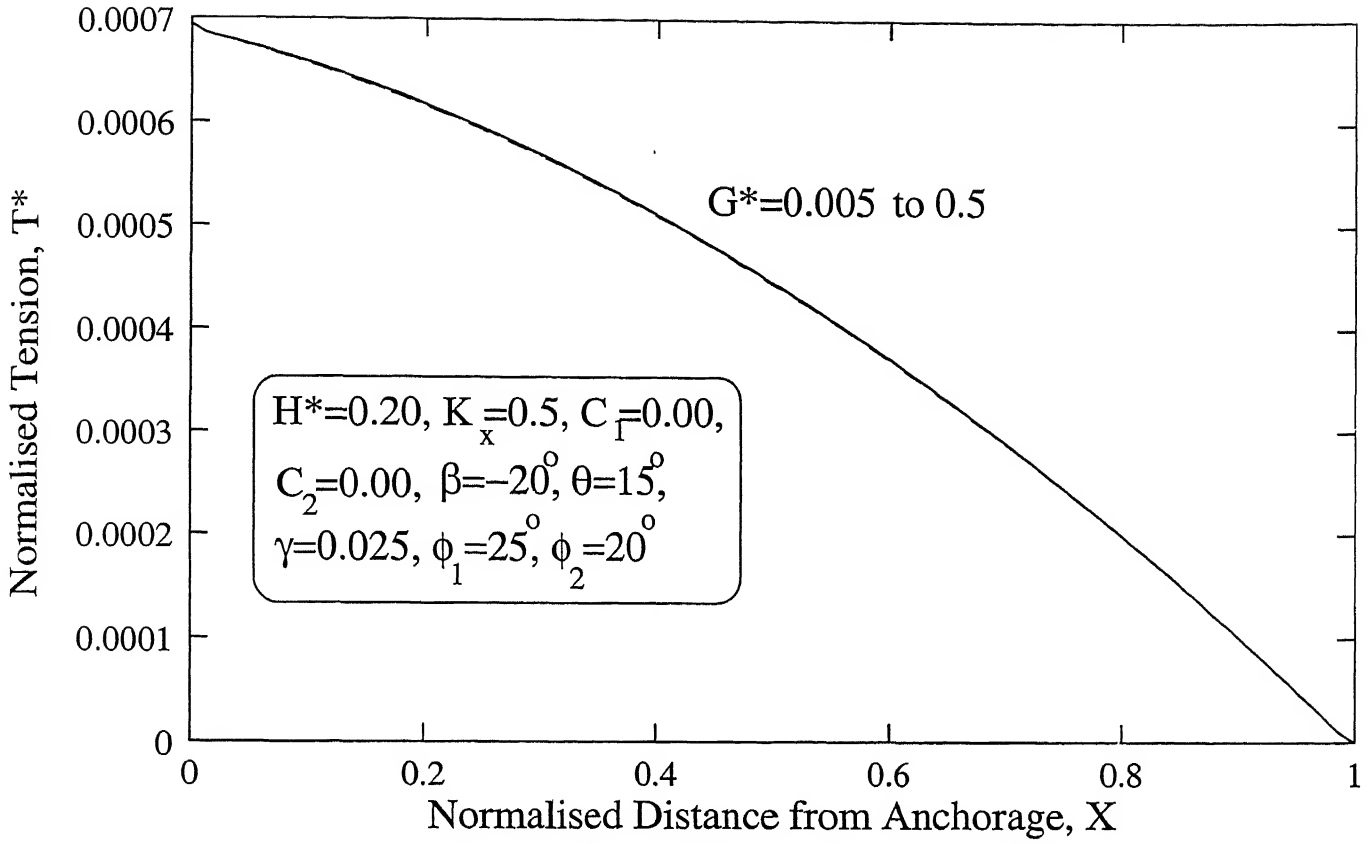

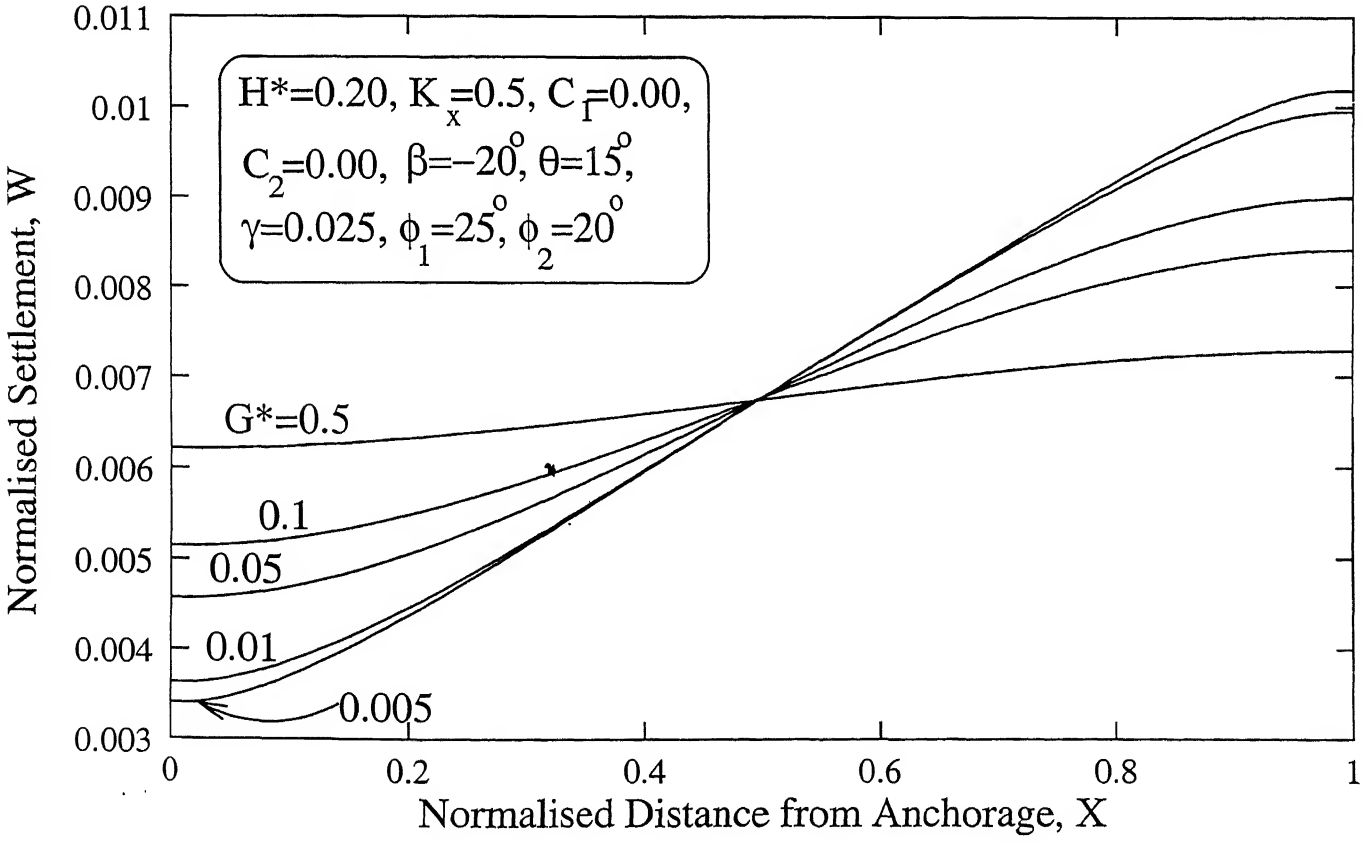

Figure 4.5.5: Variation of (a) Normalised Tension and (b) Normalised Settlement for various values of G^* (Model Study)

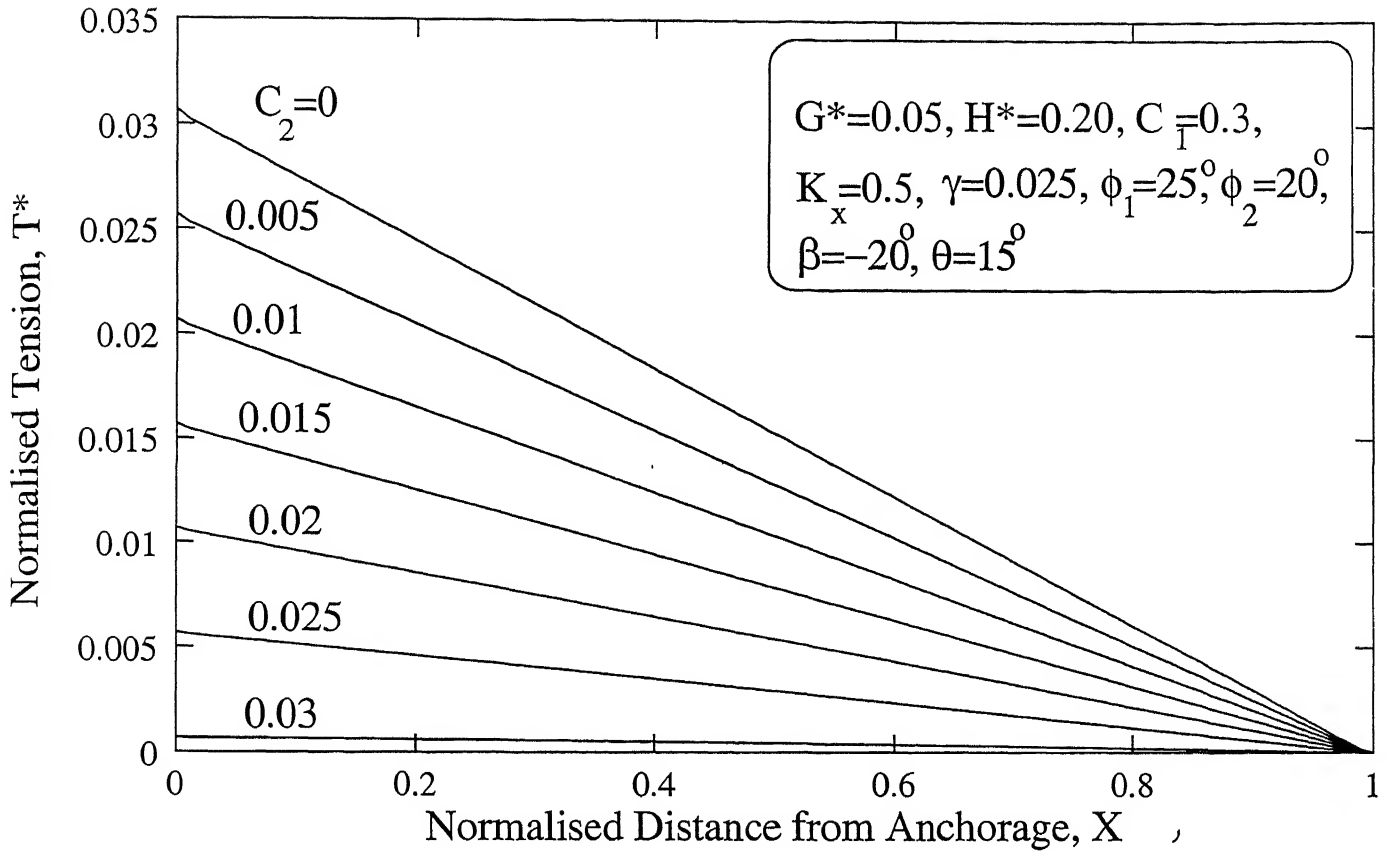

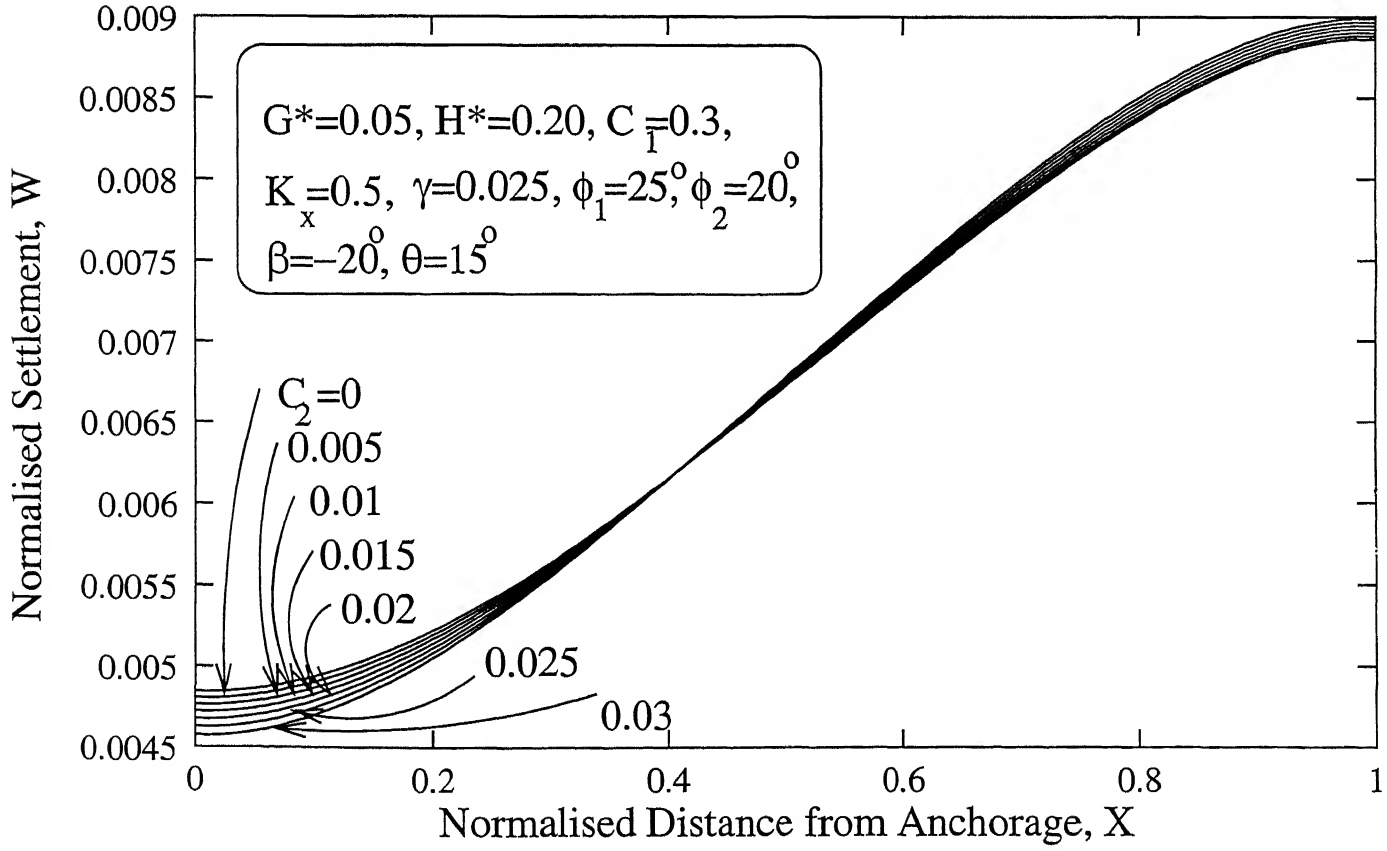

Figure 4.5.6: Variation of (a) Normalised Tension and (b) Normalised Settlement for various values of C_2 (Model Study)

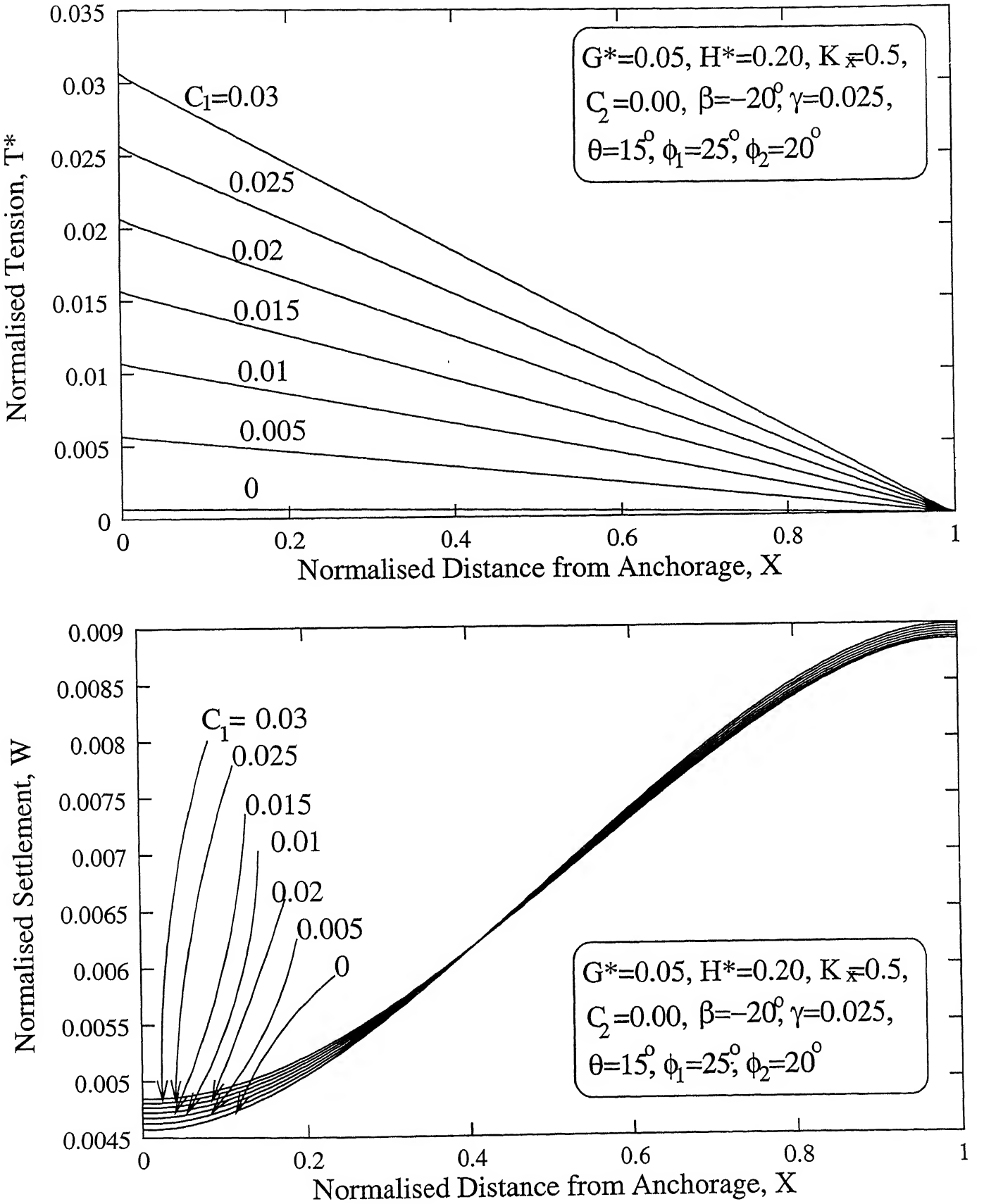

Figure 4.5.7: Variation of (a) Normalised Tension and (b) Normalised Settlement for various values of C_1 (Model Study)

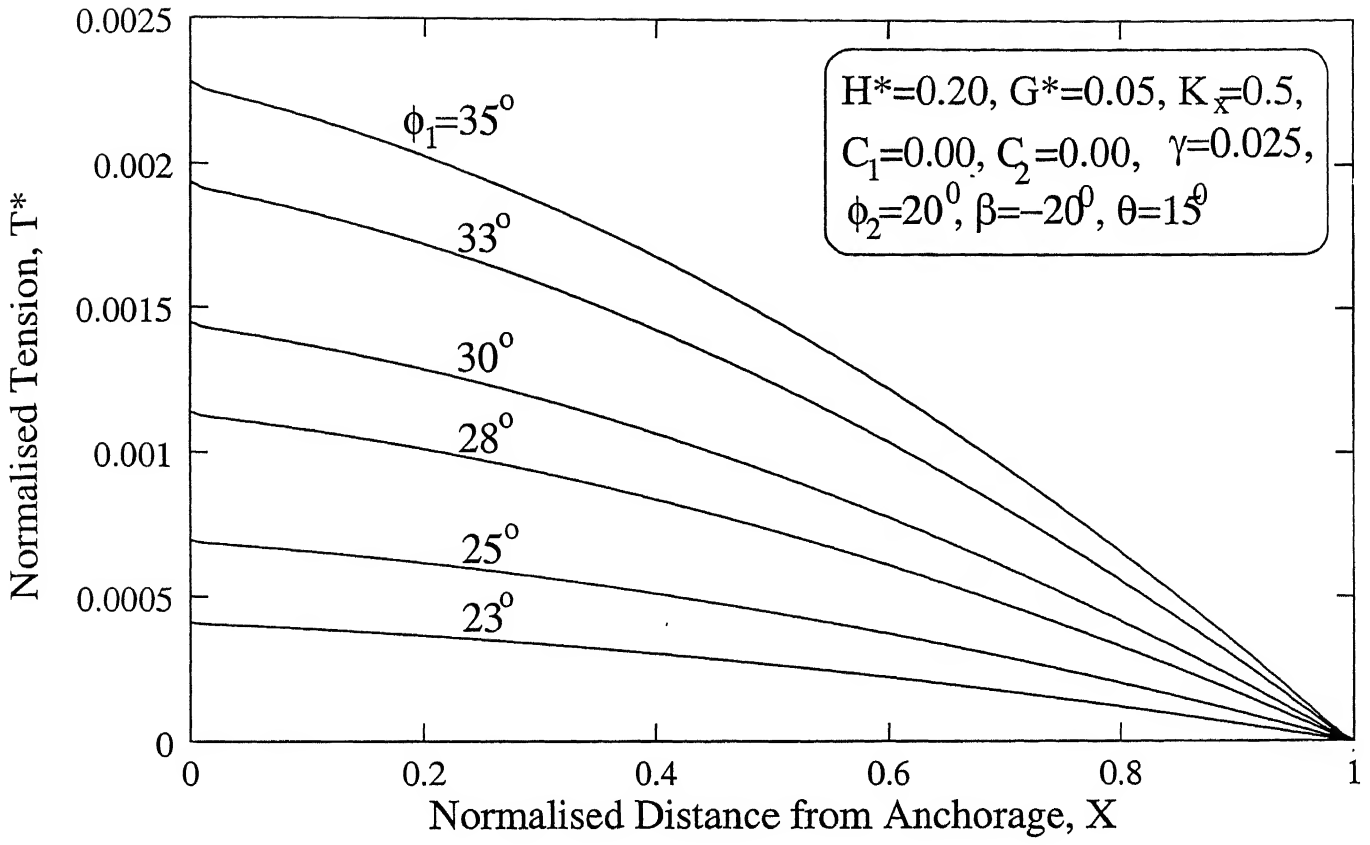

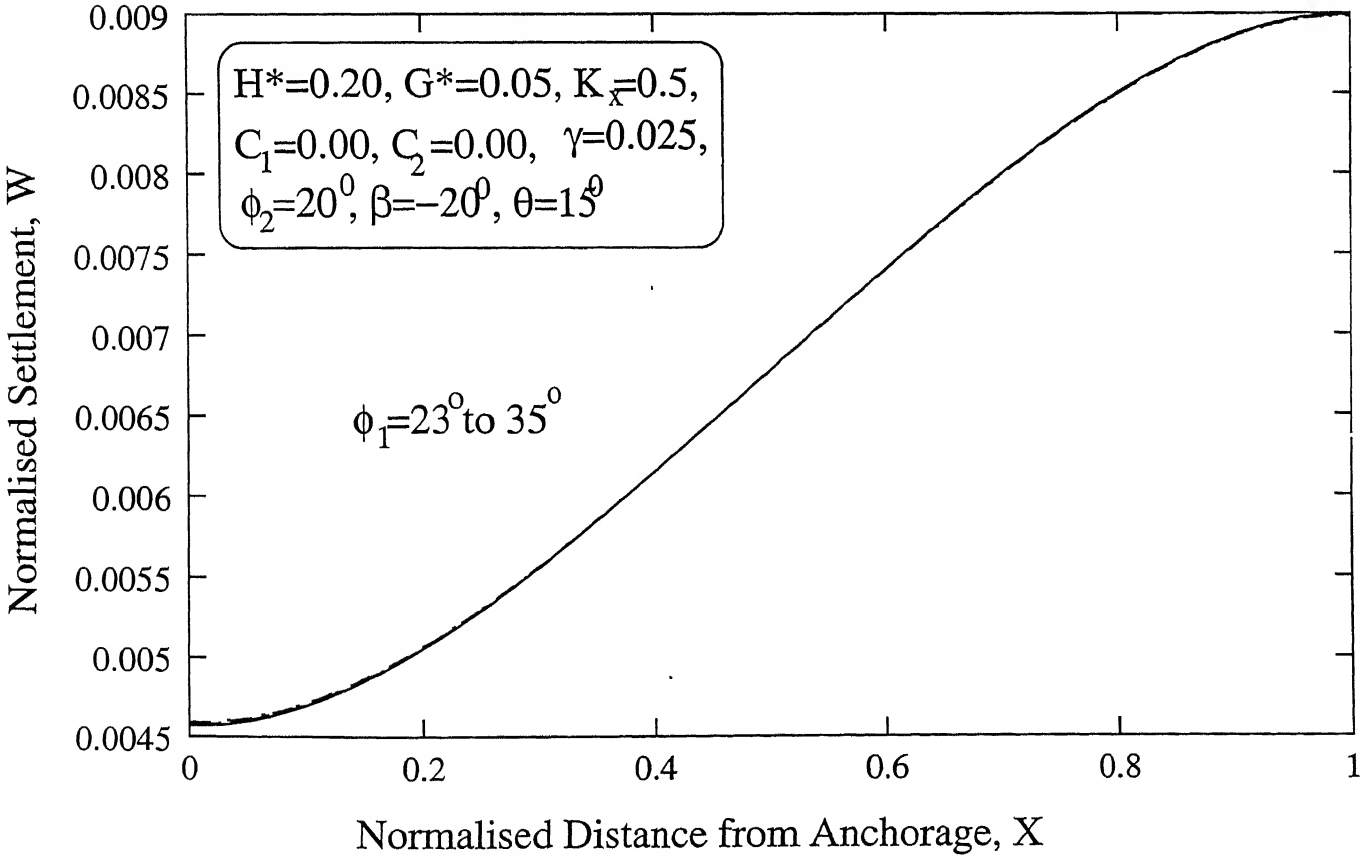

Figure 4.5.8: Variation of (a) Normalised Tension and (b) Normalised Settlement for various values of ϕ_1 (Model Study)

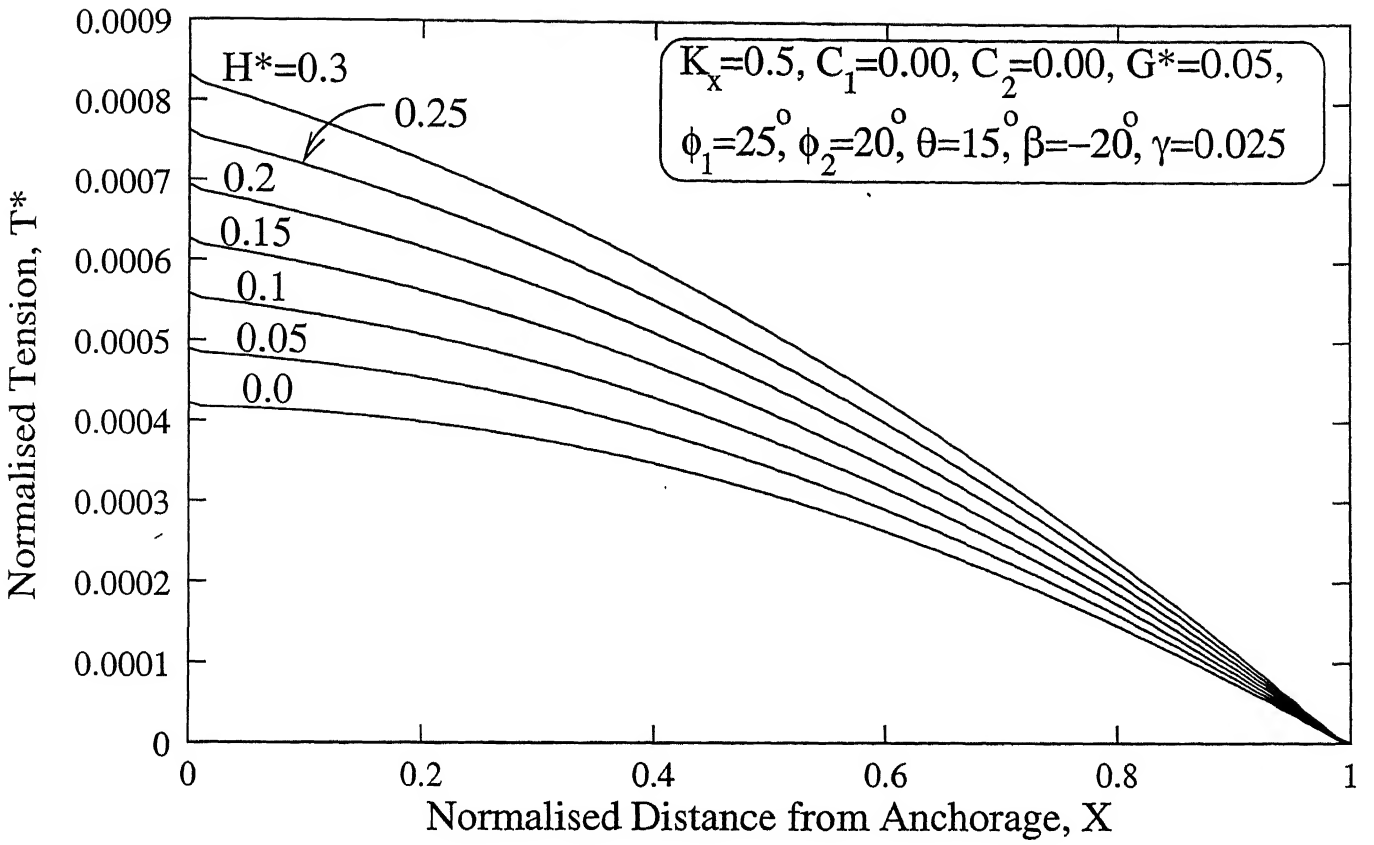

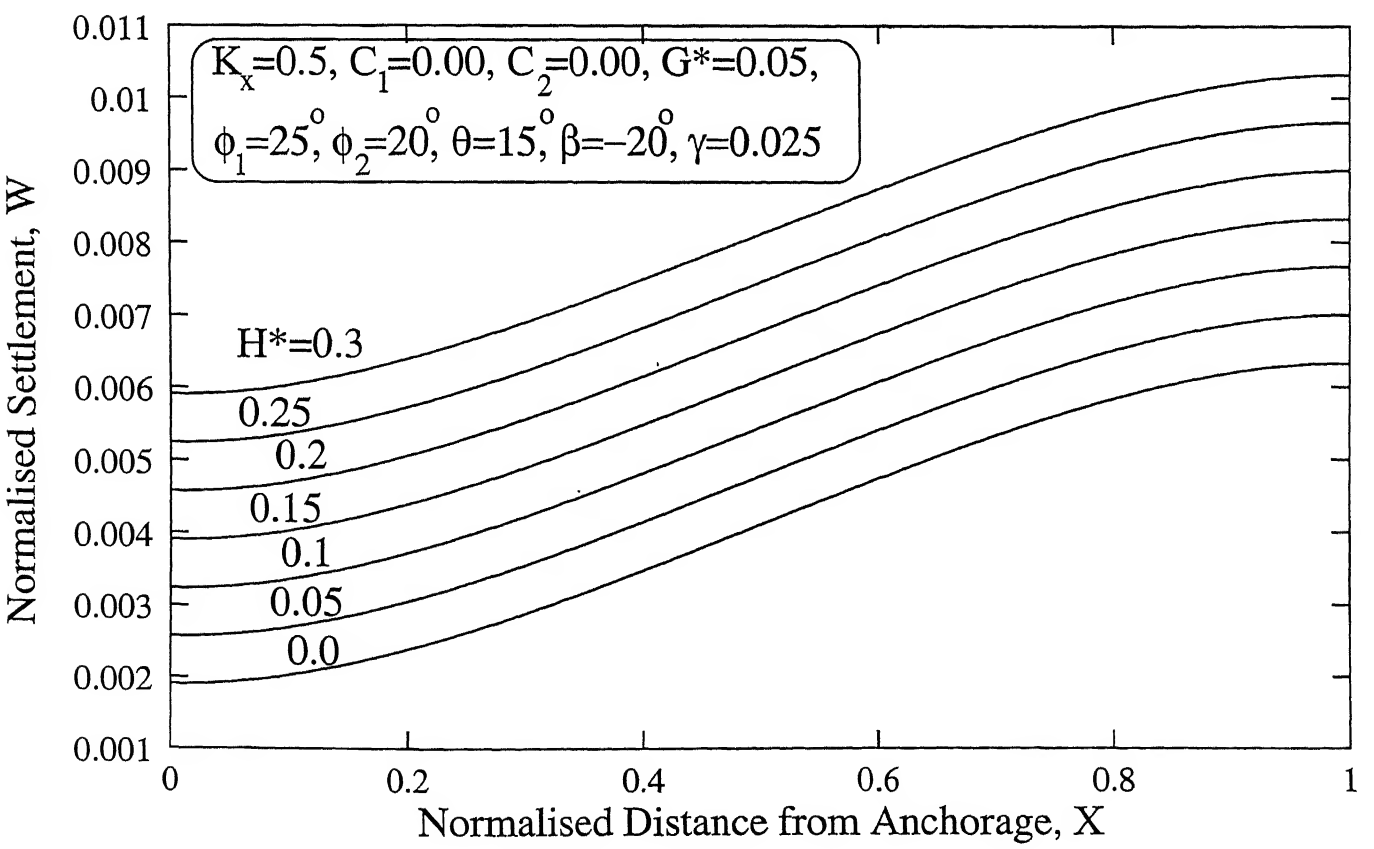

Figure 4.5.9: Variation of (a) Normalised Tension and (b) Normalised Settlement for various values of H^* (Model Study)

To study the effect of the shear modulus, G of the clay layer, the non-dimensional parameter, $G^*(= GH/k_s L^2$, depends on G/k_s) was varied. The results are presented in Figure 4.5.5. The variation of normalised tension and settlement with normalised distance from anchorage are shown in the figure. The value of normalised tension is equal to 0.00069. The profile of normalised tension is independent of G^*. The value of tension is an integral of shear stresses acting on either side of the reinforcing membrane. Full mobilisation of shear strength in the lower interface ensuresindependence of tension with G^*. The normalised settlement increases from a minimum value 0.00325 at the anchorage to a maximum value of 0.012 at the free end for $G^* = 0.005$. As G^* is increased to 0.5, the normalised settlement at the anchorage increases to 0.0062 while at the free end, it decreases to 0.0073. The settlement is the same at a normalised distance of 0.5 from the anchorage i.e., half way through the length of the geomembrane. Smaller variation can be seen in the maximum and minimum values of normalised settlement for a high value of G^*. For $G^* = 0.5$, the difference is just 0.0011, while for $G^* = 0.005$, the difference between the maximum and the minimum values is as much as 0.00875. From the results one can conclude that a stiffer clay liner with a high value of G^* is preferable as it will result in lesser differential settlement.

To study the effect of adhesion between the geomembrane and clay at the lower interface, the non-dimensional parameter, $C_2(= c_{a2}/k_s L)$ was varied. Results obtained are presented in Figure 4.5.6. Normalised tension decreases linearly with distance. The maximum value of normalised tension is 0.031 and 0.001 for $C_2 = 0$ and 0.03 respectively. The value of normalised tension decreases with increasing C_2. More resisting shear is mobilised at the lower interface for higher values of C_2, resulting in lesser values of tension induced in the geomembrane. The profile of normalised settlement is not sensitive to C_2. Similar trends were noticed when the angle of friction at the lower interface, ϕ_2 was varied from 0° to 23°.

As the shear stress at the upper interface is the disturbing force, the shear parameters, C_1 and ϕ_1 were varied to study the effect of shear parameters on the tension induced and settlement in the clay liner. Results obtained are presented in

Figures 4.5.7 and 4.5.8. The profile of variation of tension is quite similar to the previous case wherein the adhesion at the lower interface, C_2 was varied. The profile of variation in settlement is also similar to the previous case. The maximum normalised tension at the anchorage was 0.031 for C_1 = 0.03. The increase in normalised tension with increase in C_1 is because of more disturbing shear stresses, resulting in more tension, being induced at the upper interface for higher values of C_1. Similar variations can be noticed as ϕ_1 was varied from 23° to 35°. The results obtained are shown in Figure 4.5.8.

The non-dimensional factor, $H^*(= H/L)$, was varied to study (Figure 4.6.9) the effect of height of the overburden. The normalised tension is 0.00083 and 0.00042 for H^* = 0.3 and 0.0 respectively. The variation of normalised tension with normalised distance is smooth. The normalised settlement profiles are all parallel to each other. As an increase the height of overburden at the anchorage would increase the normal and shear stresses acting at the upper interface, the tension induced in the geomembrane and the settlement in the clay liner would increase with in H^*.

The effect of various parameters on tension induced in the geomembrane was studied. Tension, displacement and settlement are sensitive to all the geometric properties of a landfill and to most of the stress-strain properties of the materials and interfaces between them. The conclusions and summary of the results obtained are given in Chapter 5.

CHAPTER 5
CONCLUSIONS

Engineered landfills offer a safe solution for proper management of waste. Use of geosynthetics in the liner system has become imperative. Tension is induced in the geomembrane of a GCL because of down-slope shear stresses induced owing to the overburden material. The tension induced is effected by many aspects like the shear stress-displacement characteristics of the geomembrane-clay interface, the stress-strain characteristics of the geomembrane material etc. A three-parameter model was proposed to study the effect of settlement of the subgrade on the tension induced. An attempt has been made and the analyses presented to estimate the tension induced in the geomembrane, taking the various factors effecting the tension, into consideration. To study the effect of various parameters involved, a parametric study was carried out for their respective ranges. These parameters were the geometric parameters of the landfill, the stress-strain properties of the geomembrane material and the shear-stress characteristics of the geomembrane-clay interface. The results are presented in chapter 4.

The angles of inclination of the geomembrane and the top of the landfill with the horizontal, θ and β respectively and the height of the overburden material at the anchorage signify the geometry of the landfill. These parameters were varied and the values of tension induced in the geomembrane for all values were obtained. From the results obtained by varying the geometric properties of the landfill, the amount of tension induced is significantly effected by changes in the geometry of the landfill. Tension induced in the geomembrane increases with increasing angle of inclination, θ, of the landfill with the horizontal, θ and decreases with the angle of inclination, β, of the top of the landfill with the horizontal. The values of tension induced were increase with increasing values of the non-dimensional parameter, H^*(= H/L, where H is the height of the overburden near anchorage and L is the length of the landfill). The slope of the tension-distance from the anchorage profile was varies with the angles of inclination of the geomembrane and the top of the landfill while the slope remains the same for all values of H^*. Similar trends were noticed in the profile of displacement of geomembrane also.

The effects of the stress-strain parameters involved on the tension induced were studied by varying all the parameters within their ranges. For an increase in the value of the non-dimensional parameter, χ (= $\sqrt{k_s L^2/tE}$), the tension and the displacements induced in the geomembrane decrease, while they increase with increasing values of λ (= $\gamma L^2/tE$). Similarly as the shear parameters at the lower interface, c_{aL} and δ_L were increased, the induced tension and displacements decrease. As the coefficient of lateral earth pressure was increased, the tension and displacement induced in the geomembrane were decreasing.

The effect of displacement softening along the lower interface, on the tension and displacements induced was studied by assuming a shear stress-displacement curve as shown in Figure 3.3.2. Tension and displacements induced in the geomembrane were significantly effected by the above assumption and were very sensitive to the post-peak slope of the assumed shear stress-displacement curve, $k_{\tau 2}$. The tension and displacements induced in the geomembrane with this assumption were higher than those with a hyperbolic interface response and the variation between the resulting tensions and displacements in both the cases considerable.

To study the effect of stress-strain behavior of geomembrane material, a bilinear stress-strain response has been proposed. The effect of a bilinear stress-strain response was significant and there was considerable variation in the values of induced tension and displacement. The tension and displacements induced with this assumption were less than those with a perfectly elastic geomembrane material (linear stress-strain response).

To study the effect of settlement on the tension induced, a three-parameter mathematical model simulated the problem. Results were obtained by varying the geometric and the shear parameters representing the model. The tension induced was sensitive to all the geometric properties and the trends were similar to those of the previous case. The settlements increase with increasing angle of inclination, θ, of the geomembrane with the horizontal while it decreases with the angle of inclination, β,

of the top of the landfill. The settlements increase with the non-dimension parameter, H^*, representing the height of the overburden.

The non-dimensional parameters based on the stress-strain properties of the materials, i.e, soil, geomembrane, waste and their interfaces were varied to study their effects on tension and displacement in the geomembrane. The tension and displacement were increasing when the non-dimensional parameter, γ^*, was increased. The non-dimensional parameter, G^* had no effect on tension and for increasing values of G^*, the slope of the displacement profile decreased. For various values of the coefficient of lateral earth pressure of the overburden, k_x, the variation in tension was similar to that from the previous model while the displacements increase with increasing values of k_x. The tension induced in the geomembrane was decreases with increasing values of shear parameters, ϕ_2 and c_2, at the lower interface while it increases with the shear parameters, ϕ_1 and c_1, at the upper interface. The shear parameters had no effect on the displacement profile and it remained the same for all values of the shear parameters at both the interfaces.

In all the studies, the maximum tension was induced at the anchorage while the maximum settlement and displacement were noticed at the free end. All the parameters excepting for G^*, had some effect on the tension induced in the geomembrane. As full shear strengths are assumed to be mobilised at both the interfaces, and as tension depends mainly on them, the shear modulus of the clay underneath, G, would have no effect on the tension. The effects of the geometric properties of the landfill were more than those of the stress-strain properties of the materials and the interfaces between them. Similar trends were noticed for the displacements in the geomembrane. The settlement in the subgrade was mainly effected by the geometric properties and the shear parameters at the interfaces had no effect on the settlement.

REFERENCES

Benson, C. H. and Daniel, D. E(1990). "Influence of Clods on Hydraulic Conductivity of Compacted Clays," *Journal of Geotechnical Engineering Division*, ASCE. pp. 1231-1248.

Bowders, J. J. and Daniel, D. E. (1987). "Hydraulic Conductivity of Compacted Clays to Dilute Organic Chemicals," *Journal of Geotechnical Engineering*, ASCE, pp. 1432-1447.

Boynton, S. S. and Daniel, D. E. (1985). "Hydraulic Conductivity of Compacted Clay," *Journal of Geotechnical Engineering*, ASCE, pp. 465-467.

Broadman, B. T. (1996). "Hydraulic Conductivity of Dessicated Clay Liners," *Journal of Geotechnical Engineering Division*, ASCE, pp. 204-208.

Daniel, D. E. (1989). "In-situ Hydraulic Conductivity Tests for Compacted Clays," *Journal of Geotechnical Engineering*, ASCE, pp. 1205-1226.

Daniel, D. E. and Boynton, S. S. (1985). "Fixed Wall Versus Flexible Wall Permeameters," *Hydraulic Barriers in Soil and Rock*, ASTM. (STP874), pp. 107-126.

Daniel, D. E., Koerner, R. M., Bornaparte, R., Landreth, R. E., Carson and Scranton, H. B. (1998). "Slope Stability of Geosynthetic Caly Liner Test Plots," *Journal of Geotechnical and Geoenvironmental Engineering*, ASCE, pp. 628-637.

Datta, M. and Juneja, A. (1997). "Landfill Liners: Compacted Clays and Amended Soils," *Waste Disposal in Engineered Landfills*, Ed. by Datta, M., Narosa Publishing House, New Delhi, pp. 108-129.

Eith, A. W. and Koerner, G. R. (1997). "Assessment of HDPE Geomembrane in a Muncipal Double Liner System after Eight Years of Service," *Geotextiles and Geomembranes*, Ed. John, N. W. M., pp. 277-288.

Fox, P. J., Rowland, M. G. and Scheithe, J. R. (1998). " Internal Shear Strength of Three Geosynthetic Clay Liners,"*Journal of Geotechnical and Geoenvironmental Engineering*, ASCE, pp. 933-943.

Ghosh, C. (1991). "Modelling and Analysis of Reinforced Foundation Beds," *Ph. D. Thesis*, IIT, Kanpur.

Gilbert, R.B. (1996). "Shear Strength of Reinforced Geosynthetic Clay Liner," *Journal of Geotechnical Engineering*, ASCE, pp. 259-266.

Giroud, J. P. (1994). "Mathematical Model of Geomembrane Stress-Strain Curves with a Yield Peak," *Geotextiles and Geomembranes*, Vol. 13, pp. 1-22.

Kodikara, J. (1996). "Prediction of Tension in Geomembranes placed on Landfill Slopes," *Environmental Geotechnics*, Ed. by Kamon, Balkema, Rotterdam, pp. 557-562.

Kodikara, J. (2000). "Analysis of Tension Development in Geomembranes placed on Landfill Slopes," *Geotextiles and Geomembranes*, Vol.18, pp. 47-61.

Koerner, R. M. (1990). "Designing with Geosynthetics," 2nd Edition, Prentice Hall, Englewood Chiffs, N. J.

Koerner, R. M. and Hwu, B. L. (1991). "Stability and Tension Considerations Regarding Cover Soil on Geomembrane Lined Slopes," *Geotextiles and Geomembranes*, Vol. 10, pp. 335-355.

Koerner, R. M., Koerner, G. R. and Hwu, B, L. (1990). "Three Dimensional, Axisymmetric Geomembrane Tension Test," *Geosynthetic Testing for Waste Containment Application*, Ed. by Koerner, R. M., ASTM (STP 1081), pp. 170-184.

Mitchell, J. K., Seed, R. B. and Seed, H. B. (1990). "Kettleman Hill Waste Landfill Slope Failure 1: Liner System Properties," *Journal of Geotechnical Engineering Division*, ASCE, pp. 647-668.

Rao, G. V. (1997). "Landfill Liners: Use of Geosynthetics," *Waste Disposal in Engineered Landfills*, Ed. by Datta, M., Narosa Publishing House, New Delhi, pp. 130-147.

Rao, K. S. (1997). "Characterisation of Landfill Sites," *Waste Disposal in Engineered Landfills*, Ed. by Datta, M., Narosa Publishing House, New Delhi, pp. 68-88.

Rao, K. S. (1997). "Site Selection for Landfills," *Waste Disposal in Engineered Landfills*, Ed. by Datta, M., Narosa Publishing House, New Delhi, pp. 56-67.

Seed, R. B., Mitchell, J. K., and Seed, H. B. (1990). "Kettleman Hill Waste Landfill Slope Failure II: Stability Analysis," *Journal of Geotechnical Engineering*, ASCE, pp. 669-689.

Sharma, H. D. and Lewis, S. P. (1994). "Waste Containment Systems, Waste Stabilisation and Landfills: Design and Evaluation," *John Wiley and Sons*, Inc., New York, USA.

Stark, T. D. and Poeppel, A. R. (1994). "Landfill Liner Interface Strengths from Torsional-Ring Shear Tests," *Journal of Geotechnical Engineering,* ASCE, pp. 597-603.

Stark, T. D., Williamson, T. A., and Eid, H. T. (1996). "HDPE Geomembrane/Geotextile Interface Shear Strength," *Journal of Geotechnical Engineering*, ASCE, pp. 197-208.

Wilson-Fahmy, R. F. and Koerner, R. M. (1993). "Finite Element Analysis of Stability of Cover Soil on Geomembrane Lined Slope," *Proc. Geosynthetics' 93*, Vancouver, Canada, pp.1425-1437.

Wilson-Fahmy, R. F., Koerner, R. M. and Fleck, J. A. (1993). "Unconfined and Confined Wide Width Tension Testing of Geosynthetics," *Geosynthetic Soil Reinforcement Testing Proceedings*, Ed. by Cheng, S. C. J., ASTM (STP 1190), pp. 49-63.

APPENDIX A1

DERIVATION FOR HYPERBOLIC SHEAR STRESS-DISPLACEMENT RESPONSE

Consider a small element of geomembrane as shown in Figure A1.1. From force equilibrium in the direction parallel to that of the geomembrane,

$$\frac{dT}{dx} = \tau_l - \tau_u \qquad (1)$$

where T is the tension in the geomembrane distance x from the anchorage,

τ_l and τ_u are the shear stresses induced at the lower and upper interfaces of the geomembrane at a distance x from the anchorage.

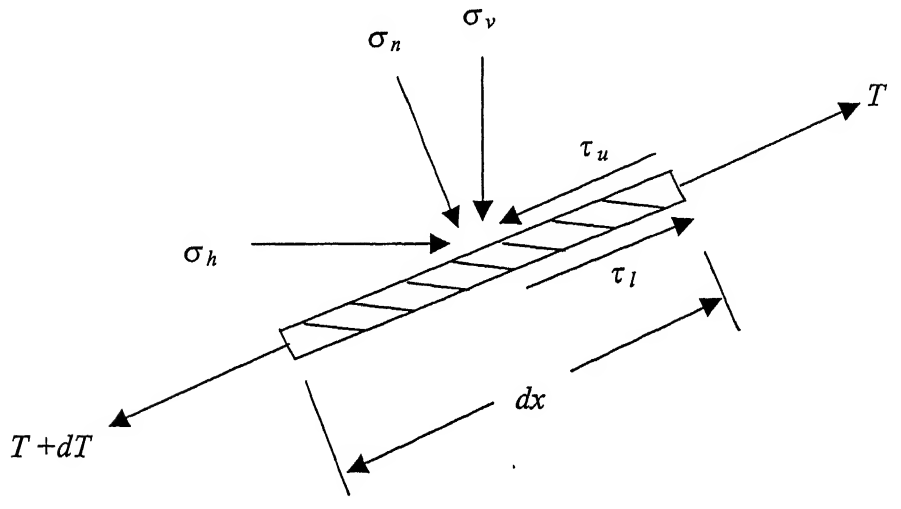

Figure A1.1: Equilibrium of an Infinitesimal Element

The stress strain relationship for the geomembrane assuming elastic response would be

$$\frac{du}{dx} = \frac{T}{tE} \qquad (2)$$

where E is the modulus of deformation of the geomembrane material and

t is the thickness of the geomembrane.

Combining equations (1) and (2), one gets

$$\frac{d^2u}{dx^2} = \frac{1}{tE}(\tau_l - \tau_u) \qquad (3)$$

From Figure A1.1, the vertical (σ_v) and horizontal (σ_h) stresses on the liner are expressed as

$$\sigma_v = h_x \gamma = (H + x \sin\theta - x \cos\theta \tan\beta)\gamma \quad (4)$$

$$\sigma_h = K_x \sigma_v \quad (5)$$

where K_x represents the ratio of horizontal to vertical stresses developed during the placement of soil and waste layers and γ represents the average bulk unit weight of the overburden over the geosynthetic liner. In the above equations, it is assumed that the water pressure at the level of the liner is not significant.

Assuming that the vertical and horizontal stress system (Eq.s (4) and (5)) represent the principal stress system for the medium above the liner, the normal, σ_n and the shear, τ_u stresses on the upper interface of the liner are

$$\sigma_n = \sigma_v \sin^2\theta + \sigma_h \cos^2\theta$$
$$= (K_x \cos^2\theta + \sin^2\theta)(H + x \sin\theta - x \cos\theta \tan\beta)\gamma \quad (6)$$

$$\tau_u = \tfrac{1}{2}(\sigma_v - \sigma_h) \sin 2\theta$$
$$= \tfrac{1}{2}(1 - K_x)(H + x \sin\theta - x \cos\theta \tan\beta)\gamma \sin 2\theta \quad (7)$$

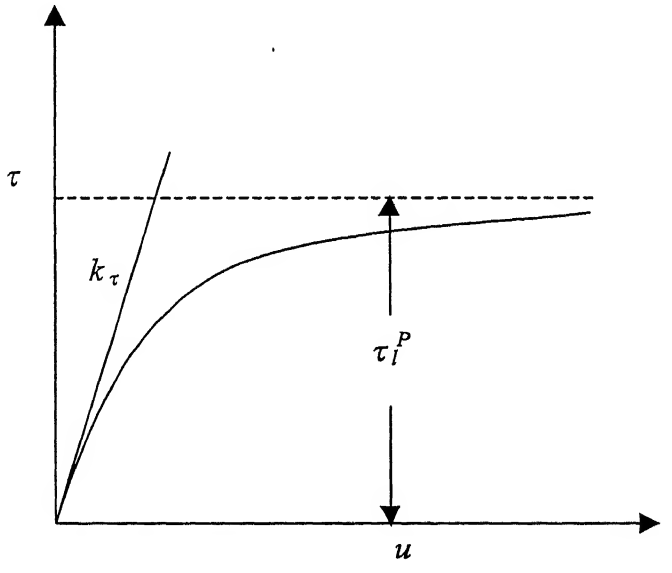

Figure A1.2: Hyperbolic Interface Response in the Present Study

The shear stresses on the lower interface depend on the shear-displacement characteristics of the geomembrane-clay interface. In the current analysis, the interface response has been assumed to be a hyperbola with an initial slope of k_τ (Figure A1.2), where k_τ is the initial slope of τ v/s u curve and τ_l^P is the maximum shear stress.

The assumed curve is defined by the following equation:

$$\tau_l = \frac{k_\tau u}{1+\frac{k_\tau}{\tau_l^P}u} \tag{8}$$

where k_τ is initial slope,

τ_l^P is the maximum shear stress.

τ_l^P is given by

$$\tau_l^P = (\sigma_n - p_l)\tan\delta_l + c_{al} \tag{9}$$

where p_l is the pore water pressure at the lower interface,

δ_l is the angle of intrinsic friction at the lower interface and

c_{al} is the adhesion between the geomembrane and clay at the interface.

Substituting equations (7) and (8) in equation (3)

$$\frac{d^2u}{dx^2} = \frac{1}{tE}\left[\frac{k_\tau u}{1+\frac{k_\tau}{\tau_l^P}u}\right] - \frac{1}{tE}\left[\frac{1}{2}(1-K_x)(H+x\sin\theta - x\cos\theta\tan\beta)\times\gamma\times\sin 2\theta\right] \tag{10}$$

Rearranging the terms in equation (10), one gets

$$\frac{d^2u}{dx^2} - \frac{1}{tE}\left[\frac{k_\tau u}{1+\frac{k_\tau u}{(\sigma_n - p_l)\tan\delta_l + c_{al}}}\right] = -\frac{1}{tE}\left[\frac{1}{2}(1-K_x)(H+x\sin\theta - x\cos\theta\tan\beta)\times\gamma\times\sin 2\theta\right] \tag{11}$$

which is the governing equation of the problem.

APPENDIX A2

DERIVATION FOR STRAIN SOFTENING IN THE SHEAR STRESS-DISPLACEMENT RESPONSE

Consider a small element of geomembrane as shown in Figure A2.1. From force equilibrium in the direction parallel to that of the geomembrane,

$$\frac{dT}{dx} = \tau_l - \tau_u \qquad (1)$$

where T is the tension in the geomembrane distance x from the anchorage,

τ_l and τ_u are the shear stresses induced at the lower and upper interfaces of the geomembrane at a distance x from the anchorage.

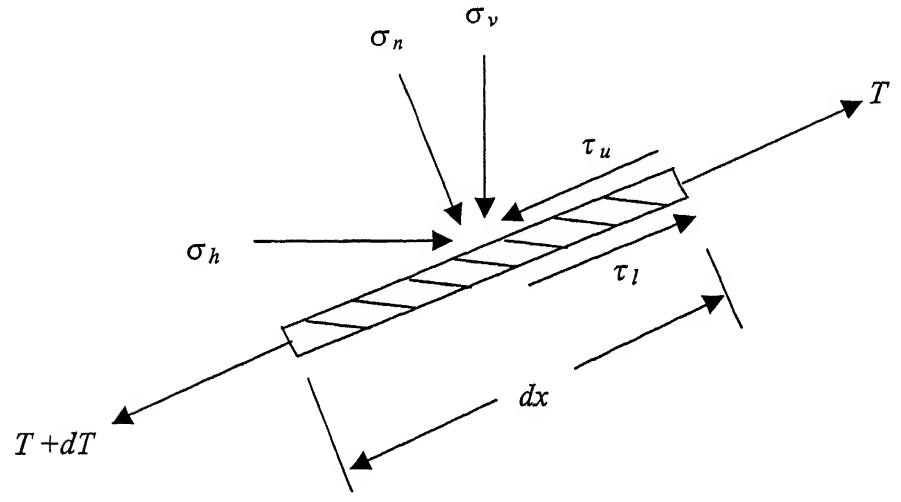

Figure A2.1: Equilibrium of an Infinitesimal Element

The stress strain relationship for the geomembrane assuming elastic response would be

$$\frac{du}{dx} = \frac{T}{tE} \qquad (2)$$

where E is the modulus of deformation of the geomembrane material and

t is the thickness of the geomembrane.

Combining equation (1) and (2), one gets

$$\frac{d^2u}{dx^2} = \frac{1}{tE}(\tau_l - \tau_u) \qquad (3)$$

From Figure A1.1, the vertical (σ_v) and horizontal (σ_h) stresses on the liner are expressed as

$$\sigma_v = h_x \gamma = (H + x \sin\theta - x \cos\theta \tan\beta)\,\gamma \quad (4)$$

$$\sigma_h = K_x \sigma_v \quad (5)$$

where K_x represents the ratio of horizontal to vertical stresses developed during the placement of soil and waste layers and γ represents the average bulk unit weight of the overburden over the geosynthetic liner. In the above equations, it is assumed that the water pressure at the level of the liner is not significant.

Assuming that the vertical and horizontal stress system (Eq.s (4) and (5)) represent the principal stress system for the medium above the liner, the normal, σ_n and the shear, τ_u stresses on the upper interface of the liner are

$$\sigma_n = \sigma_v \sin^2\theta + \sigma_h \cos^2\theta$$
$$= (K_x \cos^2\theta + \sin^2\theta)(H + x \sin\theta - x \cos\theta \tan\beta)\,\gamma \quad (6)$$

$$\tau_u = \tfrac{1}{2}(\sigma_v - \sigma_h) \sin 2\theta$$
$$= \tfrac{1}{2}(1 - K_x)(H + x \sin\theta - x \cos\theta \tan\beta)\,\gamma \sin 2\theta \quad (7)$$

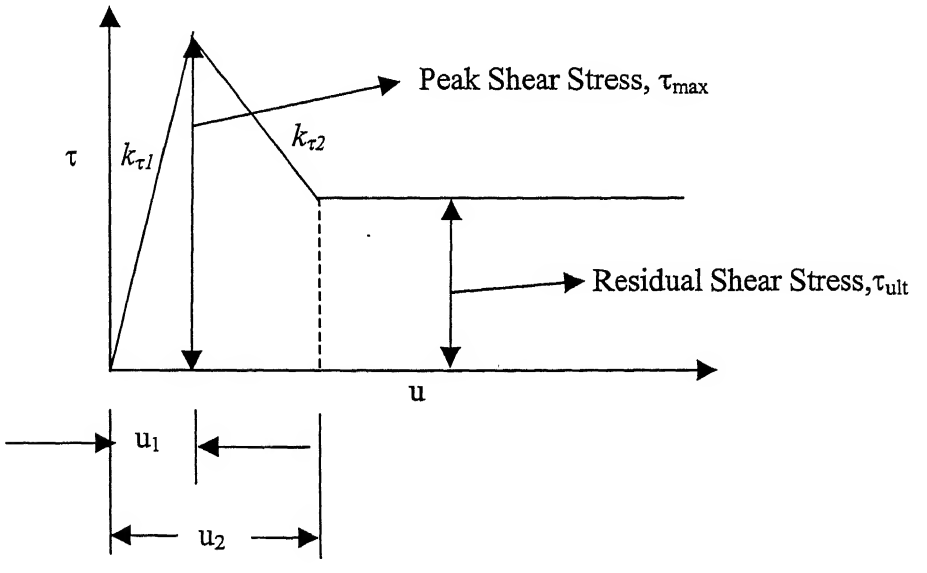

Figure A2.2: Assumed Shear Stress-Displacement Curve for Strain Softening Case

The assumed interface response is as shown in Figure A2.2 and is represented by

$$\begin{aligned} \tau_l &= k_{\tau 1} u \quad \text{if} \quad u \le u_1 \\ \tau_l &= k_{\tau 1} u_1 - k_{\tau 2}(u - u_1) \quad \text{if} \quad u_1 < u \le u_2 \\ \tau_l &= \tau_{ult} \quad \text{if} \quad u > u_2 \end{aligned} \tag{8}$$

where

τ_l is the shear stress acting on the lower interface,

u is the displacement at the lower interface,

u_1 and u_2 are displacements respectively corresponding to the peak shear stress and the point where the residual shear stress is mobilised,

$k_{\tau 1}$ and $k_{\tau 2}$ are the slope of the assumed shear stress-displacement response when $u < u_1$ and $u_1 < u < u_2$ respectively,

τ_{ult} is the residual shear stress and is given by

$$\tau_{ult} = (\sigma_n - p_l) \tan \delta_l + c_{al} \tag{9}$$

where p_l is the pore water pressure at the lower interface,

δ_l is the angle of interface friction at the lower interface and

c_{al} is the adhesion between the geomembrane and clay at the interface.

Substituting equation (7) and (8) in equation, one gets,

$$\begin{aligned} \frac{d^2u}{dx^2} &= \frac{1}{tE}\left[k_{\tau 1} u - \left[\tfrac{1}{2}(1 - k_x)(H + x\sin\theta - x\cos\theta \tan\beta) \times \gamma \times \sin 2\theta\right]\right] \quad \text{if} \quad u < u_1 \\ \frac{d^2u}{dx^2} &= \frac{1}{tE}\left[\begin{array}{l}(k_{\tau 1} u_1 - k_{\tau 2}(u - u_1)) \\ \quad - \left(\tfrac{1}{2}(1 - k_x)(H + x\sin\theta - x\cos\theta \tan\beta) \times \gamma \times \sin 2\theta\right)\end{array}\right] \quad \text{if} \quad u_1 < u < u_2 \\ \frac{d^2u}{dx^2} &= \frac{1}{tE}\left[\tau_{ult} - \left[\tfrac{1}{2}(1 - k_x)(H + x\sin\theta - x\cos\theta \tan\beta) \times \gamma \times \sin 2\theta\right]\right] \quad \text{if} \quad u > u_2 \end{aligned} \tag{10}$$

which is the governing equation of the problem.

APPENDIX A3

DERIVATION FOR BILINEAR STRESS-STRAIN RESPONSE CONSIDERATIONS FOR THE GEOMEMBRANE

Consider a small element of geomembrane as shown in Figure A3.1. From force equilibrium in the direction parallel to that of the geomembrane,

$$\frac{dT}{dx} = \tau_l - \tau_u \qquad (1)$$

where T is the tension in the geomembrane distance x from the anchorage,

τ_l and τ_u are the shear stresses induced at the lower and upper interfaces of the geomembrane at a distance x from the anchorage.

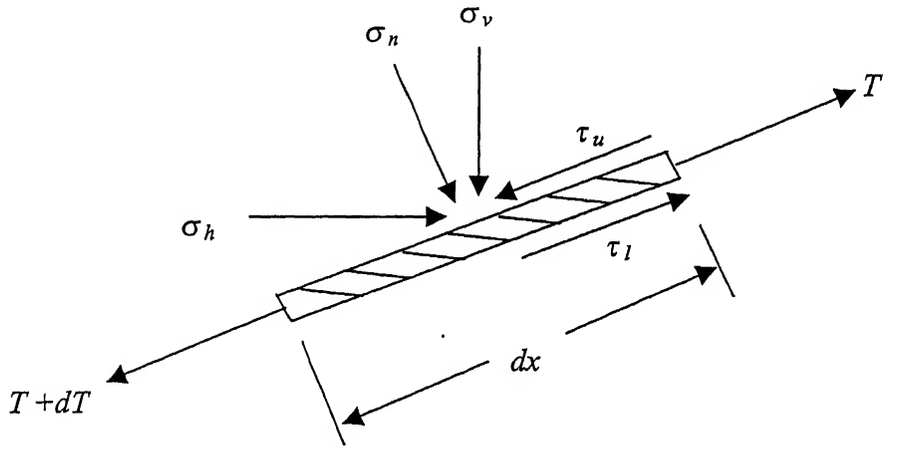

Figure A3.1: Equilibrium of an Infinitesimal Element

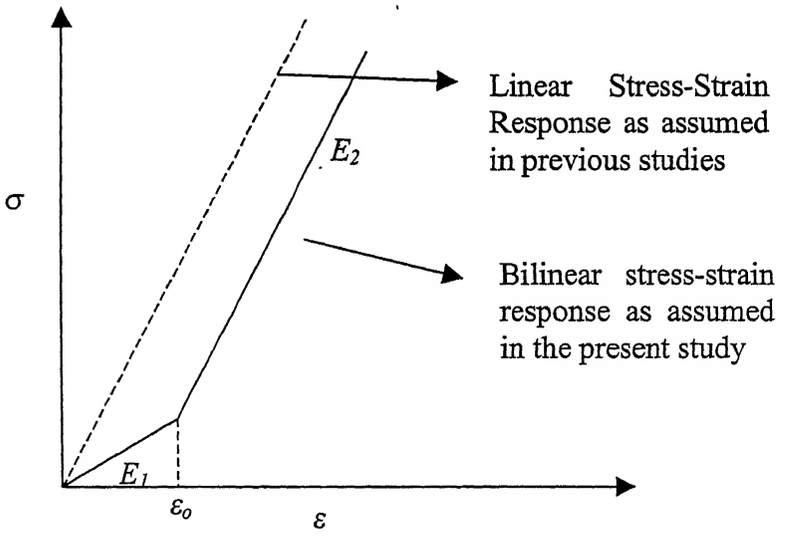

Figure A3.2: Assumed Stress-Strain Characteristic Curve of the Geosynthetics

The stress strain relationship for the geomembrane assuming bilinear response as shown in Figure A3.2 would be

$$\sigma = E_1 \varepsilon \quad if \quad \varepsilon < \varepsilon_o \tag{2.1}$$

$$\sigma = \sigma_1 + E_2(\varepsilon - \varepsilon_o) \quad if \quad \varepsilon > \varepsilon_o \tag{2.2}$$

where σ and ε are the tensile stress and strain in the geosynthetic respectively,

σ_1 is the stress corresponding to strain level at the transition and

E_1 and E_2 are the modulus of deformation for $\varepsilon < \varepsilon_o$ and $\varepsilon \geq \varepsilon_o$ respectively.

The tensile stress, σ and strain, ε at any point in a geomembrane are given by

$$\sigma = \frac{T}{t} \; and \; \varepsilon = \frac{du}{dx} \tag{3}$$

where

T is the tension induced per unit width at any point in the geomembrane,

t is the thickness of the geomembrane,

u is the displacement at that point.

Combining equation (2) and (3), one gets,

$$\frac{T}{t E_1} = \frac{du}{dx} \quad if \quad \varepsilon < \varepsilon_o$$

$$\frac{T}{t E_2} = \frac{T_1}{t E_2} + \left(\frac{du}{dx} - \varepsilon_o \right) \quad if \quad \varepsilon > \varepsilon_o \tag{4}$$

Substituting equation (4) in equation (1), one gets,

$$\frac{d^2 u}{dx^2} = \frac{1}{t E_1}(\tau_1 - \tau_u) = M_R \frac{1}{t E_2}(\tau_1 - \tau_u) \quad if \quad \varepsilon < \varepsilon_o \tag{5}$$

$$\frac{d^2 u}{d x^2} = \frac{1}{t E_2}((\tau_1 - \tau_u) \quad if \quad \varepsilon > \varepsilon_o$$

where

$$M_R = \frac{E_2}{E_1}$$

From Figure A3.1, the vertical (σ_v) and horizontal (σ_h) stresses on the liner are expressed as

$$\sigma_v = h_x \gamma = (H + x \sin\theta - x \cos\theta \tan\beta)\, \gamma \tag{6}$$

$$\sigma_h = K_x \sigma_v \tag{7}$$

where K_x represents the ratio of horizontal to vertical stresses developed during the placement of soil and waste layers and γ represents the average bulk unit weight of the overburden over the geosynthetic liner. In the above equations, it is assumed that the water pressure at the level of the liner is not significant.

Assuming that the vertical and horizontal stress system (Eq.s (6) and (7)) represent the principal stress system for the medium above the liner, the normal, σ_n and the shear, τ_u stresses on the upper interface of the liner are

$$\sigma_n = \sigma_v \sin^2\theta + \sigma_h \cos^2\theta$$
$$= (K_x \cos^2\theta + \sin^2\theta)(H + x \sin\theta - x \cos\theta \tan\beta)\gamma \quad \textbf{(8)}$$

$$\tau_u = \tfrac{1}{2}(\sigma_v - \sigma_h) \sin 2\theta$$
$$= \tfrac{1}{2}(1 - K_x)(H + x \sin\theta - x \cos\theta \tan\beta)\gamma \sin 2\theta \quad \textbf{(9)}$$

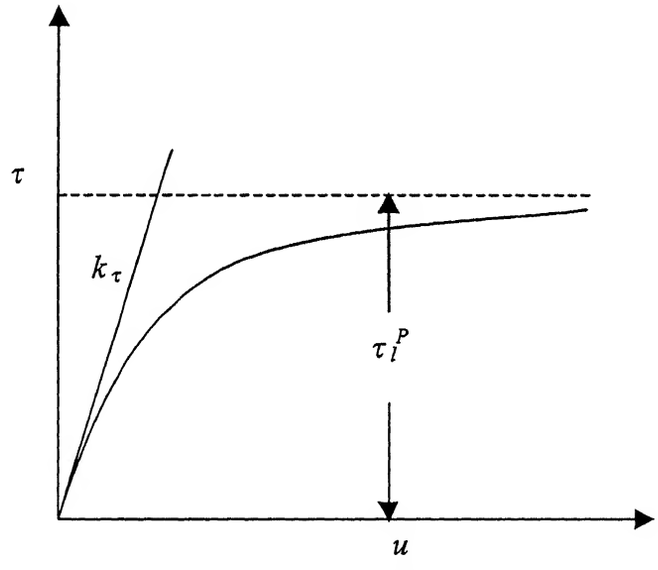

Figure A3.3: Hyperbolic Interface Response in the Present Study

The shear stresses on the lower interface depend on the shear-displacement characteristics of the geomembrane-clay interface. In the current analysis, the interface response has been assumed to be a hyperbola with an initial slope of k_τ (Figure A1.2), where k_τ is the initial slope of τ v/s u curve and τ_l^P is the maximum shear stress.

The assumed curve is defined by the following equation:

$$\tau_l = \frac{k_\tau u}{1 + \frac{k_\tau}{\tau_l^P} u} \tag{10}$$

where k_τ is initial slope,

τ_l^P is the maximum shear stress.

τ_l^P is given by

$$\tau_l^P = (\sigma_n - p_l) \tan \delta_l + c_{al} \tag{11}$$

where p_l is the pore water pressure at the lower interface,

δ_l is the angle of intrinsic friction at the lower interface and

c_{al} is the adhesion between the geomembrane and clay at the interface.

Substituting equation (9) and (10) in equation (5), one gets,

$$\frac{d^2u}{dx^2} - \frac{1}{tE_2}\left[\frac{k_\tau u}{1 + \frac{k_\tau u}{(\sigma_n - p_l)\tan\delta_l + c_{al}}}\right] = -\frac{1}{tE_2}\left[\frac{1}{2}(1 - K_x)(H + x\sin\theta - x\cos\theta\tan\beta) \times \gamma \times \sin 2\theta\right] \quad if \ \varepsilon > \varepsilon_o$$

$$\frac{d^2u}{dx^2} - M_R\frac{1}{tE}\left[\frac{k_\tau u}{1 + \frac{k_\tau u}{(\sigma_n - p_l)\tan\delta_l + c_{al}}}\right] = -M_R\frac{1}{tE_2}\left[\frac{1}{2}(1 - K_x)(H + x\sin\theta - x\cos\theta\tan\beta) \times \gamma \times \sin 2\theta\right] \quad if \ \varepsilon < \varepsilon_o \tag{12}$$

which is the governing equation of the problem.

APPENDIX A4

DERIVATION OF GOVERNING EQUATION FOR THE MODEL OF THE PROBLEM

The problem was modeled by a three parameter mathematical model as shown in Figure A4.1.

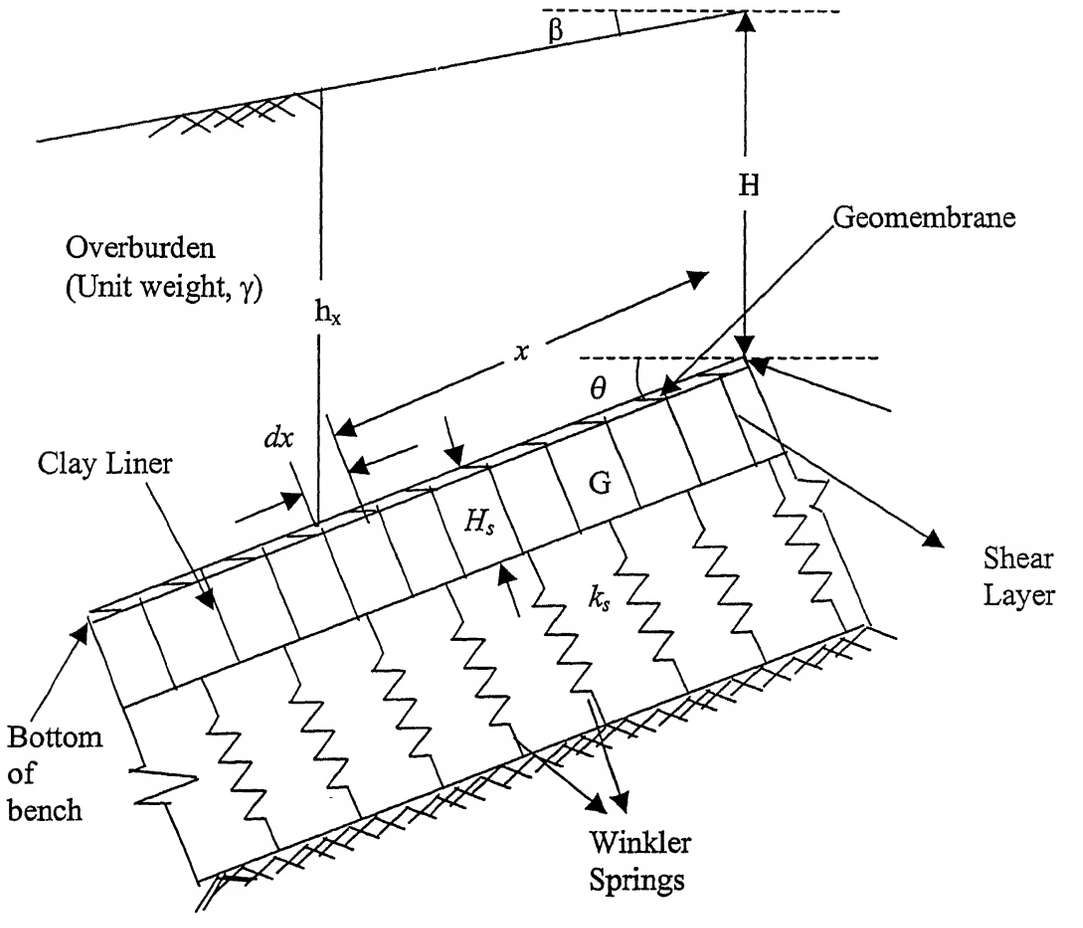

Figure A4.1: Modelling of the Problem for Prediction of Tension due to Settlement

Considering forces acting on a small element of geomembrane,

by summing up the horizontal forces one gets,

$$(T+\Delta T)(\cos(\xi+d\xi))-T\cos\xi=(\tau_1-\tau_2)\Delta x$$

$$\text{or, } \frac{d}{dx}(T\cos\xi)=(\tau_1-\tau_2)$$

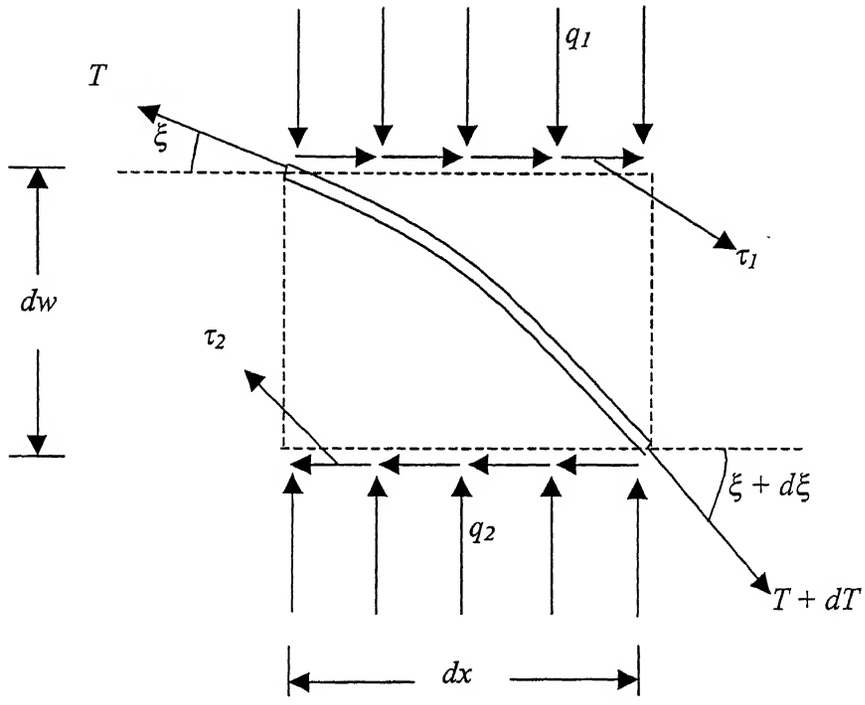

Figure A4.2: Forces acting on a Small Element of the Geomembrane

$$\text{or, } \cos\xi \frac{dT}{dx} - T\sin\xi \frac{d\xi}{dx} = (\tau_1 - \tau_2) \tag{1}$$

Similarly, by summing up the vertical forces one gets,

$$(T + \Delta T)(\sin(\xi + d\xi)) - T\sin\xi = (q_1 - q_2)\Delta x$$

$$\text{or, } \frac{d}{dx}(T\sin\xi) = (q_1 - q_2)$$

$$\text{or, } T\cos\xi \frac{d\xi}{dx} + \sin\xi \frac{dT}{dx} = (q_2 - q_1) \tag{2}$$

(1) $\times$ *sin* ξ - (2) $\times$ *cos* ξ gives,

$$-T\frac{d\xi}{dx} = (T_2 - T_1)\sin\xi - (q_2 - q_1)\cos\xi \tag{3}$$

(1) $\times$ *cos* ξ + (2) $\times$ *sin* ξ gives

$$\frac{dT}{dx} = (T_2 - T_1)\cos\xi + (q_2 - q_1)\sin\xi \tag{4}$$

The slope of the geomembrane at any point = $\tan\xi = \frac{dw}{dx}$

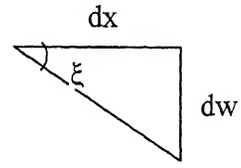

Differentiating both the sides with respect to x, one gets,

$$\sec^2\xi\frac{d\xi}{dx} = \frac{d^2w}{dx^2}$$

$$\text{or, } \frac{d\xi}{dx} = \cos^2\theta\frac{d^2w}{dx^2} \qquad (5)$$

Substituting equation (5) in equation (3), one gets,

$$-T\cos^2\xi\frac{d^2w}{dx^2} = (T_2 - T_1)\sin\xi - (q_2 - q_1)\cos\xi \qquad (6)$$

$$or,\ T\cos^2\xi\frac{d^2w}{dx^2} = (q_2 - q_1)\cos\xi - (T_2 - T_1)\sin\xi \qquad (7)$$

τ_1 and τ_2 are given by:

$$\left.\begin{aligned}\tau_1 &= c_1 + \mu_1 q_1\\ \tau_2 &= c_2 + \mu_2 q_2\end{aligned}\right\} \qquad (8)$$

Substituting this in Equation (7):

$$T\cos^2\xi\frac{d^2w}{dx^2} = (q_2 - q_1)\cos\xi - \left[\left(ca_2 + \mu_2 q_2\right) - \left(ca_1 + \mu_1 q_1\right)\right]\sin\xi \qquad (9)$$

$$\text{or, } T\cos^2\xi\frac{d^2w}{dx^2} = (q_2 - q_1)\cos\xi - \left[\left(\mu_2 q_2 - \mu_1 q\right)\sin\xi - \left(ca_2 - ca_{11}\right)\sin\xi\right] \qquad (10)$$

The reaction force q_2 is given by,

$$q_2 = K_s \cdot w - GH\frac{d^2w}{dx^2} \qquad \text{(Ghosh and Madhav, 1991)} \qquad (11)$$

Substituting equation (11) in equation (10) gives,

$$T\cos^2\xi\frac{d^2w}{dx^2} = \left(K_s \cdot w - GH\frac{d^2w}{dx^2}_2 - q_1\right)\cos\xi -$$

$$\left[\left(\mu_2 K_s \cdot w - GH\frac{d^2w}{dx^2} - \mu_1 q\right)\sin\xi - \left(ca_2 - ca_{11}\right)\sin\xi\right]$$

$$\text{or, } \frac{d^2w}{dx^2}\left[T\cos^2\xi + GH\cos\xi - \mu_2 GH\sin\xi\right] = W\left[K_s\cos\xi - \mu_2 K_s\sin\xi\right] + \left[\mu_1 q_1\sin\xi - q_1\cos\xi\right] - (ca_2)\sin\xi \quad \textbf{(12)}$$

Similarly, substituting equations (5), (8) and (11) in equation (4), one gets,

$$\frac{dT}{dx} = \left[\mu_2 k_s\cos\xi + k_s\sin\xi\right]w - \left[\mu_2 G H_s\cos\xi + G H_s\sin\xi\right]\frac{d^2w}{dx^2} - \left[\mu_1 q_1\cos\xi + q_1\sin\xi\right] + (c_{a2} - c_{a1})\cos\xi \quad \textbf{(13)}$$

APPENDIX B

VALIDATION OF RESULTS

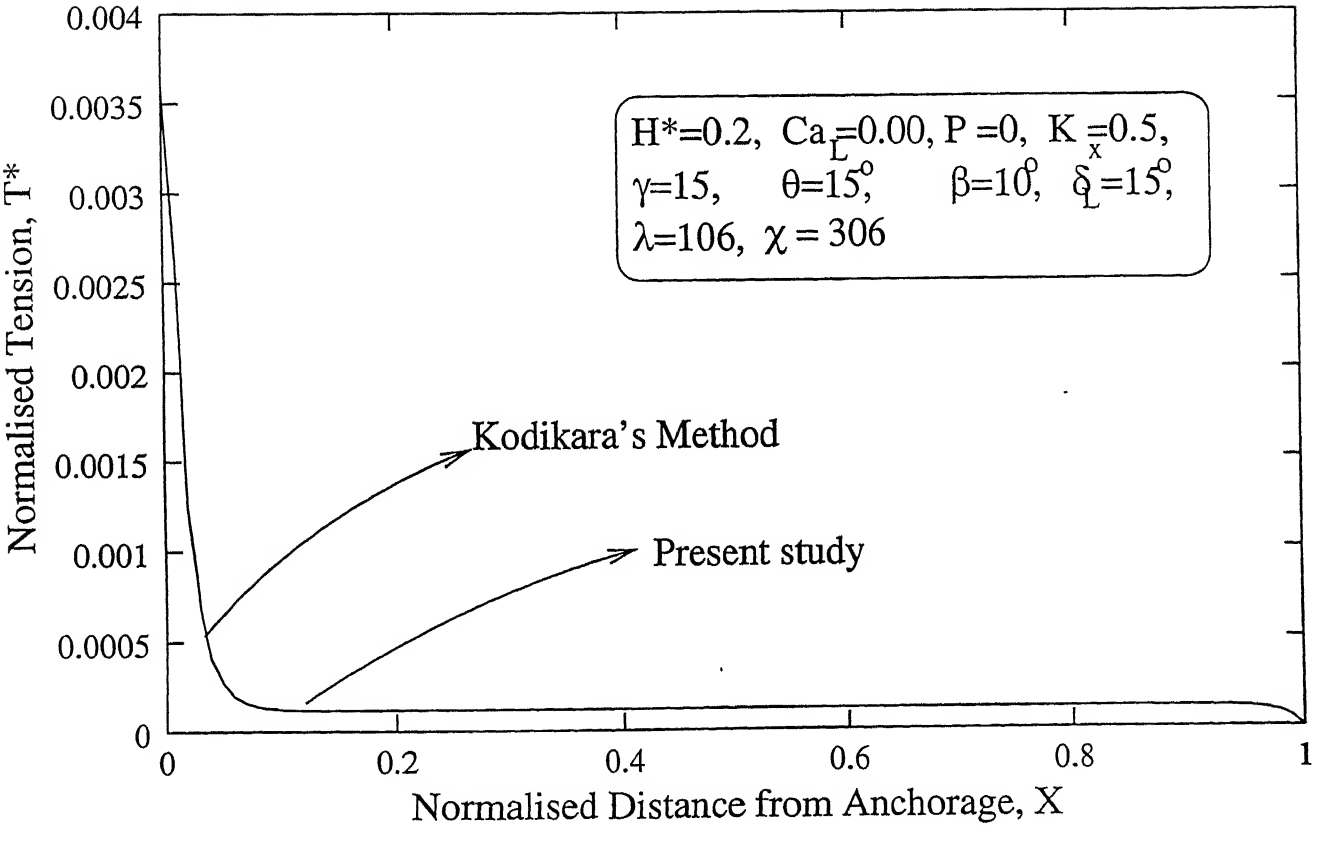

Figure B.1 Comparison between Results obtained by the Present Study and Kodikara's Results